File Copy

Capillary Flow in Agricultural Drainage

Station Bulletin 629
August 1977

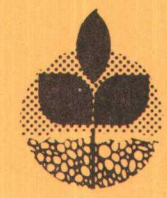

Agricultural Experiment Station
Oregon State University
Corvallis, Oregon

Western Regional
Research Project W-51

ACKNOWLEDGMENTS

The research results reported in this paper are derived from the individual efforts of numerous investigators in the western states. This research was coordinated by the Western Regional Research Committee W-51, "Dynamics of flow into drainage facilities." Individual research programs have been supported by the respective State Experiment Stations, the Agricultural Research Service, USDA, and various federal and state funding agencies as well as by federal funds administered through the Hatch Act.

The authors are indebted to numerous individuals, both technicians and graduate students, whose past efforts have helped lay the framework for this publication.

This publication is one of three concurrent publications to be issued by W-51 on different aspects of drainage research. The remaining papers and the name and location of their editors are: a) "Field performance of drains," L. G. King, Editor, Washington State University, Pullman, and b) "Factors influencing water and particle movement into drains," L. S. Willardson, Editor, Utah State University, Logan.

This paper is a contribution of the Agricultural Research Service, USDA and State Agricultural Experiment Stations of Colorado, Idaho and Oregon, through cooperative research under Western Regional Research Project W-51, "Dynamics of flow into drainage facilities."

Editor and contributors are:

Harold R. Duke, Agricultural Engineer, USDA-ARS, Fort Collins, Colorado

Royal H. Brooks, Professor, Agricultural Engineering Department, Oregon State University, Corvallis

Arthur T. Corey, Professor Emeritus, Agricultural Engineering Department, Colorado State University, Fort Collins

Delbert W. Fitzsimmons, Professor and Head, Agricultural Engineering Department, University of Idaho, Moscow

Richard R. Tebbs, Associate Professor, Department of Mathematics, Southern Utah State University, Cedar City (formerly Research Associate, Oregon State University)

CONTENTS

CAPILLARY FLOW IN AGRICULTURAL DRAINAGE

Edited by Harold R. Duke

with further contributions by
Royal H. Brooks, Arthur T. Corey, Delbert W. Fitzsimmons,
and Richard R. Tebbs

ABSTRACT

The process of drainage of soil water is customarily treated as a fully saturated flow phenomenon. Recent work of several cooperating scientists is reported to illustrate that the partially saturated zone can significantly influence the overall performance of agricultural drains, particularly with respect to maintenance of a desirable root environment and when the soils encountered are either quite shallow or very fine textured.

In the first section, the capillary properties of soils pertinent to drainage are described. Both laboratory and field measurement techniques are proposed. Experimental data illustrate the utility of these techniques. The second section details necessary considerations for modelling capillary flow systems and presents models successfully used to predict both vertical drainage of the soil profile and horizontal flow associated with a sloping water table. The final section describes results of numerical analyses of both sloping aquifers and parallel drain systems. The capillary region is shown to have considerable influence upon both the predicted water table position and the relation between water table depth and depth of soil which is adequately aerated to allow root development.

INTRODUCTION

The existence of a region within the soil profile in which capillarity dominates the movement and storage of water is well recognized. It is primarily within this region that water is infiltrated, redistributed, stored, and recovered by plants for transpiration. This region must also transmit gases produced and consumed by respiration of plant roots.

Although the capillary region is the source of virtually all water removed by subsurface drainage systems, its importance to the drainage flow regime is often debated. Because of the extremely nonlinear nature of the capillary functions, their inclusion complicates the flow equations, often to the point of rendering analytic solutions virtually impossible.

Because their methods of evaluating soil parameters force parameter values to fit a solution which neglects the capillary region, groundwater engineers and hydrologists have generally met with reasonable success in designing drains by ignoring the partially saturated zone.

It is not the intent of this paper to discourage use of this idealized design procedure, but rather to illustrate its limitations and provide the practicing designer with tools to judge whether neglecting the capillary region can be expected to give satisfactory results. Examples presented, which are typical of conditions not infrequently encountered, illustrate that, with certain geometric and soil property limitations, neglecting the effects of the capillary region can result in considerable error.

SECTION I.

CAPILLARY PROPERTIES PERTINENT TO DRAINAGE

The capillary properties of soils pertinent to drainage are those that relate to a soil's ability to retain, release, and transmit water. These properties also determine the soil's ability to exchange gases between the atmosphere and all points within the root zone of crops.

Part of the water held in soils immediately following precipitation or irrigation may be removed by downward flow in response to a finite hydraulic gradient. Water more tightly held by capillarity can be removed by plants. That remaining after plants have wilted can be removed only by evaporation and subsequent diffusion in the vapor phase. It is the first mentioned part, called "drainable" water, that is of direct concern to drainage engineers.

Briefly, the engineer needs to know how much water will be released under specified hydraulic conditions and how fast it will be released. He also needs to know how much water must be removed to provide sufficient aeration within the root zone.

Although soil textural classification conveys a vague quantification of such parameters as capillary fringe and hydraulic conductivity no visual test has yet been developed to adequately quantify the capillary properties pertinent to drainage. Thus, we must still rely on experimental evaluation of these properties. In this section, the pertinent properties are described, the most recent laboratory measurement techniques are outlined, and the most successful methods of estimating these properties in field soils are discussed.

I.1 MEASURABLE SOIL PROPERTIES by A. T. Corey

I.1.1 WATER RETENTION CHARACTERISTICS

The characteristics of soils with respect to their storage and release of water are described by the functional relationship between water content and the pressure of the water. In the past, drainage engineers usually have characterized this relationship by a single parameter called "specific yield." However, as Duke (1972) has pointed out, this parameter has been vaguely defined. For example, Todd (1959) defines specific yield as "the volume of water that an aquifer releases from or takes into storage per unit change in the component of head normal to that surface." This definition implies that specific yield is independent of water pressure (i.e., water table depth or flux) and, therefore, is a constant. Such an assumption is a valid approximation only if the water table is already at a safe depth and the flux of water through the region above the water table is negligible with respect to the saturated hydraulic conductivity.

It is preferable to describe the relationship (between water retained and water pressure) over the ranges of pressure existing during significant drainage. These pressures range from atmospheric to considerably less than atmospheric. That is, the gauge pressure of the soil water during drainage is usually negative. As the pressure of water becomes more negative, water content decreases. However, the relationship between water content and gauge pressure is subject to hysteresis; that is, water content is greater as a soil drains to a particular pressure than when it undergoes imbibition to the same pressure. In fact, an infinite number of relationships are possible, depending on the water content at the time a soil starts to drain or to imbibe.

Drainage engineers are concerned with describing the relationship (between water retained and water pressure) primarily during drainage. Such a relationship is shown in Figure I-1. In this figure, the water content is expressed as a volume ratio, called saturation, which is defined

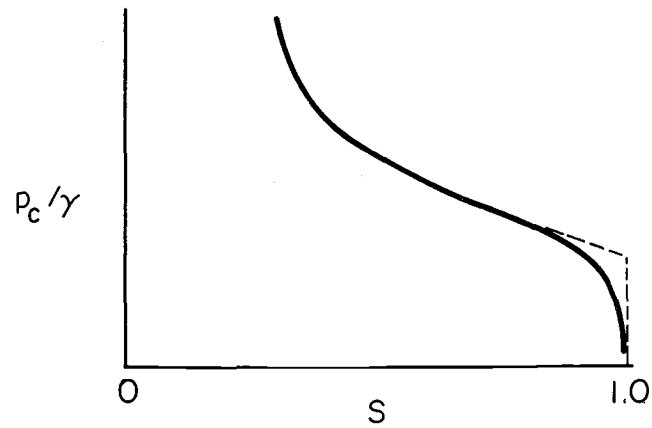

Figure I-1. Relationship between water content and negative water pressure head on a drainage cycle.

as the ratio of volume of water to volume of pore space. The negative pressure is expressed as the difference in pressure between air and water divided by the specific weight of water. This quantity is called capillary pressure head, p_c/γ , and has a positive sign. It is similar to what soil scientists call "suction" head, "tension", or matrix suction, which they usually express in centimeters of water.

The relationship shown in Figure I-1 is a type that can be obtained in a laboratory for a soil sample that is initially fully saturated with water by evacuating

all of the air. It is not probable that such a relationship applies often in a field soil because a mechanism for evacuating all of the air does not exist. We would expect, therefore, to find (in the field) a water retention relationship somewhat similar to Figure I-1, except that the water saturation at zero gauge pressure would be less than 1.0. Experience indicates that a maximum saturation of 0.85 to 0.90 could be expected. However, it is convenient to define another ratio to express the water content for the field saturation. In this case, saturation is defined as the ratio of volume of water to the maximum volume of water following imbibition, entrapped air being regarded as part of the soil matrix. With this definition of saturation, the field retention characteristics are typically similar to that shown in Figure I-1.

Several characteristics of the water retention relationship should be noted. For example, the soil remains essentially fully saturated over a finite range of p_c/γ . The curve shown in Figure I-1 indicates a gradual transition from the fully saturated state to a condition of rapid desaturation with respect to change in p_c/γ . However, White, et al (1970) have shown that this transition is produced by the relatively large boundary effect on small laboratory samples. In the field, where only the surface of the soil constitutes an exposed boundary, the transition region of the curve can be expected to be greatly reduced. In this case, a valid approximation might be represented by the dashed line shown in Figure I-1.

In any case, it is important to consider the magnitude of the maximum p_c/γ at which the soil remains essentially fully saturated. Brooks and Corey (1964) have called this value of p_c/γ the "bubbling" pressure head, p_b/γ . They defined it as the value of p_c/γ at which an extrapolation of the retention curve (shown by the dashed line) intersects the abscissa representing a saturation of 1.0. Brooks and Corey believed that at values of p_c/γ greater than p_b/γ , the gas phase is continuous within the soil and aeration is possible. However, White, et al (1970) observed from very refined experiments that continuity of the gaseous phase first occurs at a slightly higher value of p_c/γ , represented by the pressure at which the dashed extrapolation intersects the measured curve.

Another aspect of the retention curve which needs to be noted is that saturation, S , appears to approach a minimum value and further increases in p_c/γ produce a very small decrease in S . Brooks and Corey (1964) have called this limiting value of S the "residual" saturation, S_r . When this water content is expressed as a

fraction of the dry weight of the soil, it should correspond to a standard laboratory evaluation of "field capacity." The water that drains from the soil (from the maximum saturation S_m to the minimum saturation S_r) should be a measure of "specific yield", provided that the latter is evaluated by lowering the water table from an already great depth.

Another significant aspect of the retention curve is the way in which S varies with p_c/γ and the p_c/γ corresponding to S_r . According to Brooks and Corey (1964) this characteristic of soils depends on their "pore-size" distribution. They characterized the pore-size distribution in terms of an index λ , obtained from data such as are shown in Figure I-2.

To obtain λ , Brooks and Corey replotted these data on a log-log plot after first "normalizing" the variable S . The water saturation is normalized by defining a new variable, called "effective" saturation S_e , as

$$S_e = \frac{S - S_r}{S_m - S_r} \tag{I-1}$$

where S_r is the residual saturation and S_m is the maximum saturation. When $\log S_e$ is plotted as a function of $\log p_c/\gamma$, the result, typically, is as shown in Figure I-2. This plot is usually linear except within the region of S_e influenced

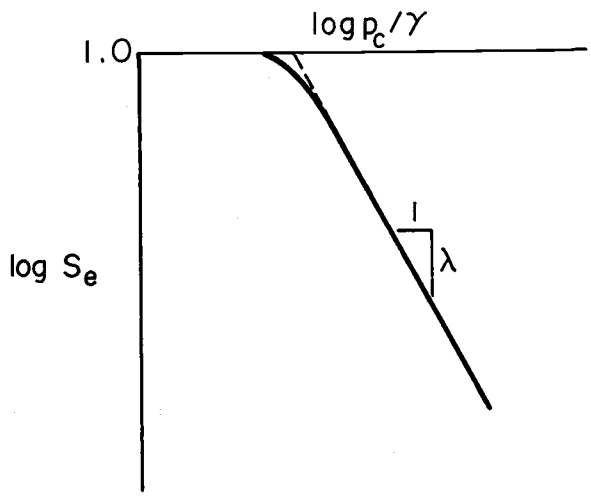

Figure I-2. Logarithmic plot of effective saturation as a function of capillary pressure head used to determine pore size distribution index, λ .

by the previously mentioned boundary effect. Consequently, it is easy to determine a value of p_b/γ by extrapolating the linear portion of the plot to the abscissa

representing $S_e = 1.0$. Moreover, the negative of the slope of this plot gives the value of λ. From theoretical considerations, Brooks and Corey thought that this slope is a measure of the relative range of pore dimensions, being larger the more uniform the pore size. For example, it is clear that if the pore size were completely uniform, all pores would drain at the same value of p_c/γ and the slope would be infinitely large. They, therefore, called λ the pore-size distribution index.

In making a plot such as Figure I-2, Brooks and Corey recommended first estimating S_r from a plot such as Figure I-1. The estimated value of S_r is then modified until a plot of $\log S_e$ vs. $\log p_c/\gamma$ is as nearly linear as possible (within the range $S_e < 1.0$). The definition of S_r is then implicit in the way it is determined. It is also convenient to use a computer program to determine p_b/γ, S_r and λ directly from data for S as a function of p_c/γ. Such a program has been developed by Corey and Stauffer and is presented in Appendix C.

Once these three parameters have been determined, the only other parameter needed to describe the pertinent water retention characteristics of the soil is the "effective" or "drainable" porosity ϕ_e. The latter parameter is related to the total porosity ϕ by the relation

$$\phi_e = (S_m - S_r)\,\phi \,. \tag{I-2}$$

The value of S_e is given by

$$S_e = \left(\frac{p_b}{p_c}\right)^{\lambda} \tag{I-3}$$

for $p_c \geq p_b$ and

$$S_e = 1.0 \tag{I-4}$$

for $p_c \leq p_b$. These expressions for S_e obviously neglect the transition portion of the curve shown in Figure I-1, that is, the portion representing saturations greater than that for which the gaseous phase is continuous. The rationale for neglecting this portion of the measured data is that it is probably not applicable to large masses of soil in the field, as suggested by White, et al (1970).

I.1.2 WATER TRANSMISSION CHARACTERISTICS

The transmission of water through soils during drainage usually can be described by combining Darcy's equation for flow of water with a continuity equation. The result is

$$\text{div } [K \nabla (p_c/\gamma - z)] = -\phi_e \frac{\partial S_e}{\partial t} \qquad \text{(I-5)}$$

in which K is the soil water conductivity, a function of saturation and probably aeration and position in space. Time is represented by t, and z is the vertical ordinate. In order to apply this equation (or any analagous equation), it is necessary to describe the functional relationships among S_e, p_c/γ, and K.

The relationship between S_e and p_c/γ is approximated by equations (I-3) and (I-4) which are functions of the pore-size distribution index. From theoretical considerations it is to be expected that the relationships among K, S_e, and p_c/γ are also functions of λ. Brooks and Corey (1964) have presented experimental as well as theoretical evidence that this is the case.

Brooks and Corey measured the relative conductivity, $K/K_{1.0}$, as a function of p_c/γ for a variety of soils and porous rocks, $K_{1.0}$ being the maximum value of K, that is, when $S_e = 1.0$. They presented their data as plots of $\log (K/K_{1.0})$ vs. $\log p_c/\gamma$, an example of which is shown in Figure I-3. They noted that such plots,

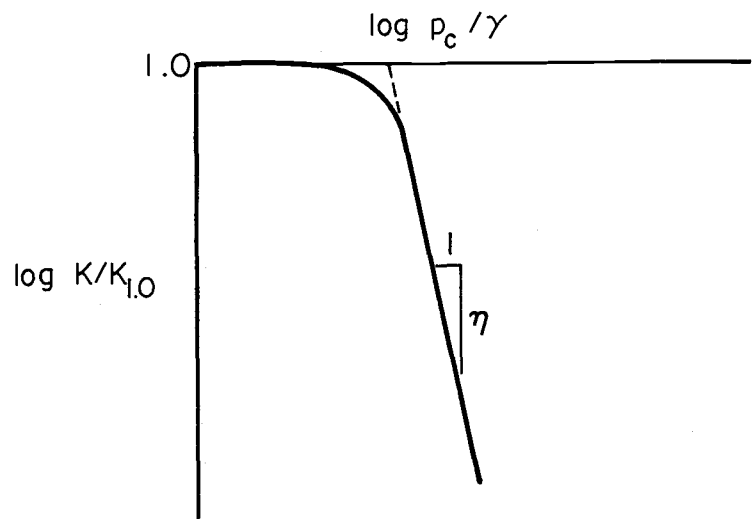

Figure I-3. Relative conductivity as a function of p_c/γ.

typically, were also linear over all except the region influenced by the sample boundary, that is, values of p_c/γ close to or less than p_b/γ. It was observed that the linear portion of the plot, when extrapolated to a zero value of $\log (K/K_{1.0})$ provided another evaluation of p_b/γ yielding the same result as obtained from the $S_e - p_c/\gamma$ function.

Consequently, it is possible to express the relationship between $K/K_{1.0}$ and p_c by the equation

$$\frac{K}{K_{1.0}} = \left(\frac{p_b}{p_c}\right)^{\eta} \qquad \text{(I-6)}$$

for $p_c \geq p_b$, and

$$\frac{K}{K_{1.0}} = 1.0 \qquad \text{(I-7)}$$

for $p_c \leq p_b$. This again obviously ignores the transition portion of the measured curve, which is justified on the basis that the transition is presumed to be a result of sample boundary effects.

Brooks and Corey reasoned that η should be related to λ. They presented the theoretical relationship

$$\eta = 3\lambda + 2 \qquad \text{(I-8)}$$

which was found experimentally to be a valid approximation. According to these results, the only parameter needed to describe the water transmission characteristics of soils during drainage (other than those needed to describe the retention characteristics) is the value of $K_{1.0}$, obtained after the soil has imbibed a maximum amount of water.

I.1.3 PROPERTIES OF SOIL PROFILES

A distinction is made between the capillary properties of soils and those of soil profiles. A soil profile frequently consists of layers of soil, either distinct or gradually varying, each layer having properties different from others in the profile. The response of a soil profile during drainage can be determined only by analyzing the

flow through a system of layers, the properties of each individual layer having been specified.

The thickness and slope of the individual layers, as well as their hydraulic properties, must be taken into account in any valid analysis of drainage of heterogeneous soil profiles. It is not possible to describe such systems in terms of average properties of the profile, no matter how such an average is obtained.

I.2 LABORATORY EVALUATION OF SOIL CAPILLARY PROPERTIES by A. T. Corey

As pointed out in the previous section, the capillary properties of soils can be evaluated in terms of the following parameters:

1) porosity - ϕ ,
2) maximum conductivity - $K_{1.0}$,
3) residual saturation - S_r ,
4) air-entry or "bubbling pressure" - p_b ,
5) pore-size distribution index - λ .

Methods of evaluating the parameters listed above (on laboratory samples) have been described by Brooks and Corey (1964) and Laliberte and Corey (1967). A more convenient and faster variation of their methods recently has been developed by Corey. The latter method is described here.

The method involves a determination of all five of the parameters listed by a single experiment in which p_c , S and the flow rate, q , are measured directly while the sample is continuously draining. Downward flow is established through a short cylindrical sample of undisturbed soil under conditions such that p_c (therefore S) is nearly uniform throughout. The rate of inflow is allowed to decrease gradually with time so that the outflow from the bottom of the sample is always slightly greater than the inflow. The average discharge through the sample is measured along with p_c and S at intervals of time until the inflow has practically stopped.

Undisturbed soil samples are obtained using a sleeve-type sampler similar to that described by Laliberte and Corey (1967). With this procedure the soil sample is retained in a thin-walled acrylic inner sleeve that fits inside the sampler and is removed after the sampling operation. The inner sleeve contains two 90 degree openings cut in the sleeve wall which may be about 5 cm apart longitudinally. During the sampling operation, the openings are filled with plastic inserts. Afterwards, the inserts are replaced by tensiometers consisting of capillary barriers mounted in acrylic plastic curved to fit the sample over a 90 degree segment of its surface at the sleeve wall openings.

The inner sample sleeve should have an internal diameter of about 2.5 - 5 cm, the exact diameter depending upon the strength of the source used for gamma attenuation

measurements to obtain the water saturation. It should be about 13 cm in length, allowing about 4 cm of sample length beyond each of the tensiometers.

When the sleeve containing a sample is removed from the sampler, it is first dried in a vacuum oven at not more than 70°C. After drying, the dry weight of the sample is determined. This, along with the particle density of the soil and volume of the cylinder, permits calculation of the porosity, ϕ .

Figure I-4 illustrates schematically the apparatus used to evaluate the capillary properties of the soil core. The sleeve containing the sample is placed on a saturated capillary barrier that is mounted on an acrylic end plate to which a siphon tube is attached. Initially, water in the capillary barrier is maintained at a negative pressure such that imbibition into the dry sample will proceed at a negligible rate. Good contact between the sample and the barrier is important. It is also important to use a barrier which has a minimum impedance, but with an air-entry value permitting desaturation of the sample without air getting into the outflow siphon. An unconsolidated barrier consisting of very fine sand resting on several thin layers of progressively coarser sand has proved ideal for many soil types. Good contact between sample and barrier is more easily obtained with unconsolidated barriers than with rigid plates such as fritted glass or ceramic.

A beam of gamma rays is directed at the column. The gamma rays are collimated so that they pass through a thin longitudinal slice of the sample midway between the two tensiometers. An Americium source (about 100 mc) is ideal for this purpose provided the column diameter is not more than about 4 cm. The gamma count is then recorded for the dry state.

Next, the tensiometer barriers are placed in contact with the soil and held by a device such as rubber bands so that they will remain in contact as the soil swells and shrinks during imbibition and drainage. The tensiometer barriers and leads should be presaturated and connected to pressure transducers before being placed in contact with the soil. It should be possible, however, for air to enter the sample in the vicinity of the tensiometers.

The soil is then allowed to imbibe water through the bottom barrier to its maximum capacity or until the capillary pressure is nearly zero. The maximum water saturation

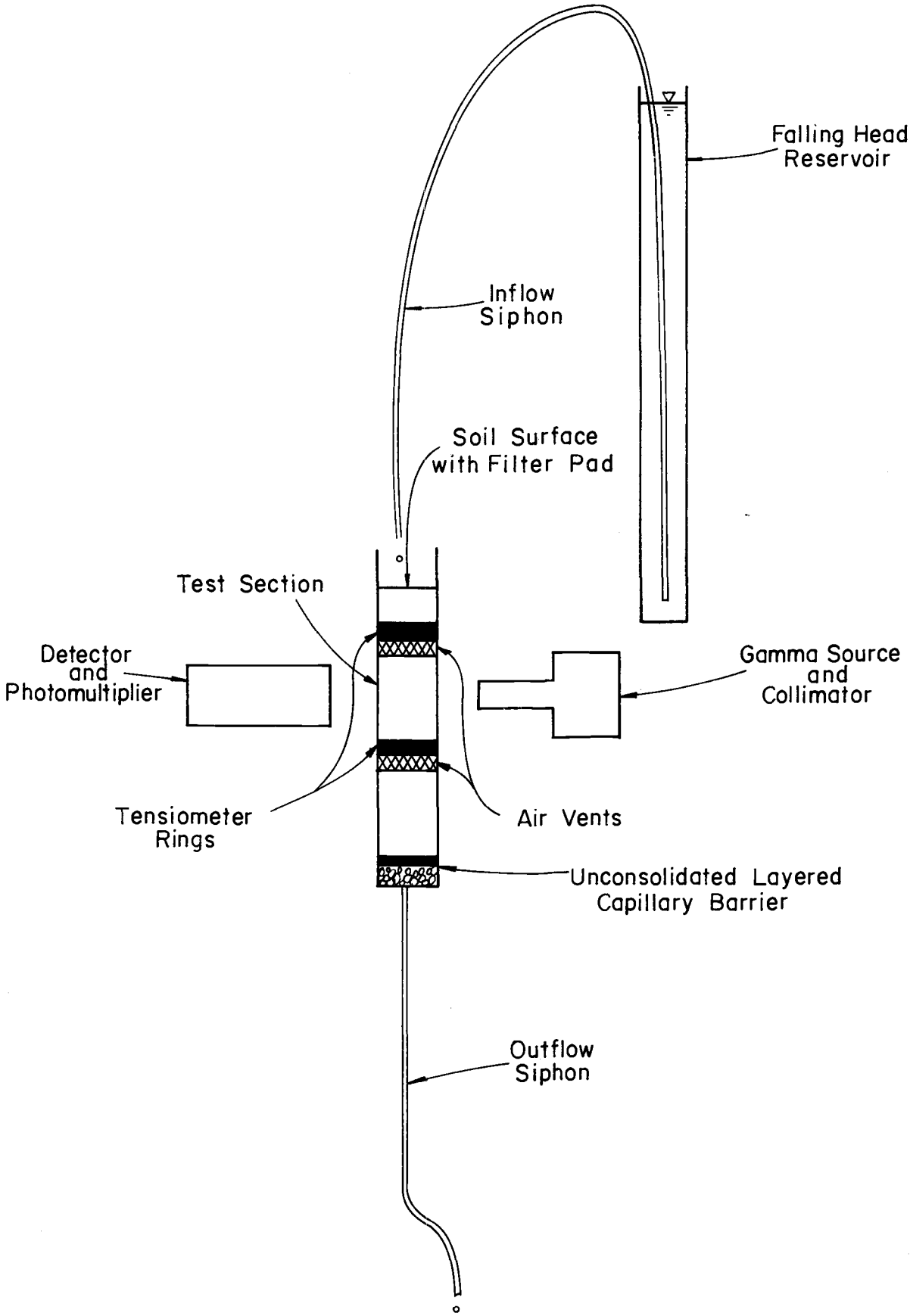

Figure I-4. Schematic diagram of equipment for laboratory evaluation of soil properties.

is considered to be that which is obtained about 30 minutes after the top of the sample is entirely wet and the rate of increase of water saturation becomes very slow. It is useful to record the volume of water imbibed by the sample so that the value of the maximum water content can be computed. For this purpose, it is important to keep the pressure of water in the barrier slightly less than atmospheric so that no water is lost from the air vents.

After the sample has reached maximum saturation, the gamma count rate is again determined. The difference in count rate between the dry state and maximum saturation respectively provides the basis for computing the saturation at intermediate saturations. It is desirable to relate the count rate through the sample to the count rate through a standard absorber for each measurement in order to correct for drift of the gamma system due to a variety of causes.

In some cases, the air entry pressure of the sample may be sufficiently small that the top of the sample will not reach its maximum saturation by imbibition from a barrier at zero pressure, since the sample is about 13 cm in length. In that case, the maximum saturation will be obtained only after downward flow through the sample has been established. In any case, the establishment of downward flow through the sample is the next step.

Inflow to the top of the sample is provided by a siphon from a reservoir with a falling head. The reservoir consists of a vertical acrylic tube with a diameter that depends on the maximum conductivity of the soil being investigated. A tube with a diameter in the range of 3-5 cm is suitable for many soils. A larger diameter might be preferable for very permeable sands. The length of the tube should be about 1-2 meters.

The reservoir is positioned so that the bottom is at least slightly below the level of the sample surface. At the beginning of the experiment, the reservoir is filled. A small diameter tube is used to siphon water from the reservoir to the top of the sample, which is covered with a pad of blotting paper to buffer the discrete drops of water. The top of the sample sleeve is fitted with a short empty extension to retain excess water during the initial adjustment period when the inflow rate may momentarily exceed the outflow rate.

The siphon tube is selected of such diameter and length that the rate of inflow will equal the outflow when the hydraulic gradient is unity and the reservoir is full. This hydraulic gradient is obtained by adjusting the level of the outflow siphon. Nylon tubes are suitable for the siphons since they minimize the accumulation of air by diffusion through the tube walls. Air bubbles may seriously affect the operation of siphons especially at very small flow rates. For this reason, it is also important to de-aerate the water used in the reservoir.

The reservoir should preferably be filled with drainage water from the site where the sample was obtained. The water should be filtered as well as de-aerated before filling the reservoir. This procedure is followed so that the degree of swelling of the clay minerals will be similar to that which occurs in the field.

It is necessary to provide a means for measuring both the inflow and outflow independently. This can be accomplished by calibrating the drops from the inflow and outflow siphons. It is convenient to provide tips for both siphons which are cut from the same section of tubing so that the drop size from the two siphons will be identical. It has been found that drop size will vary depending on the angle at which the tip is oriented. It is good practice to always orient the tips downward. The drop size will also vary somewhat with the flow rate so that one should calibrate the drop size at intervals of time as the flow rate decreases.

The inflow drop rate will start decreasing immediately, of course, because the level of water in the reservoir falls continuously. In the beginning, however, the outflow may remain constant or possibly even increase slightly if the water piles up at the surface of the sample. During this period, only the outflow rate needs to be recorded since the sample is not desaturating. This rate, along with the measured hydraulic gradient is used to compute $K_{1.0}$. It is good practice to obtain several measurements of $K_{1.0}$ so that a valid average can be determined.

As soon as the inflow drop rate decreases sufficiently to permit a negative water pressure to develop at the top of the sample, the hydraulic gradient within the saturated portion will decrease abruptly. It will be necessary to lower the outflow siphon to maintain the hydraulic gradient close to unity during this period, so that when the sample begins to desaturate, it will desaturate more or less evenly from top to bottom. The sample cannot desaturate completely evenly, of course, because the air

can enter only at the top of the sample and around the tensiometers. Furthermore, it is not likely that the sample will be completely homogeneous.

It is necessary for the operator to work rather quickly during the period of initial desaturation to obtain the necessary measurements of the gamma count rate, inflow, outflow, and the two tensiometer readings. In fact, during this period, it may be necessary to have two operators.

As soon as the sample has undergone significant desaturation, the outflow siphon is lowered to its final position. This position should be such as to create a negative pressure at the bottom of the sample at least equal to the maximum negative pressure for which one needs to measure the water saturation. For most agricultural soils, this will usually not be greater than 150-200 cm of water.

Lowering the outflow siphon will affect the tensiometer readings only slightly if the bottom capillary barrier is, at least, 4-5 cm below the bottom tensiometer, and if the sample has already reached the stage at which a continuous air phase exists. Thereafter, the tensiometer readings will be affected only by the inflow rate and the homogeniety of the sample, not by the position of the outflow siphon.

The hydraulic gradient within the test section will automatically adjust itself to a value close to 1.0 provided the sample is relatively homogeneous. A greater negative pressure will be measured at the tensiometer where the soil has the smaller pores. Thus, the hydraulic gradient may be greater or less than 1.0 depending upon where the smaller pore-size exists in the sample. In any case, it will not be possible to adjust the hydraulic gradient to 1.0 by changing the level of the outflow siphon. This level should remain the same throughout the remainder of the experiment. For non-homogeneous samples, it will be necessary to assign a value of conductivity to the average negative pressure measured at the two tensiometers. This procedure should give satisfactory results provided the difference in pressure head is not more than 1-2 cm of water.

After the flow rate has decreased to about 1/2 to 1/3 of its initial value, the experiment will usually proceed smoothly and one may obtain data at intervals of time as short or as long as desired in order to define the necessary functional relationships. Ordinarily, it is possible to obtain all the conductivity data necessary in

a single 8-hour work day. It is usually desirable to allow the column to drain over night to obtain a saturation corresponding to a higher negative pressure so that a better definition of the residual saturation is obtained.

It is obvious that the procedure described, although it provides a direct measurement of the variables involved, is not a "steady state" method. The sample drains continuously and, therefore, one might describe the procedure as a "pseudo" steady state or, more properly, a dynamic method.

Although one might question the rigor of the procedure, it has many advantages over all direct measuring procedures previously employed. The major advantage is that the experiment is finished before trouble is encountered from air collecting in the outflow siphon, capillary barriers becoming plugged, algae accumulating in the soil sample, etc. Also, as compared to steady state methods, the tendency for the sample to inadvertently jump to an imbibition cycle (at some time during the experiment) is avoided. Consequently, the results are more likely to be consistent and reproducible than those obtained by other methods. Furthermore, the results are obtained for conditions similar to those existing during drainage of the soil profile in the field.

The curves of K vs. p_c obtained by the method described are similar to those obtained by steady state methods except in the range of initial desaturation. In this range the curves differ in that with the dynamic method, the values of K and S both remain unchanged until p_c exceeds p_b at which time K and S are reduced abruptly. During this abrupt desaturation, the values of p_c may actually decrease slightly; that is, pressure hysteresis takes place. A typical log-log plot of K vs. p_c is shown in Figure I-5.

An explanation for the pressure hysteresis is that under dynamic conditions, air will have to replace water by bulk flow. There is not time for significant air to enter by diffusion or to escape from solution. Consequently, no significant desaturation can take place until the air entry pressure of the sample is reached. Once a continuous air phase exists, however, air is free to enter numerous larger pore spaces that may previously have been isolated by water. When these start to empty, the value of p_c decreases measurably. The decrease is more noticeable for soils having a large range of pore sizes. The decrease for sands having a very uniform pore size may be very small.

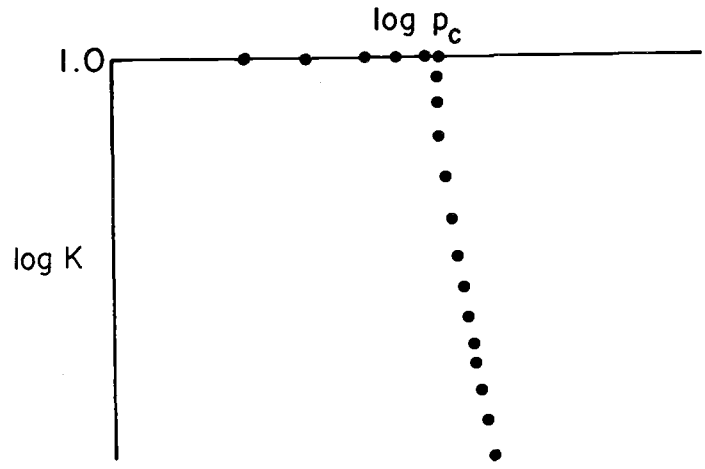

Figure I-5. Typical experimental relation between hydraulic conductivity and capillary pressure.

During the period when the value of p_c is actually decreasing, the value of K continues to decrease rapidly, but accurate measurements are not possible because the water pressure changes too rapidly. By the time p_c has resumed its upward climb, the value of K will have dropped to about $.5\ K_{1.0}$. Therefore, a typical curve obtained by the dynamic method indicates a constant K equal to $K_{1.0}$ over a range of p_c less than or equal to the air entry pressure. At this pressure the value of K drops abruptly to about 50 percent of $K_{1.0}$, usually without any change of p_c that can be accurately recorded.

This type of behavior is clearly not in accordance with predictions based upon present theories of soil water "diffusivity." It can be understood only by a consideration of flow of the air phase as well as the water. The resistance to the entrance of air is significant during a laboratory drainage situation and there is no reason to suppose that this is not also the case in the field. Nevertheless, the measured curves of K as a function of p_c usually can be described with reasonable accuracy by the empirical approximation of Brooks and Corey, that is,

$$\frac{K}{K_{1.0}} = \left(\frac{p_b}{p_c}\right)^{\eta} \qquad \text{(I-6)}$$

for $p_c \geq p_b$, and

$$\frac{K}{K_{1.0}} = 1.0 \qquad \text{(I-7)}$$

for $p_c \leq p_b$. However, the approximation may not be sufficiently accurate for extremely heterogeneous soils.

At the end of the experiment described above, data are available for the calculation of all of the parameters listed at the beginning of the section. The value of λ may be approximated by the relationship of Brooks and Corey (1964)(I-8), that is,

$$\lambda = \frac{\eta - 2}{3} \quad , \qquad \text{(I-9)}$$

or it may be obtained directly from plots of the $\log S_e$ as a function of $\log p_c$. Such plots require the determination of S_r which also is needed for the determination of the "drainable" porosity.

Brooks and Corey (1964) and Laliberte et al (1968) have described a trial and error graphical method for determining S_r such that the relationship between $\log S_e$ and $\log p_c$ is most nearly linear. However, a more convenient method of calculating S_r and λ from data for S as a function of p_c has been developed recently by Stauffer and Corey. The method employs a Fortran program (shown in Appendix C) to do more or less the same thing as the graphical procedure. This program computes S_r , p_b , η , λ and a correlation coefficient for the fit of the actual data with the empirical function computed. The data input for this program include values of saturation corresponding to values of p_c greater than an estimated value of p_b . Instructions for using the program are included in Appendix C.

I.3 CAPILLARY PROPERTIES OF FIELD SOILS by D. W. Fitzsimmons

The importance of the capillary region to water movement is emphasized in other sections of this paper. However, before these principles can be applied to field problems, the necessary capillary parameters must be evaluated for the soil *in situ*. Relations between water pressure and soil water content have been measured routinely since the conception of the tensiometer. Although these data are not obtained without questionable accuracy, nor without difficulty, it will be assumed that the water content-pressure function can be measured.

Measurement of flow characteristics, however, is not so readily dismissed. Many techniques have been devised for estimating the saturated hydraulic conductivity, ranging from infiltrometer tests through various groundwater pumping schemes, depending on the region of the profile of interest. Several attempts have been made to develop methods for measuring unsaturated hydraulic conductivity *in situ*. So far, these attempts have met with limited success due to difficulties encountered in making precise measurements under field conditions. Laboratory methods such as described in the previous section are of limited use, due in part to the uncertainty of obtaining samples which are actually undisturbed.

Because of the difficulties involved in obtaining hydraulic conductivity data either in the field or in the laboratory numerous attempts have been made to relate the hydraulic conductivity of a soil to other soil characteristics which are easier to measure. Most methods of calculating hydraulic conductivity do not work well for a range of soil types. One method seems to work quite well for one type of soil while another works well for a different soil. Some investigators have had to use factors of twenty or more in order to match calculated hydraulic conductivities with experimental values for some types of soil.

Relating the hydraulic conductivity to desaturation characteristics appears to be the most promising of these methods. Rose (1949), Burdine (1953), Millington and Quirk (1961), Brooks and Corey (1964) and Brutsaert (1968) are among those who have developed equations for calculating the hydraulic conductivity from desaturation data.

The study reported here describes a method for calculating unsaturated hydraulic conductivity of field soils from the desaturation characteristics of disturbed samples of the same soil.

I.3.1 BASIC EQUATIONS

Carman (1937) modified the Kozeny (1927) equation to obtain an equation for the permeability of a soil which can be expressed as

$$k = \frac{R^2 \phi S}{cT} \tag{I-10}$$

where R is the hydraulic radius of a pore, S is the saturation, ϕ is the porosity, c is a shape factor and T is a tortuosity factor. Assuming that the pores are cylindrical, the hydraulic radius, R, of a pore is $r/2$, where r is the radius of the pore. Defining relative permeability, $k.$, as $k/k_{1.0}$ where k is the permeability at any given saturation and $k_{1.0}$ is the saturated permeability of the soil (permeability when $S = 1$), Equation (I-10) becomes

$$k. = \frac{(r)_S^2 \phi S/cT_S}{(r)_{1.0}^2 \phi/cT_{1.0}} \quad . \tag{I-11}$$

According to Burdine (1953), the average value of r^2 should be used for porous media, and $T_{1.0}/T_S$ can be expressed as

$$\frac{T_{1.0}}{T_S} = \left[\frac{S-S_r}{1-S_r}\right]^2 \tag{I-12}$$

where S_r is the residual saturation of the soil as defined by Brooks and Corey (1964). Using Burdine's work, Equation (I-11) can be expressed as

$$k. = \left[\frac{S\bar{r}_S^2}{\bar{r}_{1.0}^2}\right]^2 \tag{I-13}$$

where $\bar{r}^2$ is the average value of r^2 for all pores filled with water at saturation, S. Although Equation (I-13) is presented in terms of permeability, it is equally adaptable to calculating hydraulic conductivity, since it represents the value relative to its saturated value.

Equation (I-13) can be used to calculate the unsaturated hydraulic conductivity of a soil from its desaturation characteristics. The saturation values taken directly from the capillary pressure head-desaturation relationship for the soil and the values of $\bar{r}^2$ can be calculated using the equation presented in the following paragraphs.

A computer program for carrying out these calculations has been presented by Sinclair (1973).

The incremental change in the volume of water in the pores of a soil associated with an incremental change in saturation can be expressed as

$$dV = \phi V_s \, dS \tag{I-14}$$

where V_s is the bulk volume of the soil. The number of pores, F , which desaturate or saturate due to an incremental change in saturation can be expressed as

$$F = \frac{\phi V_s \gamma}{4(2\sigma) \pi r^2} \frac{dS}{d(\frac{1}{p_c/\gamma})} \tag{I-15}$$

where γ is the specific weight of water, σ is the surface tension of water and $d(\frac{1}{p_c/\gamma})$ is the incremental change in the reciprocal of the capillary pressure head corresponding to a given incremental change in saturation. The values of dS and $d(\frac{1}{p_c/\gamma})$ can be obtained from a capillary pressure head saturation relationship for the soil. The rest of the values are constant for a given soil and fluid.

A typical capillary pressure head-saturation relationship is shown in Figure I-6. This curve can be divided, as shown, into arbitrary increments of capillary pressure head $(p_1/\gamma, p_2/\gamma, \ldots\ldots, p_n/\gamma)$ and corresponding increments of saturation $(S_1, S_2, \ldots\ldots, S_n)$. The average capillary pressure head (PA) and saturation (SA) for each increment are

$$PA_{n-1} = (p_{n-1} + p_n)/2 \tag{I-16}$$

and

$$SA_{n-1} = (S_{n-1} + S_n)/2 \, . \tag{I-17}$$

The average radius of the pores corresponding to the average capillary pressure head for each increment can be calculated using the equation

$$RA_{n-1} = (2 \sigma \cos \alpha)/PA_{n-1} \tag{I-18}$$

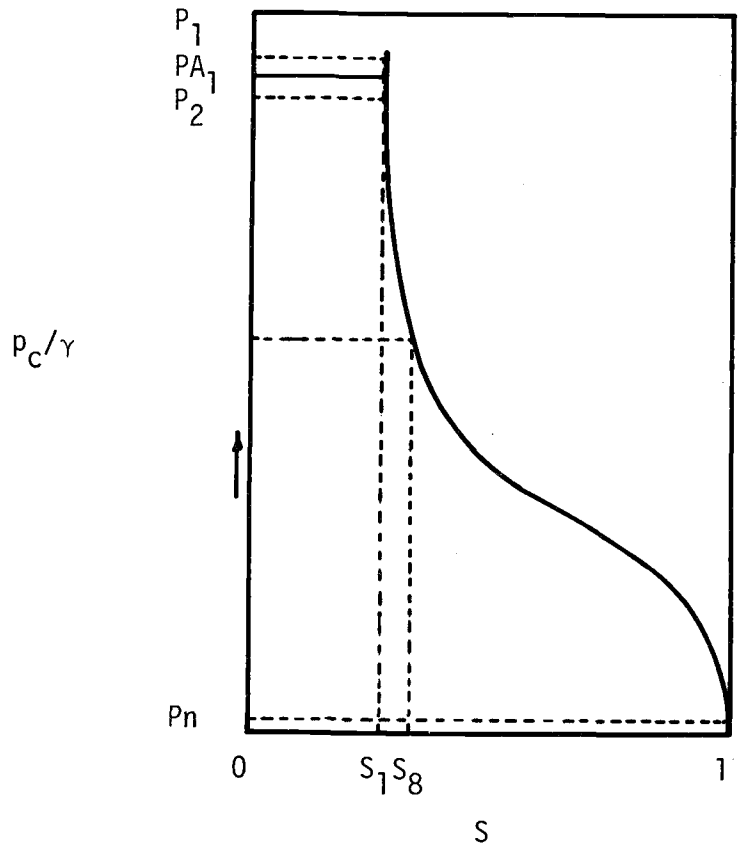

Figure I-6. Typical capillary pressure head-saturation curve showing panel points for calculating distribution of pore sizes.

where α is the contact angle of water against the wall of a pore. These values are used in Equation (I-15) to determine how many pores in an increment would desaturate for a given incremental change in saturation. A hypothetical curve showing the number of pores, F , plotted versus the average radius, RA , of the pores in each panel is shown in Figure I-7. This plot shows the pore size distribution of the soil and is used to determine the values of $\bar{r}^2$ to be used in Equation (I-13).

Before the values of $\bar{r}^2$ can be determined, the pore size distribution function must be normalized so that it will represent a probability density function. This can be done by dividing each F_{n-1} by the area under the curve in Figure I-7. The area under the curve (FNORM) can be calculated using the trapezoidal formula on each panel and summing the areas of each panel; that is,

$$FNORM = \sum_{n=1}^{n=ND-1} (F_{n+1} + F_n)(RA_{n+1} - RA_n)/2 \qquad (I\text{-}19)$$

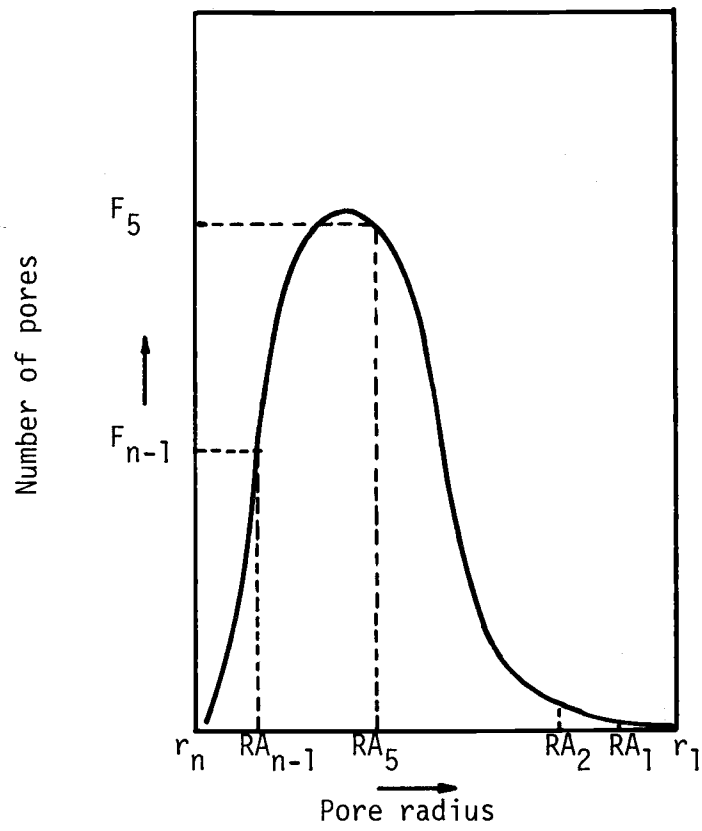

Figure I-7. Hypothetical pore size distribution curve showing the panel points calculated from the saturation curve.

where ND is the number of increments chosen to divide the curve in Figure I-6.

The average value of $\bar{r}^2$ can be calculated using the formula

$$\bar{r}_a^2 = \sum_{n=a}^{n=ND-1} \frac{[(RA_n^2)(F_n) + (RA_{n+1}^2)(F_{n+1})](RA_{n+1}-RA_n)}{2(FNORM)} \qquad (I\text{-}20)$$

where a is the subscript of the capillary pressure head at which the hydraulic conductivity is to be calculated using Equation (I-13).

I.3.2 LABORATORY EXPERIMENTS

Experimental data were gathered for seven agricultural soils. Both hydraulic conductivity and desaturation data were obtained for undisturbed samples of each soil. Desaturation data were also obtained for disturbed samples of these soils. These data

made it possible to calculate the hydraulic conductivity of the soils from the desaturation characteristics of both disturbed and undisturbed samples of a soil, and to compare these calculated values with experimentally determined values.

Undisturbed cores of the field soils were taken with a soil sampler developed by Hayden and Heineman (1968). This is a double tube, split sleeve type sampler which takes 7.5 cm diameter cores up to 23 cm in length.

Once the cores were obtained, they were encased in heat shrinkable plastic tubing for protection and to prevent fluid from flowing along the walls of the samples during the hydraulic conductivity tests.

Once the samples were prepared, the relation between hydraulic conductivity and capillary pressure head was determined using a technique similar to that of Brooks and Corey (1964). Saturation-capillary pressure head data were obtained by a technique similar to that described by Sinclair (1970).

Desaturation data were obtained from disturbed soil samples in a similar manner. Soil from undisturbed samples was crumbled carefully to avoid destroying the small peds, then passed through a No. 10 sieve. The soil was then placed in a sample container and packed by the dropping method described by Reeve and Brooks (1953).

These desaturation data were used, with Equations (I-13) and (I-15) to calculate the p_c/γ - K relationships for the seven soils. The calculated values are compared with corresponding relationships obtained from undisturbed cores.

A typical p_c/γ - K relationship for a uniform porous medium, such as glass beads, is shown in Figure I-8. The features of such a relationship are discussed in detail in a previous section of this paper.

Experimental and calculated p_c/γ - K relationships for the Ritz silt loam are compared in Figure I-9. The experimental data were obtained for two different samples of the same soil. The fact that the data plot as essentially one curve is an indication that the method used to determine hydraulic conductivity gives reproducible results.

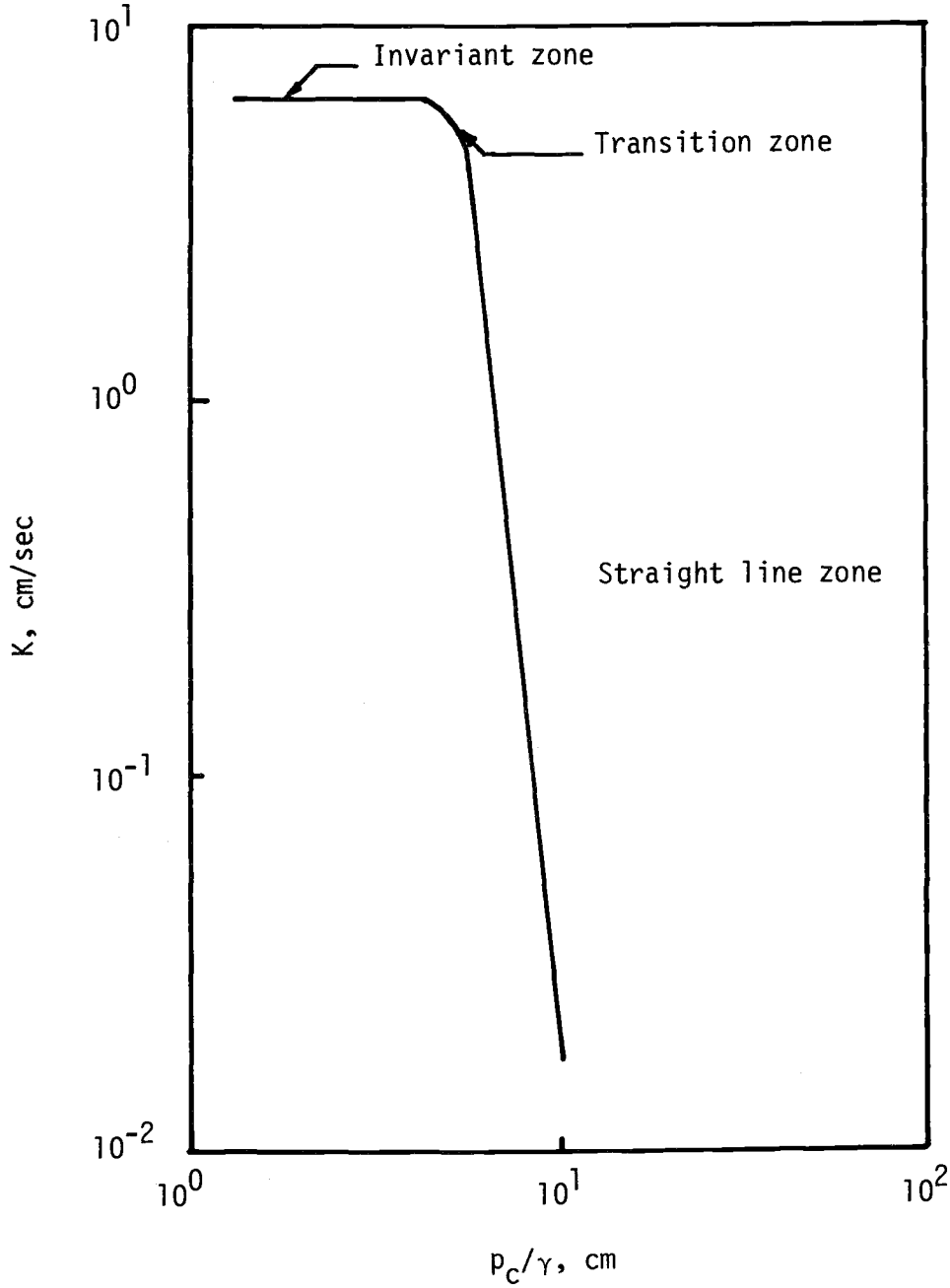

Figure I-8. Typical capillary pressure head-hydraulic conductivity relationship for uniform porous media.

Referring to Figure I-9, it appears that the saturated hydraulic conductivity of this soil is about .001 cm/sec and is essentially constant until a capillary pressure head of about 40 cm is reached. Compared to the p_c/γ - K relationship for a uniform soil, the experimental relationship has a long transition zone and a poorly defined straight-line zone. The long transition zone and continuously curving plot of the data points at the higher capillary pressure heads seem to be characteristic of undisturbed agricultural soils. This is the reason that some theories developed

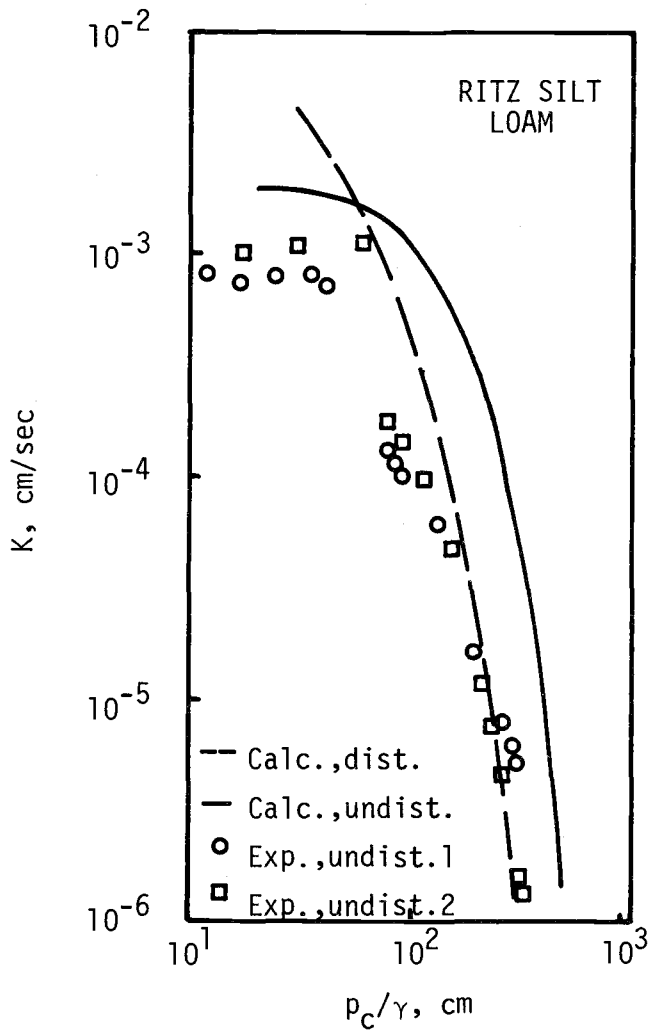

Figure I-9. Capillary pressure head hydraulic conductivity relationships for Ritz silt loam soil (calc.-calculated value, exp.-experimental value, dist.-disturbed sample, undist.-undisturbed core)

for uniform materials such as glass beads do not predict the hydraulic characteristics of agricultural soils very well.

The p_c/γ - K relationship calculated using the p_c/γ - S data for the undisturbed sample of this soil (solid line) seems to predict the saturated hydraulic conductivity of this soil reasonably well. As pointed out above, it also predicts the shape of the experimental relationship quite well. It does not however, predict the hydraulic conductivity well at the higher values of capillary pressure head.

The p_c/γ - K relationship calculated using the p_c/γ - S data for the disturbed soil samples (dashed line) predicts the experimental hydraulic conductivity values quite

well at higher values of capillary pressure head. It does not do a good job, though, of predicting the saturated permeability of this soil. Even so, either of the calculated p_c/γ - K relationships shown in Figure I-9 would be quite useful in making unsaturated flow calculations for this soil. For making flow estimates, the ease of obtaining these p_c/γ - K relationships might easily justify their use.

If more accurate flow estimates are needed, the agreement between the calculated and experimental relationships can be improved by scaling. In this study it was found that scaling the relationships by dividing the hydraulic conductivity by the saturated hydraulic conductivity and the capillary pressure head by the bubbling pressure head of the soil produced the best results. Scaled p_c/γ - K relationships for the Ritz silt loam soil are shown in Figure I-10. As can be seen, the calculated scaled p_c/γ - K relationship for the disturbed soil samples fits the scaled experimental data just as well as the p_c/γ - K relationship calculated for the undisturbed sample.

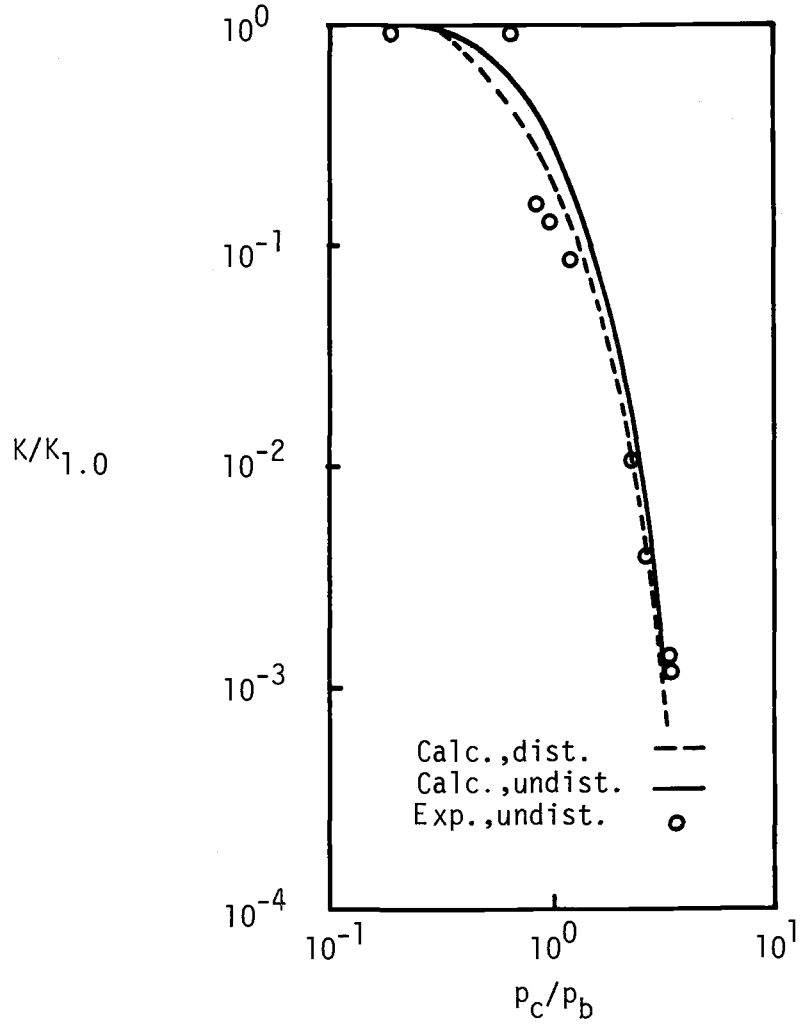

Figure I-10. Scaled capillary pressure head-relative hydraulic conductivity relationships for Ritz silt loam soil.

Thus it appears that this method provides a means of calculating the capillary properties if bubbling pressure head and saturated hydraulic conductivity can be measured in the field.

Once these two parameters are known, the p_c/γ - K relationship for the field soil can be determined by multiplying scaled values by the scaling parameter. The time required to measure the bubbling pressure head and saturated hydraulic conductivity of a soil in the field is partially offset by the fact that only the p_c/γ - S relationship for disturbed samples of the soil is needed to calculate the p_c/γ - K relationship for the field soil.

Scaled capillary pressure head-hydraulic conductivity relationships for the other five soils are presented in Figure I-11. In general, the results obtained for these soils were essentially the same as those for the Ritz silt loam soil.

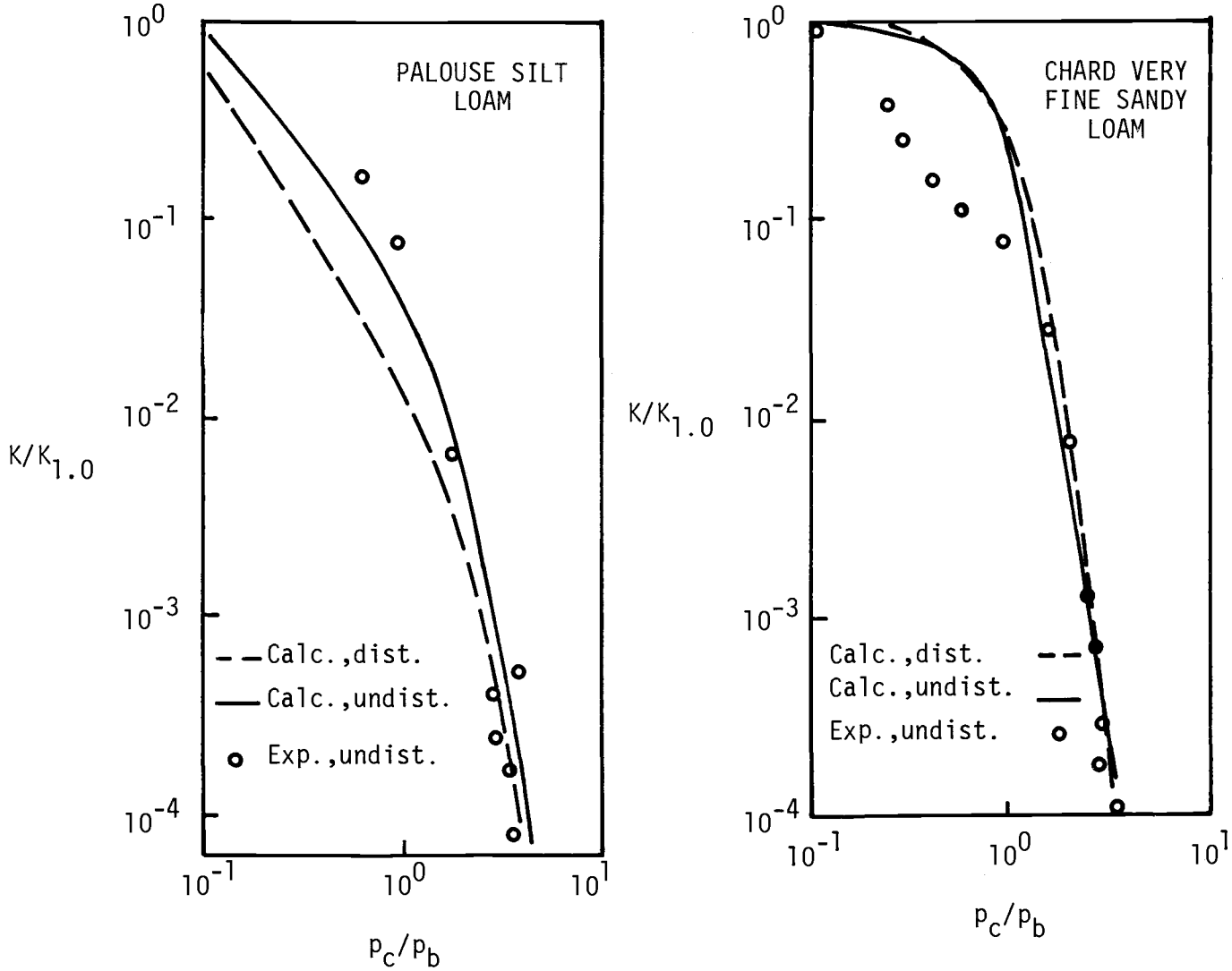

Figure I-11. Scaled capillary pressure head-hydraulic conductivity relationships for five soils.

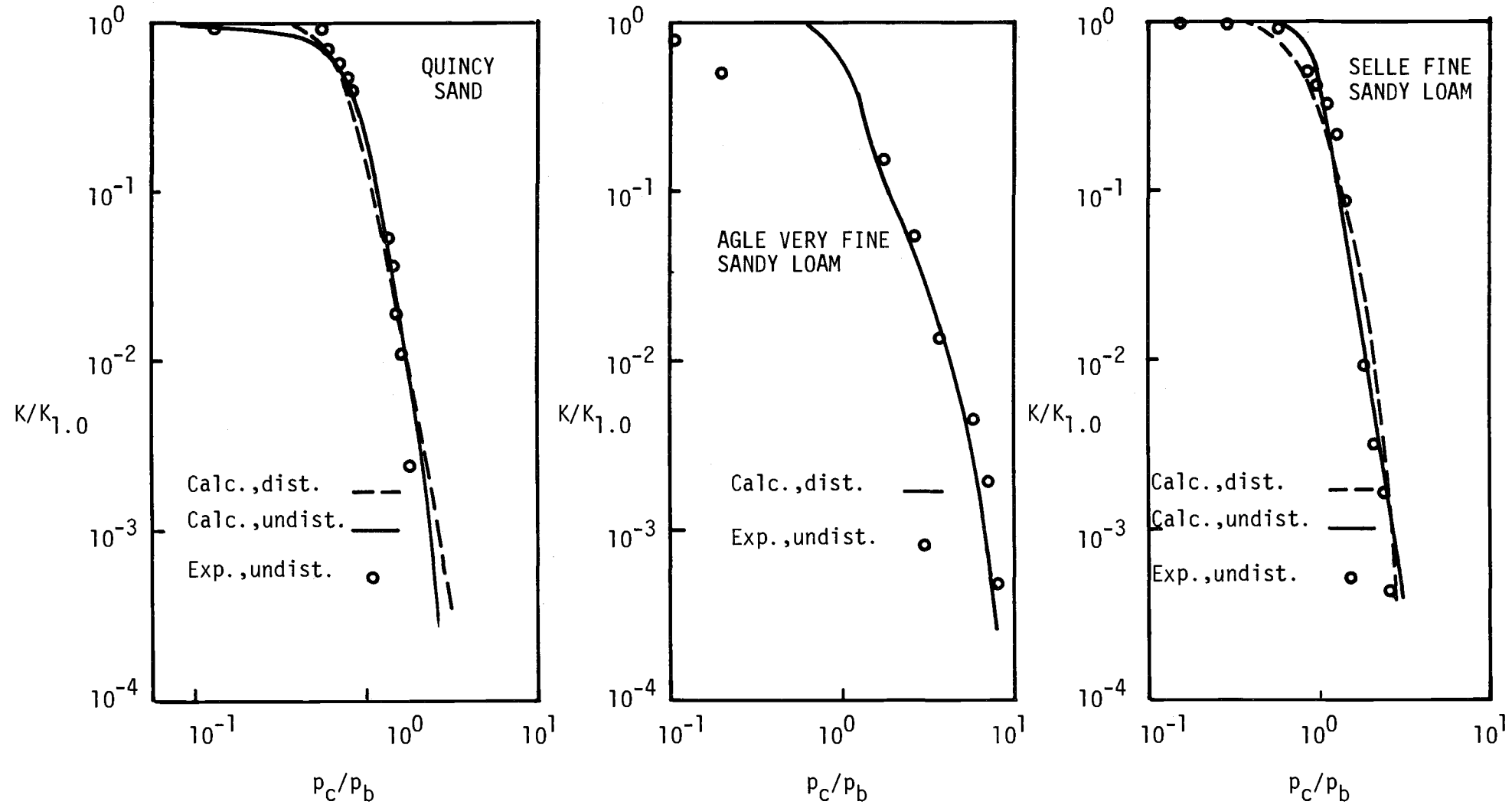

Figure I-11. (Continued) Scaled capillary pressure head-hydraulic conductivity relationships for five soils.

It should be noted that calculated p_c/γ - K relationships presented in Figure I-12 for Chard non-calcareous fine sandy loam soil do not fit the experimental p_c/γ - K relationship for this soil very well. The slopes of the calculated p_c/γ - K relationships are not nearly as steep as the slope of the experimental relationship apparently because this soil is anisotropic. Scaled p_c/γ - K relationships have not been presented for this soil since the methods of calculating these relationships are apparently valid only for isotropic soils.

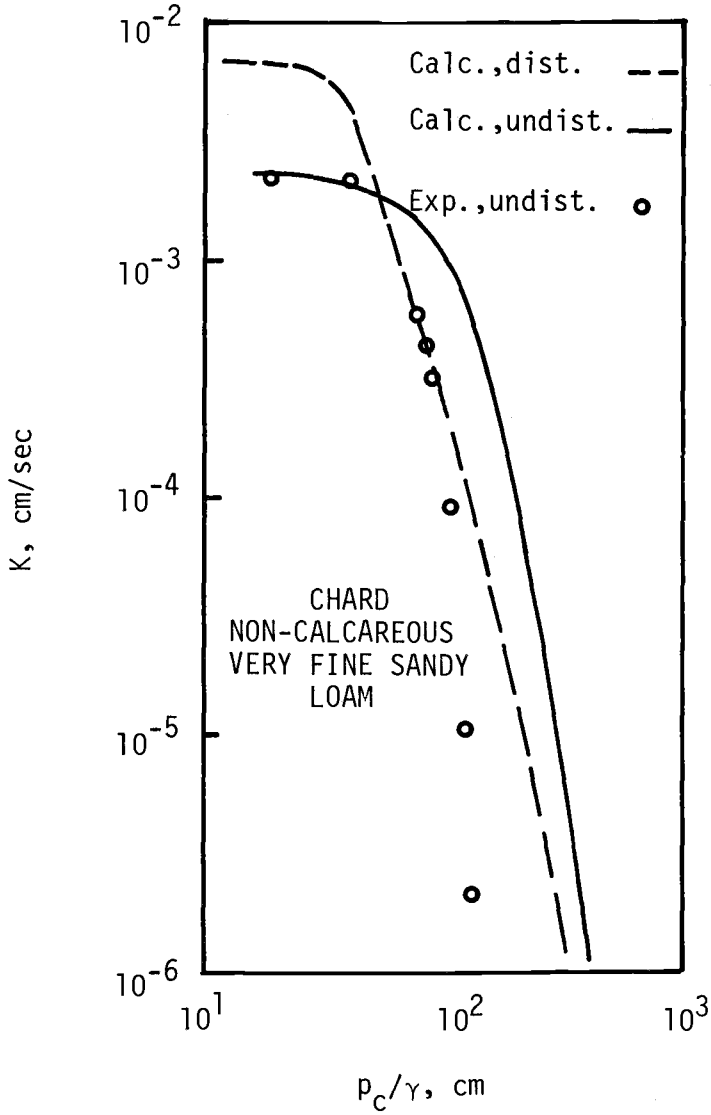

Figure I-12. Capillary pressure head-hydraulic conductivity relationships for the Chard non-calcareous very fine sandy loam.

SECTION II.

MODELING CAPILLARY FLOW SYSTEMS

The objective of model construction, whether physical or mathematical, is to predict the performance of a full-sized system without the expense and time required to observe the response of the full-sized system to the range of stimuli that may be expected to occur naturally. Such models must necessarily be simplifications of nature's system in order to quantify the parameters considered pertinent to the desired results.

Whenever one constructs a physical model for observing fluid flow in porous media, it is immediately obvious that the geometric dimensions of the model must be somehow related to those of the prototype if the model is to behave similarly. Yet, mathematical models are very often constructed without regard to similitude, or formulation in terms of dimensionless parameters, which allows extension of results to prototypes of similar geometry.

This section describes procedures for satisfying criteria of similitude in cases of both saturated and partially saturated flow, and describes the dimensionless variables necessary for consideration of the effects of the partially saturated region.

II.1 SIMILITUDE CRITERIA by R. H. Brooks

The literature is replete with the solution of various boundary value problems that have application only to one prototype situation. Some of these solutions were obtained with mathematical models while others were obtained using a physical model. Extrapolation of results to other specific conditions are virtually impossible because the solutions have not been presented in terms of scaled variables or scaled boundaries that satisfy similarity criteria.

By satisfying similarity criteria, one not only may extend the results to a similar prototype, but generalizations can be made that provide an insight into the physical nature of the performance of the system. Without similar criteria it becomes nearly impossible to make generalized conclusions.

There are two generally accepted methods for establishing criteria of similitude. The first is usually called dimensional analysis and is commonly used by hydraulic engineers. The second method is called inspectional analysis and requires that the differential equation describing the physical processes be known.

The purpose of this section is not to review or discuss the various methods of establishing similitude requirements, but rather to apply criteria that have been previously developed to the flow of fluids in porous media.

The similitude requirements proposed by Brooks and Corey (1964) will be reviewed and applied to the mathematical model described herein. They found that by applying the method of inspectional analysis to the general flow equation of one fluid moving in a homogeneous medium, a set of similitude requirements could be established. They discovered that if these requirements were satisfied, the solutions of the differential equations yielded identical particular solutions in terms of scaled variables.

The basic equation for the flow of fluids in porous media is obtained by combining Darcy's Law with the continuity equation. The basic units in this equation are force, length, and time. The properties of the fluid and the medium can be defined in terms of these three basic units. For example, permeability can be expressed in terms of length.

If the basic equation is written in terms of energy per unit volume, then the equation may be appropriately scaled by using a standard unit of energy that contains standard units of force and length. Since hydraulic conductivity may be a variable, then a standard unit of hydraulic conductivity must be chosen also.

The basic flow equation, Darcy's Law, may be expressed in terms of energy per unit volume as

$$q = \frac{k}{\mu} \nabla(-p_c + \gamma z) \qquad \text{(II-1)}$$

where q is the volumetric flux per unit area and μ is fluid dynamic viscosity. The standard units of energy and hydraulic conductivity are chosen for the present as p_o and K_o respectively. This standard energy unit is a standard pressure. The physical significance of these terms will be pointed out later in the development. By dividing each energy term by the standard energy and hydraulic conductivity by the standard hydraulic conductivity, the standard units for the other terms in the equation may be deduced. Thus, Equation (II-1) becomes

$$q/K_o = \frac{kp_o}{K_o\mu} \nabla(-p_c/p_o + \gamma z/p_o) \qquad \text{(II-2)}$$

since $k = \frac{K\mu}{\gamma}$, then Equation (II-2) may be expressed as

$$q/K_o = \frac{K}{K_o} \frac{(p_o)}{(\gamma)} \nabla(-\frac{p_c}{p_o} + \frac{\gamma z}{p_o}) \; . \qquad \text{(II-3)}$$

The standard unit of length for the gradient, ∇ , must be p_o/γ and the standard flux, q , must be K_o , the saturated hydraulic conductivity.

Using simplified notation and rewriting, Equation (II-3) becomes

$$q. = K. \nabla.(-p. + Z.) \qquad \text{(II-4)}$$

which is identical in form to Equation (II-1). The dot notation is defined as:

$q.$ = scaled flux, q/K_o ,

$\nabla.$ = scaled gradient, $L_o\nabla$,

$p.$ = scaled pressure, p_c/p_o ,

$Z.$ = scaled elevation above an arbitrary datum, z/L_o , and L_o is the standard length, p_o/γ .

Obviously, if one chooses a standard pressure as the standard unit of energy, the characteristic length for similitude must be p_o/γ or some characteristic pressure head.

For saturated media, K_o is a constant and the standard pressure head p_o/γ may be any characteristic pressure head related to the flow geometry or any characteristic length. The properties of the medium do not become part of the similitude criteria. As long as the medium is always saturated, the only similitude criteria that must be satisfied are those for geometric similarity, i.e.,

1. The macroscopic boundaries of the model must have a shape and orientation similar to the prototype.
2. The size of the model must be such that the ratio of all corresponding lengths must be the same for model and prototype,

$$(\frac{L}{D})_m = (\frac{L}{D})_p \qquad \text{(II-5)}$$

where L and D are any arbitrary length dimensions and the subscripts p and m denote prototype and model respectively.

If at any time in the flow system the medium becomes partially saturated so that

$$K = f(p_c) \tag{II-6}$$

then a geometric characteristic length is not sufficient for use as a standard pressure head or as a standard length. In other words, for the general case, the standard pressure head and standard permeability cannot be arbitrarily chosen. If the relative flux, $q.$, in Equation (II-4) must be the same for both prototype and model, the functional relationship given by Equation (II-6) must be identical for both model and prototype.

Even though the relationship given by Equation (II-6) is different for wetting and drying of media, the standard units used in Equation (II-6) should be intrinsic media properties and independent of the type of flow. If the standard units for affinity and similarity are to be practical, they should also be measurable properties.

In studies dealing with the drainage of liquids from porous media, Brooks and Corey (1964) found that effective saturation and capillary pressure could be related by a power function. These relationships are described in Section I of this paper.

If the functional relationships given by Brooks and Corey are valid, the bubbling pressure head p_b/γ and the saturated hydraulic conductivity $K_{1.0}$ reduce the functional relationship among the variables to one that is the same for all soils having identical values of λ . Therefore, these two hydraulic properties of porous media logically become the standard pressure head and hydraulic conductivity for satisfying the general similitude and affinity requirements for flow in porous media. The requirements necessary and sufficient for two partially saturated systems to be affine are that the pore size distribution index λ must be the same for two media. Furthermore, similarity criteria will be satisfied if the characteristic or standard length is the bubbling pressure head. In other words, the size of the model must be such that

$$\frac{L_p}{L_m} = \frac{(p_b/\gamma)_p}{(p_b/\gamma)_m} \tag{II-7}$$

and

$$\lambda_m = \lambda_p \ , \tag{II-7}$$

where L is any geometric dimension. Corey, Corey, and Brooks (1965) demonstrated that if the above requirements were satisfied for the drainage cycle, the two systems would be affine on the imbibition cycle as well.

The general scaled differential equation for imbibition or drainage is obtained by combining scaled Darcy's Law with the scaled continuity equation. The continuity equation is scaled in a manner similar to Darcy's Law and in dimensional form it may be written as

$$\text{div}\left(\frac{q}{\phi_e}\right) = - \frac{\partial S.}{\partial t} \tag{II-8}$$

where ϕ_e is effective porosity.

If q is scaled by $K_{1.0}$, t by t_o, and div by p_b/γ, then Equation (II-8) becomes

$$\frac{t_o K_{1.0}}{\phi_e p_b/\gamma} \frac{p_b}{\gamma} \text{ div } \frac{q}{K_{1.0}} = - \frac{\partial S.}{\partial t/t_o} \tag{II-9}$$

or

$$\frac{t_o K_{1.0}}{\phi_e p_b/\gamma} \text{ (div. q.)} = - \frac{\partial S.}{\partial t.} \tag{II-10}$$

where dots designate scaled dimensionless variables. Since Equation (II-10) must be identical in form to Equation (II-8) and must yield identical particular solutions, let

$$\frac{t_o K_{1.0} \gamma}{\phi_e p_b} = 1 \tag{II-11}$$

or

$$t_o = \frac{p_b \phi_e}{\gamma K_{1.0}} \ . \tag{II-12}$$

Thus, for unsteady flow in porous media, the standard time is given by Equation (II-12) and the general scaled equation for flow of a fluid in partially saturated media becomes

$$\text{div.}[K.\nabla.(-p. + Z.)] = \partial S./\partial t. \qquad \text{(II-13)}$$

where the dots designate scaled variables or operators with respect to scaled variables.

The scaled partial differential equation, (II-13), may be rearranged in terms of other dependent variables, e.g., scaled saturation, $S.$, or scaled hydraulic head, H .

Equation (II-13) may be solved using any suitable relationship among saturation, capillary pressure, and permeability provided these variables are scaled with the standard quantities previously mentioned. If the pore size distribution index is known, then the results will have application to other similar boundary conditions having the same pore size distribution index. The relationship among saturation, capillary pressure, and permeability need not be in functional form. They may be a set of tabular values and they may be for either imbibition, drainage, or a combination of various types of flow.

The standard units of permeability, capillary pressure, and saturation are intrinsic properties of the medium and one need not be concerned with the type of function (or tabular data) used to describe the flow process so long as the media properties described by Brooks and Corey are definable. If they cannot be defined, then the solutions are not transferable to other similar conditions.

A summary of the standard units used in Equation (II-13), and other hydraulic properties of media, is given in Table II-1 below. Other standard units may be defined from those given in Table II-1, e.g., diffusivity and hydraulic head.

Table II-1. Standard Units and Hydraulic Properties of Media

Length	$L_o = p_b/\gamma$
Time	$t_o = p_b\phi_e/\gamma K_{1.0}$
Permeability	$K_o = K_{1.0}$
Capillary pressure	$p_o = p_b$
Pore size distribution index	λ
Effective porosity	$\phi_e = \phi(1-S_r)$
Residual saturation	S_r

II.2 VERTICAL DRAINAGE OF SOIL PROFILE by R. H. Brooks

An application of the concept of similarity to drainage of one-dimensional soil profiles is presented to illustrate the usefulness of this concept in studying the drainage characteristics of soils.

If the soil is homogeneous and the soil profile of interest is nowhere saturated, then the combined continuity equation and Darcy's Law may be transformed into a diffusivity-type equation where soil-water content is the only independent variable. The transformation assumes capillary pressure and hydraulic conductivity are single valued functions of water content. The unscaled diffusivity equation for one-dimensional vertical drainage is expressed as

$$\frac{\partial \theta_e}{\partial t} = \frac{\partial}{\partial z} \left[D(\theta_e) \frac{\partial \theta_e}{\partial z} + K \right] \qquad \text{(II-14)}$$

in which the variables θ_e, z, and t are: the effective volumetric water content of the soil, the elevation above a boundary of constant water content such as the capillary fringe, and time, respectively. Effective volumetric water content is defined as

$$\theta_e = \frac{\theta - \theta_r}{\phi - \theta_r}$$

where θ_r is the residual water content and ϕ is the porosity of the soil. The diffusivity function, $D(\theta)$, is defined as the product of the capillary conductivity function and the slope of the capillary pressure-water content curve, i.e.

$$D(\theta) = -K \frac{\partial p_c/\gamma}{\partial \theta_e} \quad . \qquad \text{(II-15)}$$

The equations of Brooks and Corey (1969) for relating capillary pressure and hydraulic conductivity can be expressed in terms of water content as

$$K = K_{1.0} \, (\theta)^{(2 + 3\lambda)/\lambda} \qquad \text{(II-16)}$$

and

$$p_c = p_b \, (\theta_e)^{-1/\lambda} \qquad \text{(II-17)}$$

in which $K_{1.0}$ = the saturated hydraulic conductivity; Θ_e = the effective water content defined earlier; p_b = the bubbling pressure of the media, and λ = the pore-size distribution index.

Substituting Equations (II-16) and (II-17) into Equation (II-15) yields

$$D(\Theta) = \frac{K_{1.0}\, p_b}{\phi_e \lambda \gamma} (\Theta_e)^{(1 + 2\lambda)/\lambda} \quad . \tag{II-18}$$

Equation (II-18) may be scaled by letting $D_o = K_{1.0}\, p_b/(\phi_e \lambda \gamma)$, therefore

$$\frac{D(\Theta)}{D_o} = (\Theta_e)^{(1 + 2\lambda)/\lambda} \tag{II-19}$$

or

$$D. = (\Theta.)^{(1 + 2\lambda)/\lambda} \tag{II-20}$$

in which $D. = D(\Theta)/D_o$ and $\Theta. = \Theta_e$.

By scaling the diffusion equation (II-14), identical particular solutions may be obtained for a large number of drainage systems that have specified absolute boundaries provided that the initial and boundary conditions and media of the system are similar to those of the mathematical model. When the standard units are chosen to satisfy the similarity criteria discussed in the previous section, and making use of Equations (II-16, 17 and 18), Equation (II-14) reduces to the appropriate scaled diffusivity equation, i.e.

$$\frac{\partial \Theta.}{\partial t.} = \frac{1}{\lambda} \frac{\partial}{\partial Z.} \left[\Theta.^{(1 + 2\lambda)/\lambda} \frac{\partial \Theta}{\partial Z.} + \lambda \Theta.^{(2 + 3\lambda)/\lambda} \right] . \tag{II-21}$$

It is apparent that for Equation (II-21) to yield identical particular solutions, the pore-size distribution index, λ , must be the same for any two systems. If Equation (II-21) is solved using specific boundary and initial conditions, and for several soils having various values of λ , one can determine how pore-size distribution affects water content above the water table during vertical drainage.

The initial and boundary conditions imposed upon Equation (II-21) are as follows:

$$\theta.(Z.,0) = 1 \text{ for } 0 \leq Z. \leq L. \qquad \text{(II-22)}$$

in which $L. = L/L_o$ and L = the height of the soil profile measured from the water table to the soil surface:

$$\theta.(Z.,t) = 1 \text{ for } 0 \leq Z. \leq 1.0 \qquad \text{(II-23)}$$

$$\theta.(L.,t.) = 1 - q. \text{ for } t. \geq 0 \qquad \text{(II-24)}$$

where $L. \geq 1.0$.

The predictor-corrector finite-difference scheme introduced by Douglas and Jones (1963) was used to solve the one-dimensional diffusion equation (II-21) shown previously. The advantages of this numerical method over various other finite-difference methods are that it is algebraically explicit, it is second order accurate in both the space and time variables, and it is unconditionally stable. The development of this method of solution for the one-dimensional diffusion equation is not within the scope of this section. For the details of the development, the reader is referred to the thesis by Ng (1968).

Equation (II-21) was solved for various soil profile depths and various pore-size distribution indices. A total of 58 soil profiles were investigated. With scaled profile depth and λ as parameters, scaled water content was plotted as a function of scaled elevation above the water table, and scaled time. Some of the data are shown in Figures II-1 and II-2. The scaled profile depths are 2.0 and 7.0, respectively. Scaled elevation above the water table begins with unity on each set of curves since $\theta. = 1.0$ for $0 \leq Z. \leq 1.0$. The equilibrium value of $\theta.$, or the static distribution of water content is represented by the curve $t. = \infty$. This curve was obtained from Equation (II-17) by letting $Z. = P.$ which results in $\theta. = (Z.)^{-\lambda}$. The numerical solution converges to the equilibrium value as noted by the coincidence of the curves in Figure II-2(a) for $t. = 590$. In most cases it was not practical to carry the numerical solution to times approaching infinity. The largest scaled time used was 590.

To convert scaled variables to dimensioned variables, one must multiply by the standard units. For example, if Figure II-2 represents a soil profile with a bubbling

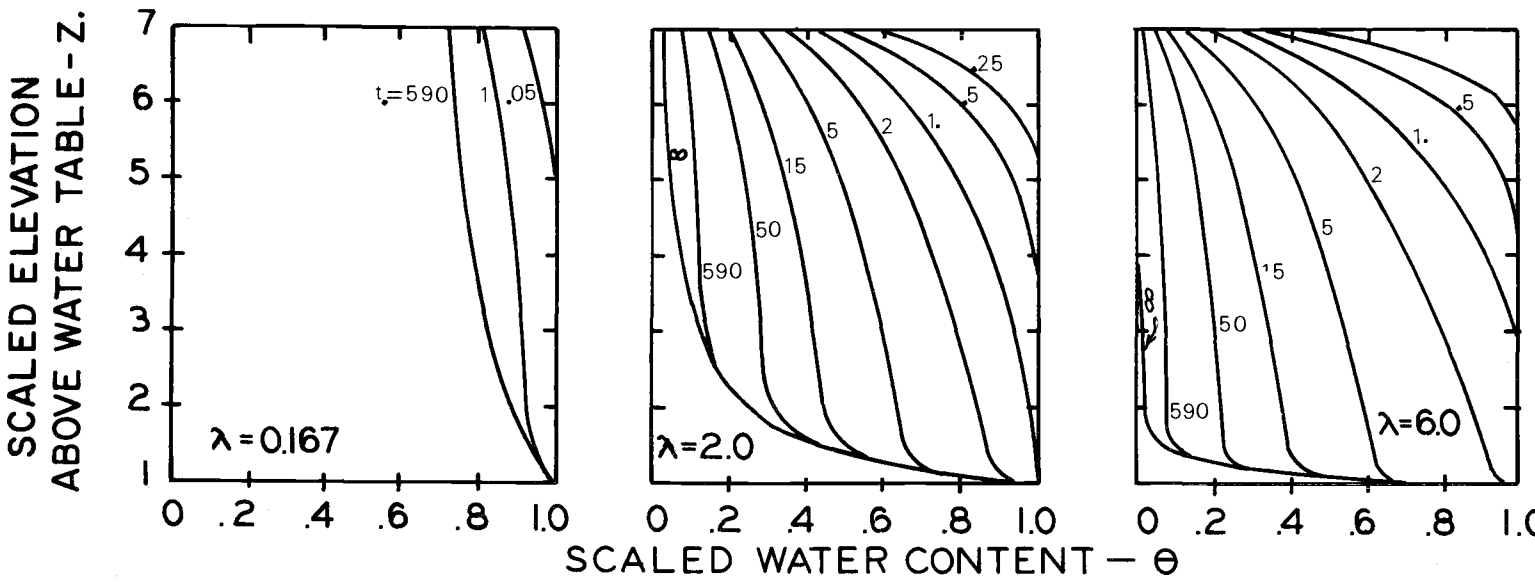

Figure II-1. Scaled water content as a function of scaled elevation above the water table for three pore-size distribution indices, Z. = 7.

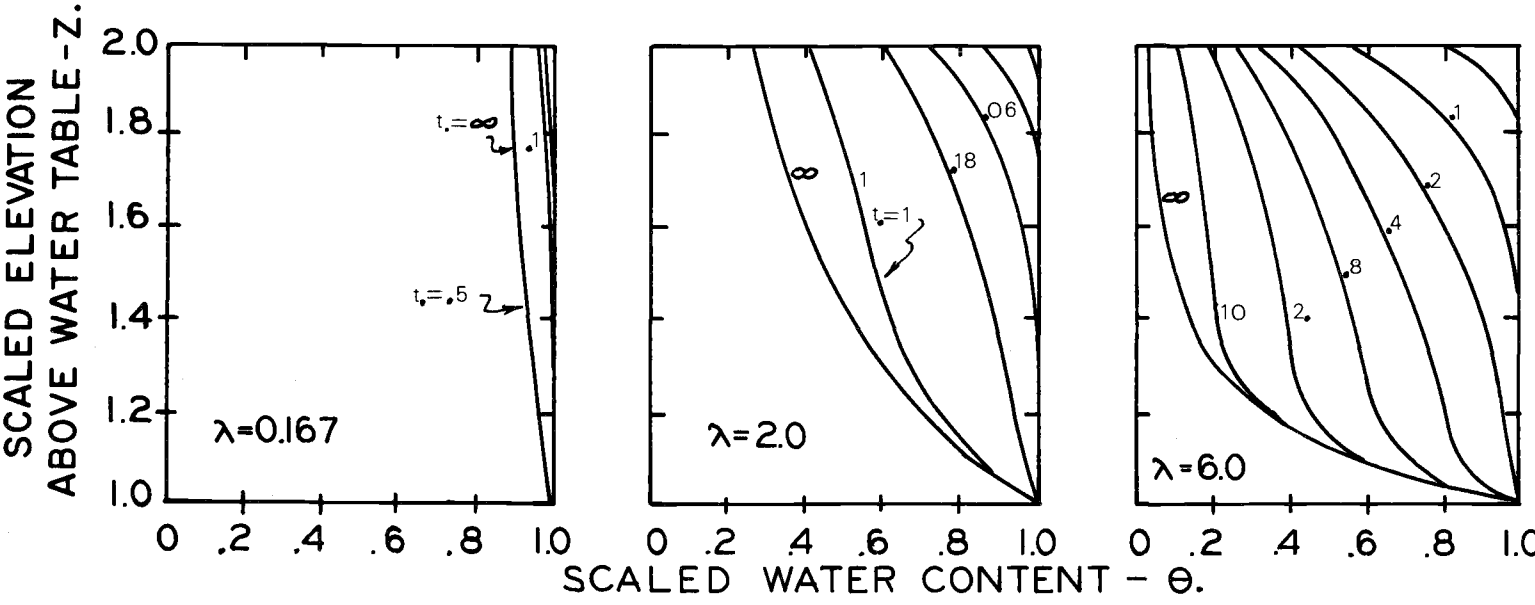

Figure II-2. Scaled water content as a function of scaled elevation above the water table for three pore-size distribution indices, Z. = 2.

pressure head of 1 foot, hydraulic conductivity of 1 foot per day, and effective porosity of 0.25, then a scaled time of unity is equal to 6 hours of real time. If, for the example given above, λ is 6.0 and the profile depth is 7 feet, (see Figure II-2(c)) after 30 hours ($t_. = 5.0$) the profile is approximately 50 percent drained. On the other hand, if $\lambda = 0.167$ (Figure II-2(a)), then equilibrium is closely approached in 48 hours ($t_. = 12$, curve not shown).

Field capacity has been defined as the equilibrium water content after 48 hours of drainage. The definition is used often without qualification. In the above example where drainage of similar profile depths are compared with soils of two different pore size distributions, field capacity is a function of the type of soil as well as the profile depth. If agricultural soils tend to have small values of λ and small values of $p_b/\rho g$, then the term field capacity as defined above may have general application. However, one should recognize its limitations.

In addition to obtaining the aforementioned data, volume of water drained was obtained as a function of time. Scaled volume may be obtained by integrating under the curves of Figures II-1 and II-2. Accumulative scaled volume may be expressed as

$$V._i = (L._ - 1) - \int_1^{L._} \theta_.(Z._, t._i)dZ. \qquad \text{(II-25)}$$

in which the i subscript refers to a particular time. The results of $V_.$ as a function of $t_.$ shown in Figures II-3 and II-4 were obtained by numerical integration. The curves are for various pore-size distribution indices and for various scaled profile depths. Experimental data points for six soil columns are shown also in the figures.

An increase in the profile depth has a similar effect to an increase in the pore-size distribution index, other things being equal.

All of the theoretical curves seem to be linear for small values of scaled time, i.e., $V_. \simeq t_.$ In other words, the scaled volume seems to be independent of the pore size distribution and profile depth during early stages of drainage.

The scaled mathematical solution is compared with experimental results from a physical model in Figures II-5 and II-6. The results from these two systems, as

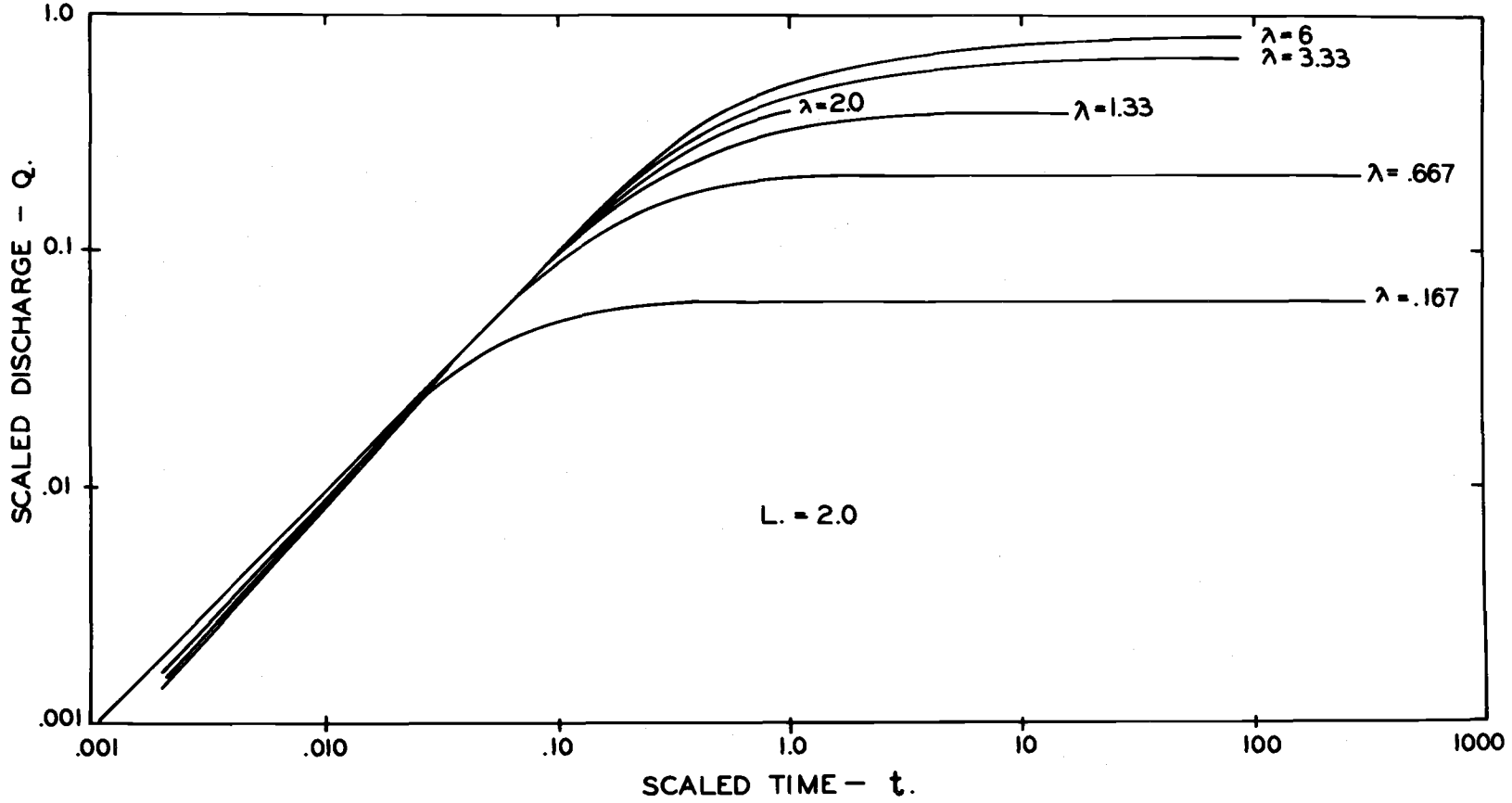

Figure II-3. Scaled discharge as a function of scaled time for drainage from a scaled column length of 2.0 and for various pore-size distribution indexes.

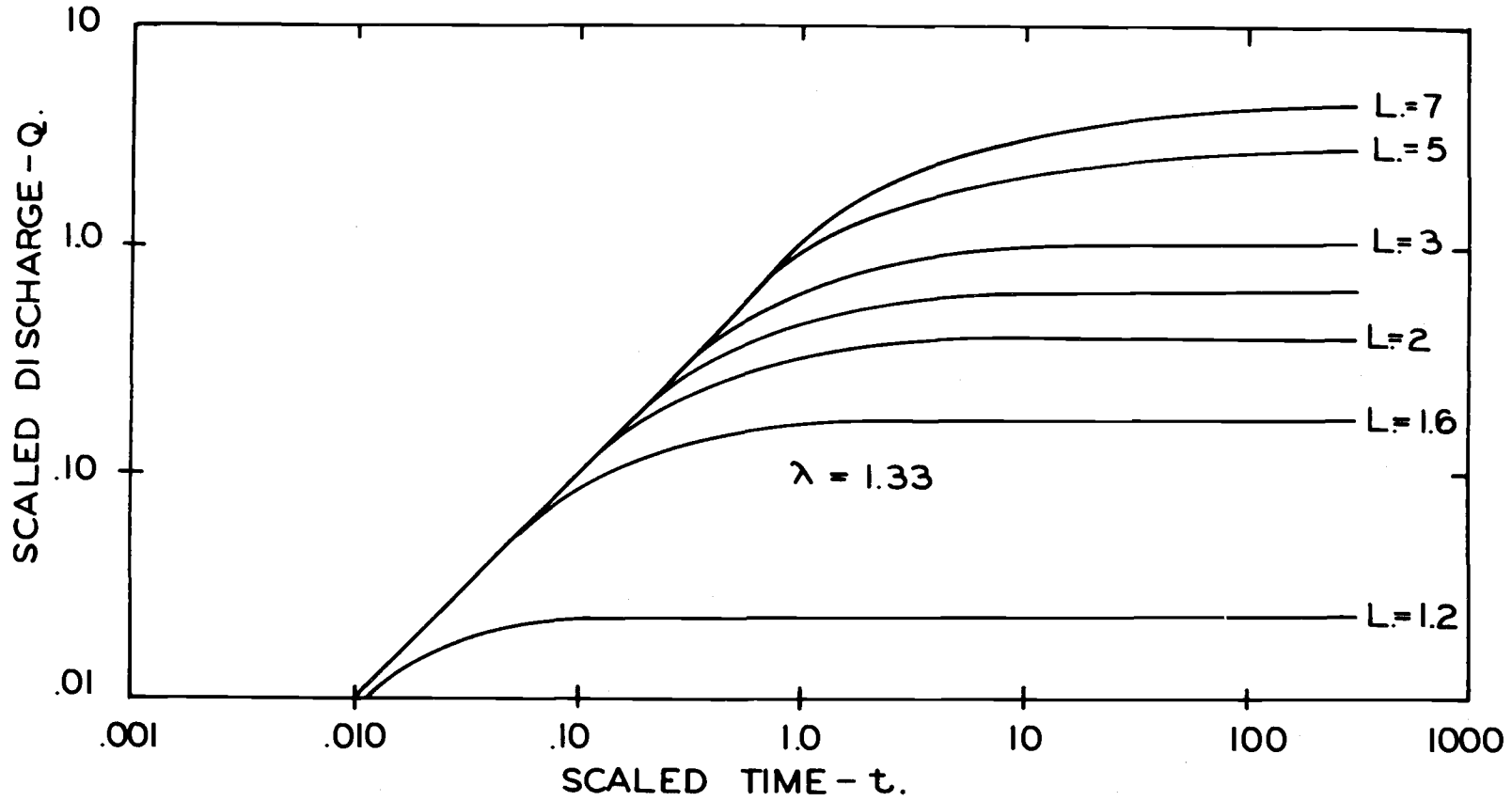

Figure II-4. Scaled discharge as a function of scaled time for drainage from various scaled column lengths having a pore-size distribution index of 1.33.

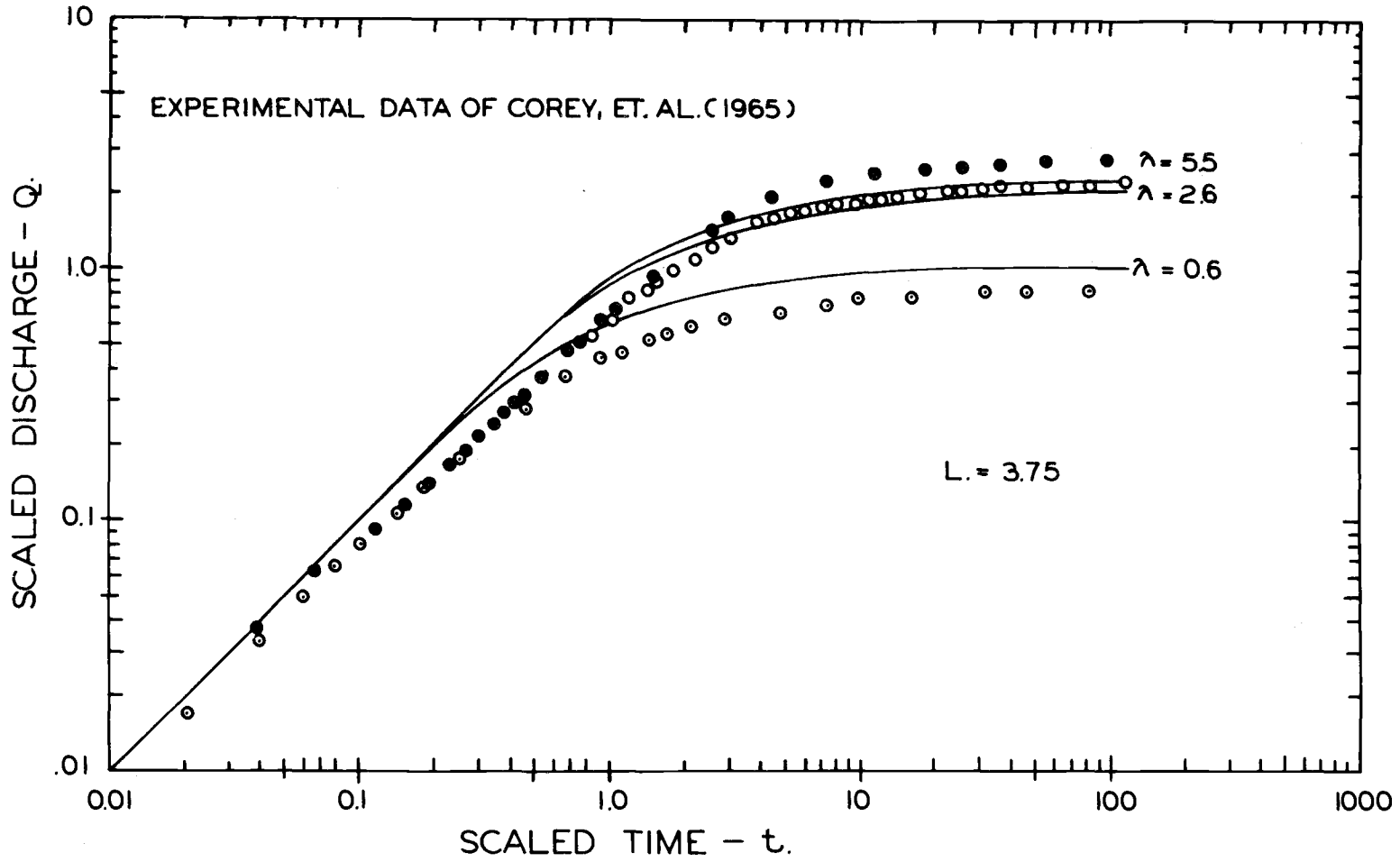

Figure II-5. Experimental data from Corey, et al. (1965) of scaled discharge as a function of scaled time compared with numerical solutions of the diffusion equation for scaled column lengths of 3.75.

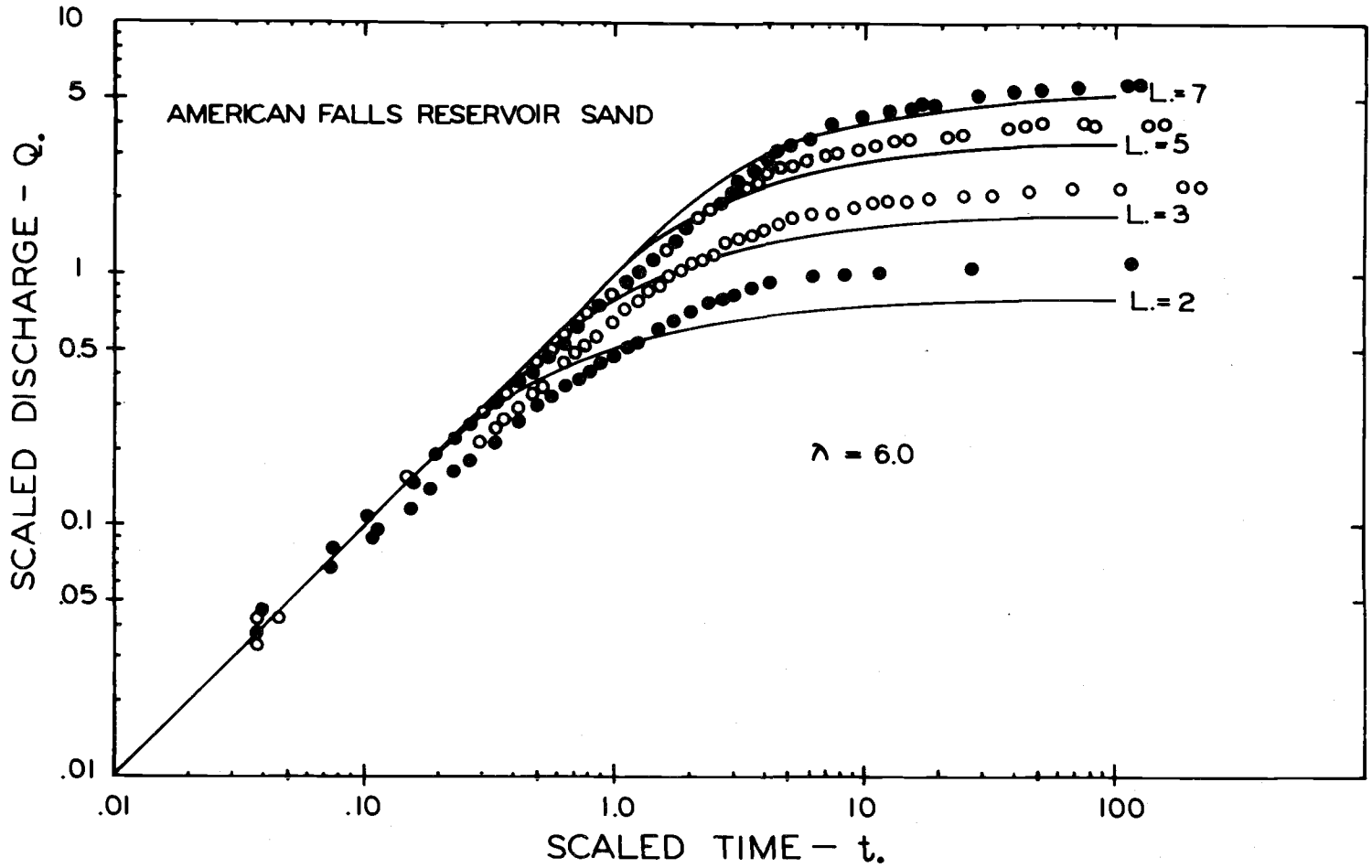

Figure II-6. Theoretical scaled discharge as a function of scaled time compared with experimental data for American Falls Reservoir Sand of various column lengths.

measured by volume as a function of time, are in close agreement. The hydraulic properties (standard units) of the physical model were obtained in separate experiments from the experiment of volume vs time.

Discrepancies between the mathematical model and the physical model may be due largely to the inadequacy of the Brooks-Corey equations to describe exactly the relationships among capillary pressure, water content and capillary conductivity, especially in the so-called "transition" zone, i.e., the downward concavity of the curve of P_c vs S. However, the differences between the mathematical model and the physical experiment are not great and these data lend support to both the similitude criteria presented by Brooks and Corey and to the Brooks-Corey approximations for predicting fluid flow in porous media.

The assumption that drainage occurs instantaneously in the partially saturated region above the water table is simply not valid and will result in inadequate design of subsurface drainage systems when the flow region is relatively shallow. The specific yield or volume associated with drainable porosity may not be obtained from a drainage profile for a considerable period of time.

II.3 HORIZONTAL FLOW ABOVE THE WATER TABLE by H. R. Duke

Most drainage research investigators have recognized the existence of horizontal flow above the water table and delayed drainage of soils as the water table recedes. Donnan (1947), for example, found that increasing the flow depth by the height of the capillary fringe improved the results of equilibrium drainage calculations. Many subsequent investigations have followed similar lines of reason. However, the contribution of the capillary region is not uniquely dependent upon the height of the saturated region above the water table, but depends as well upon the distribution of pore sizes, the flux through the partially saturated region, the celerity of the water table, and the depth of the water table below the soil surface. In the following analysis, it will be assumed that water table movement is sufficiently slow that the soil water can be considered in equilibrium with the water table, that the soil is uniform and stable, and that only mechanical potential gradients exist.

Based on the Dupuit-Forchheimer assumptions and the assumptions enumerated above, the mass continuity equation can be expressed as

$$\phi_e \frac{\partial Y_s}{\partial t} = \frac{\partial}{\partial x} \left(K_{1.0} Y_k \frac{\partial Y}{\partial x}\right) + Q \qquad \text{(II-26)}$$

where ϕ_e is the effective, or drainable, porosity; $K_{1.0}$ is the saturated hydraulic conductivity; Q is the strength of the distributed water source; x is the horizontal space coordinate; and t is time. The horizontal gradient, $\partial Y/\partial x$, (Y is the water table elevation referred to the impermeable lower boundary) is assumed to be uniform along a vertical line, both above and below the water table. If this equation is to represent both partially saturated and saturated flow, the storage term, Y_s, and horizontal flow term, Y_k, must account for the effects of capillary storage and capillary conductivity, respectively. Since the flow problem is analyzed as a one-dimensional problem, the effect of the capillary region is incorporated in the form

$$Y_k = Y + H_k \,, \qquad \text{(II-27)}$$

where H_k is a fictitious depth of saturated soil having the same capacity for horizontal flow as the capillary zone, and

$$Y_s = Y + H_s \ , \qquad \text{(II-28)}$$

where H_s is a fictitious depth of saturated soil having a volume of drainable water equal to that in the capillary zone. The concepts of an equivalent permeable height, as suggested by Myers and van Bavel (Bouwer, 1964) and of an equivalent saturated height used by Hedstrom, et al (1971) are employed.

II.3.1 EQUIVALENT PERMEABLE HEIGHT

The effectiveness of the capillary region in conducting water horizontally toward a drain is given by an expression suggested by Myers and van Bavel (Bouwer, 1964) as

$$H_k = \frac{1}{K_{1.0}} \int_0^H K \, dz \qquad \text{(II-29)}$$

where K is the capillary conductivity as a function of capillary pressure; z is elevation above the water table, and H is the distance from the water table to the soil surface. When H is less than the bubbling pressure head, p_b/γ, the soil remains saturated to the surface and $H_k = H$. If $H > p_b/\gamma$ the conductivity depends upon elevation and any vertical flux which may exist.

II.3.1.1 Static equilibrium. When the soil profile is in static equilibrium with the water table, as is assumed here for the case of transient drainage, $z = p_c/\gamma$, where p_c/γ is the capillary pressure head and z can be substituted for p_c/γ in the Brooks-Corey relations. Substituting the Brooks-Corey relation for K when $z = p_b/\gamma$ in Equation (II-29) and equating p_c/γ to z_r gives

$$H_k = \frac{1}{K_{1.0}} \left[\int_o^{p_b/\gamma} K_{1.0}^{dz} + \int_{p_b/\gamma}^{H} (p_b/\gamma)^{\eta} \, z^{-\eta} \, dz \right] \qquad \text{(II-30)}$$

which, when integrated results in

$$H_k = \frac{p_b}{\gamma} \left[\frac{\eta - H^{1-\eta} \, (p_b/\gamma)^{\eta-1}}{\eta - 1} \right] . \qquad \text{(II-31)}$$

Dimensionless variables $H.$ and $H_k.$ are defined by dividing by the bubbling pressure head, a characteristic parameter of dimension length, so that $H. = H/(p_b/\gamma)$. In terms of these scaled variables, the effective permeable height is

$$H_{k\cdot} = \frac{\eta - H_{\cdot}^{1-\eta}}{\eta - 1} \quad . \tag{II-32}$$

II.3.1.2 Steady downward flow. During steady percolation to a water table, the capillary pressure head is, at every point, less than the elevation above the water table. It is apparent from Figure II-7 that the relation between capillary pressure head and elevation above the water table exhibits three separate regions delineated by Z' , Z'' , and H . Before Equation (II-29) can be applied to this case, these elevations and their corresponding capillary pressures must be evaluated. In the region between the water table and the point at which the capillary pressure equals the bubbling pressure, $(0 < Z \leq Z')$, the hydraulic conductivity remains constant at the saturated value (see Figure II-7).

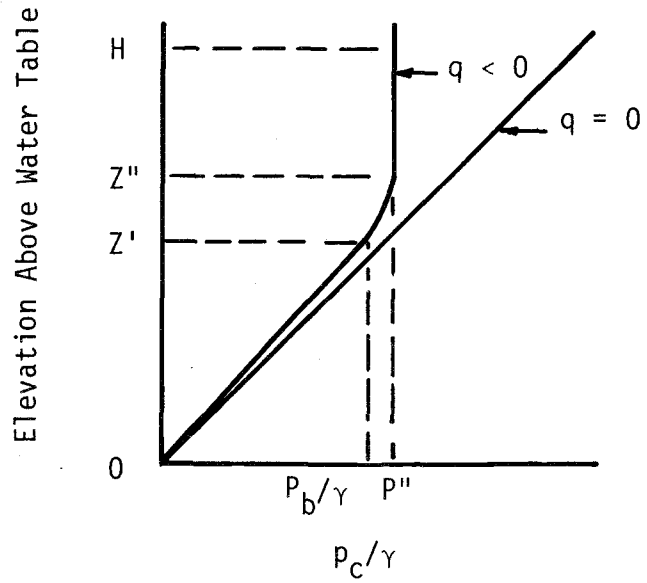

Figure II-7. Capillary pressure profile in a soil with a steady downward flux of water

As elevation increases above Z' , capillary pressure increases, and conductivity decreases. Thus, the gradient of capillary pressure must decrease. If the soil profile is sufficiently deep, the hydraulic conductivity continues to decrease with increasing elevation until it approaches the flux in magnitude. That elevation at which $K = -\varepsilon q$, is defined as Z'' , where q is the volumetric flux rate, positive upward, and ε is a constant greater than, but arbitrarily near unity.

After evaluating the elevations Z' and Z'' , at which the conductivity function changes form, the equivalent permeable height is evaluated from Equation (11-29),

which can be expressed as

$$H_k = \frac{1}{K_{1.0}} \left[\int_0^{Z'} K_{1.0}\, dZ + \int_{Z'}^{Z''} K\, dZ + \int_{Z''}^{H} (-\varepsilon q.)\, dZ \right] , \qquad \text{(II-33)}$$

which in terms of scaled variables reduces to

$$H_{k.} = 1 - \varepsilon q.H. + \int_1^{(-\varepsilon q.)^{-1/\eta}} \frac{1 + \varepsilon q.P_.^{\eta}}{P_.^{\eta}(1+q.P_.^{\eta})}\, dP. \quad . \qquad \text{(II-34)}$$

It is important to emphasize that $q.$ is defined positively upward, so that for the case considered here, values of $q.$ are negative.

Since the effective hydraulic conductivity depends upon saturation, the shape of the saturation profile strongly influences the ability of the capillary region to transmit water toward the drain. Figures II-8 and II-9 show the effects of η and scaled depth to water table, $H.$, upon the effective permeable height, $H_{k.}$, for static profiles and the case of steady downward flux, respectively. It is apparent

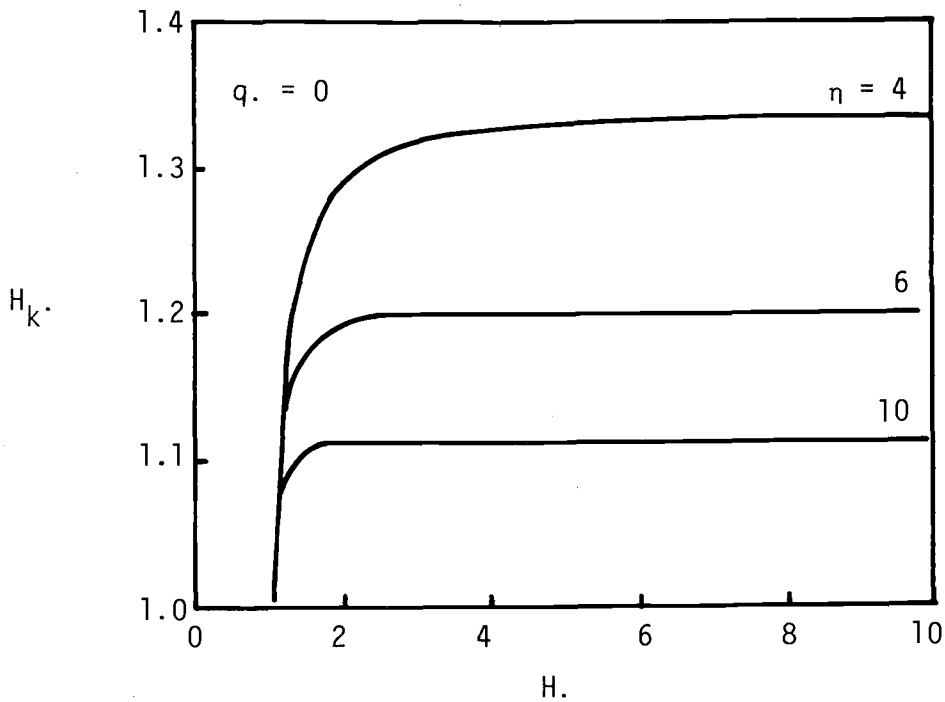

Figure II-8. Scaled effective permeable height as a function of scaled water table depth, static equilibrium.

that the major contribution to $H_{k.}$ occurs within a relatively short distance above the water table. $H_{k.}$ is influenced by water table depth to greater depth for small values of η and is more sensitive to changes in η for small values of η. Regardless of the value of η, $H_{k.}$ is never less than unity when $H. > 1$.

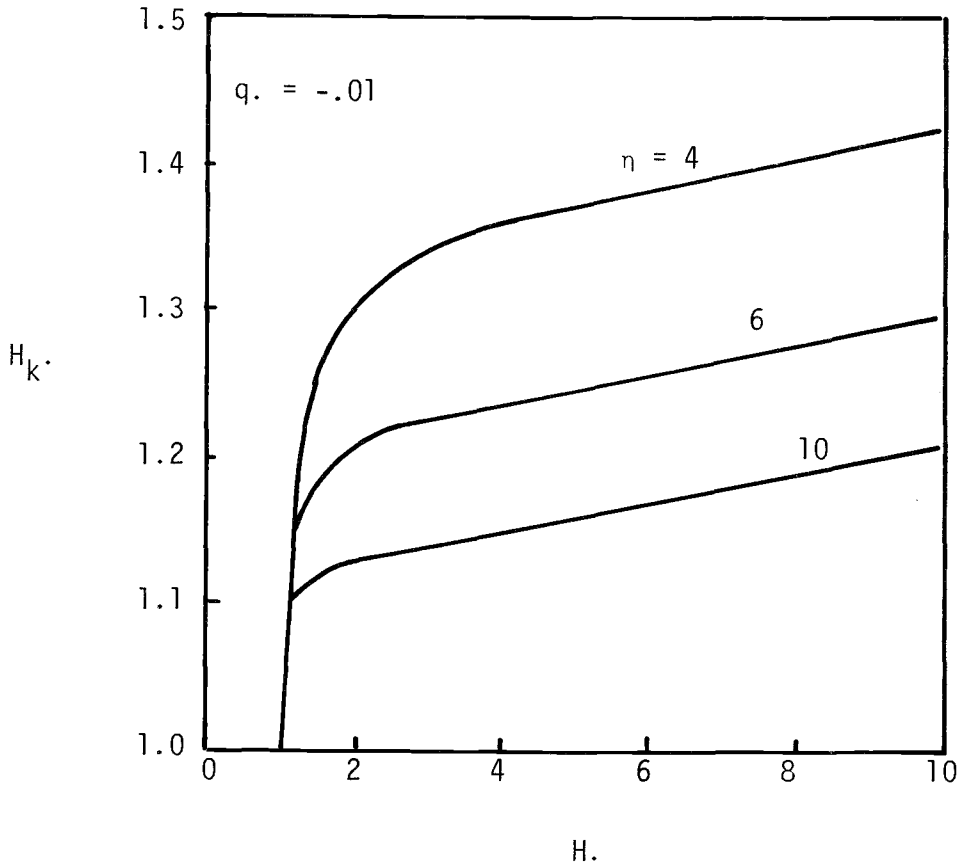

Figure II-9. Scaled effective permeable height as a function of scaled water table depth, steady downward flux.

As previously mentioned, when the flux is downward, the hydraulic conductivity is nowhere less than the magnitude of the flux. Therefore, downward flux increases the effective permeable height, as indicated by Equation (II-34) and shown graphically in Figure II-9. The same general observations apply to this case as to the case of static equilibrium. However, $H_{k.}$ does not approach a constant as water-table depth increases. Rather, as indicated by the second term in Equation (II-34), $H_{k.}$ increases linearly with H. at higher values of H. (i.e., H. > Z."). Therefore, the entire depth of profile can contribute to horizontal flow and the water table depth becomes an important consideration in evaluating the total flow system.

Figure II-10 shows the influence of q. upon $H_{k.}$ for a selected value of H. and η . The rate of increase of $H_{k.}$ with increasing q. is not great, except when q. is relatively large. This suggests that $H_{k.}$ can be calculated from the static equilibrium equation with little error as long as q. is small. The rate of

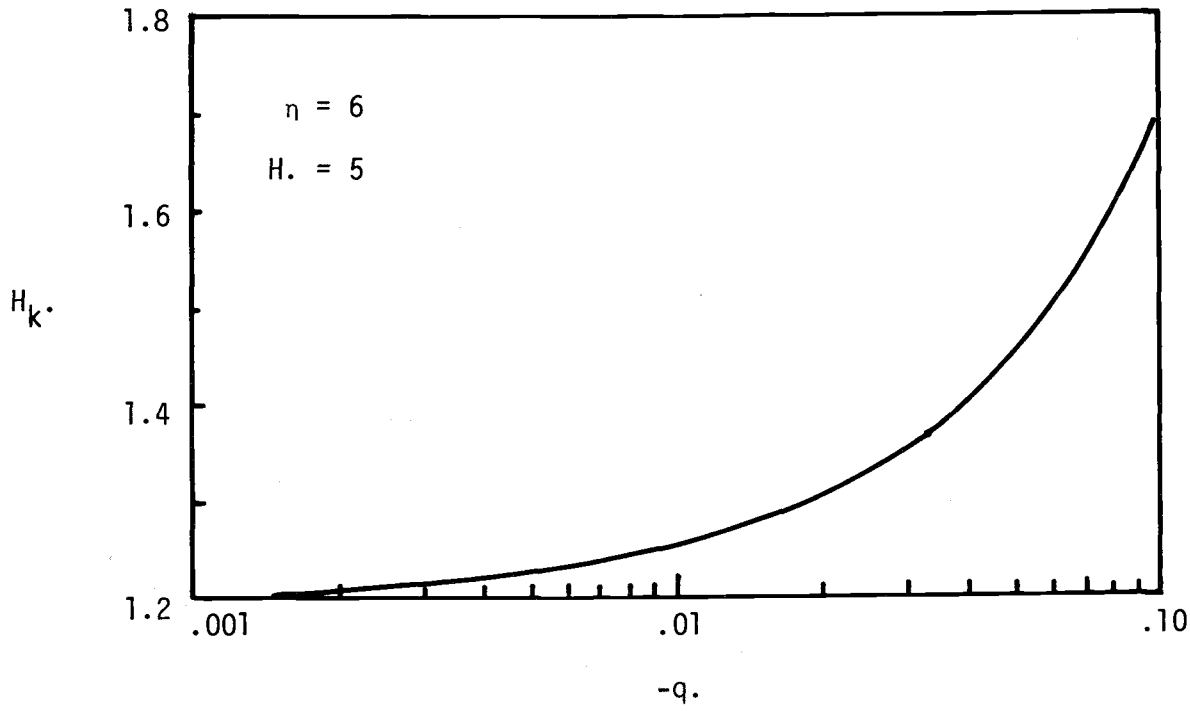

Figure II-10. Effect of flux upon effective permeable height

change of H_k. with respect to q. is also dependent upon η (and upon H. for shallow water table depths). As η increases, the deviation from the equilibrium value increases.

II.3.2 EQUIVALENT SATURATED HEIGHT

When the water table depth varies significantly with time, the capillary region influences the flow in a second way. The volume of water released from storage for a unit decrease of the water table is dependent upon the depth to the water table. This dependence has been discussed by Childs (1960), Duke (1972), and others. Such a dependence of the specific yield upon depth to the water table can be treated analogously to the previously discussed effective permeable height. A fictitious column of saturated soil of height H_s that contains the same volume of drainable water as the partially saturated soil profile is defined by

$$H_s = \int_o^H S_e \, dZ \, , \qquad \text{(II-35)}$$

where S_e, the effective saturation, is defined by $S_e = (S - S_r)/(1 - S_r)$. The volume of drainable water per unit area of soil in this fictitious column is given by

$$V_d = \phi(1 - S_r)H_s \qquad \text{(II-36)}$$

where V_d is the total water volume; ϕ is total porosity; and S_r the residual saturation. Volume V_d is equal to the volume of drainable water in a unit area of soil of height, H, above the water table. Thus, the volume of water, V_r, released per unit area from the soil by a unit decline in the water table is given by

$$V_r = \phi[1+(H_s)_H - (H_s)_{H+1}] \qquad \text{(II-37)}$$

where the subscripts refer to the depth to water table at which H_s is evaluated.

By applying the Brooks-Corey expression

$$S_e = (p_b/p_c)^{\lambda} \qquad \text{(II-38)}$$

where λ is the pore-size distribution index, with the appropriate limits on Equation (II-35), the effective saturated height is evaluated in the same manner as the effective permeable height.

Carrying out these evaluations gives

$$H_{s.} = \frac{\lambda - H_.^{1-\lambda}}{\lambda - 1} \qquad \text{(II-39)}$$

for the case of static equilibrium, where $H_{s.}$ is the effective saturated height scaled by the bubbling pressure, and λ is the pore size distribution index defined by Brooks and Corey.

For the case of steady downward flux,

$$H_{s.} = \frac{1-(\varepsilon q_.)^{\lambda/\eta}}{1+q_.} + (-\varepsilon q_.)^{\lambda/\eta} H_. + \int_1^{(-\varepsilon q_.)^{-1/\eta}} \frac{P_.^{-\lambda} - (-\varepsilon q_.)^{\lambda/\eta}}{1+q_. P_.^{\eta}} dP_. \quad . \qquad \text{(II-40)}$$

Since $\eta = 2 + 3\lambda$ (according to Brooks and Corey, 1964), $H_{s.}$ is always greater than $H_{k.}$ for a given soil and water table depth. This means that the effect of differences in depth to the water table is more significant with respect to the effective storage height than to the effective permeable height.

Figure II-11 illustrates the influence of water table depth, $H.$, upon $H_{s.}$, as computed from Equation (II-39), when the soil profile is in static equilibrium with the water table. The scaled effective saturated height, $H_{s.}$, exhibits much the same relation to water table depth as does $H_{k.}$. However, since the exponent of capillary pressure, p_c, is larger (i.e., a smaller negative number, $\lambda < \eta$) in the equation relating S_e to p_c, than in the equation relating relative conductivity, $K_{1.0}/K$,

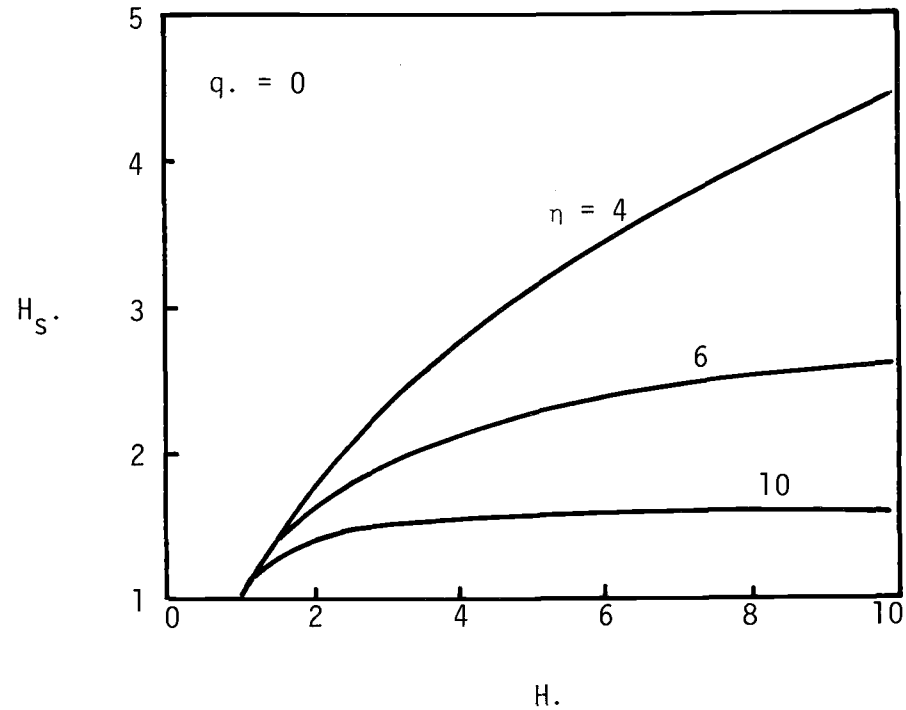

Figure II-11. Scaled effective saturated height as a function of scaled water table depth, static equilibrium.

to p_c, $H_{s.}$ is much larger than $H_{k.}$ at a particular water table depth. $H_{s.}$ is much more sensitive to $H.$ and to η than is $H_{k.}$. Therefore the effective specific yield continues to change as the water table declines to relatively large depths.

As in the case for $H_{k.}$, a downward flux can significantly increase the magnitude of $H_{s.}$ as shown in Figure II-12. Because of the magnitude of λ relative to η, $H_{s.}$ is influenced by the vertical flux more than is $H_{k.}$. Therefore, use of the equilibrium equation to calculate $H_{s.}$ may result in significant errors. Since the case of steady percolation with a falling water table was not considered in this study,

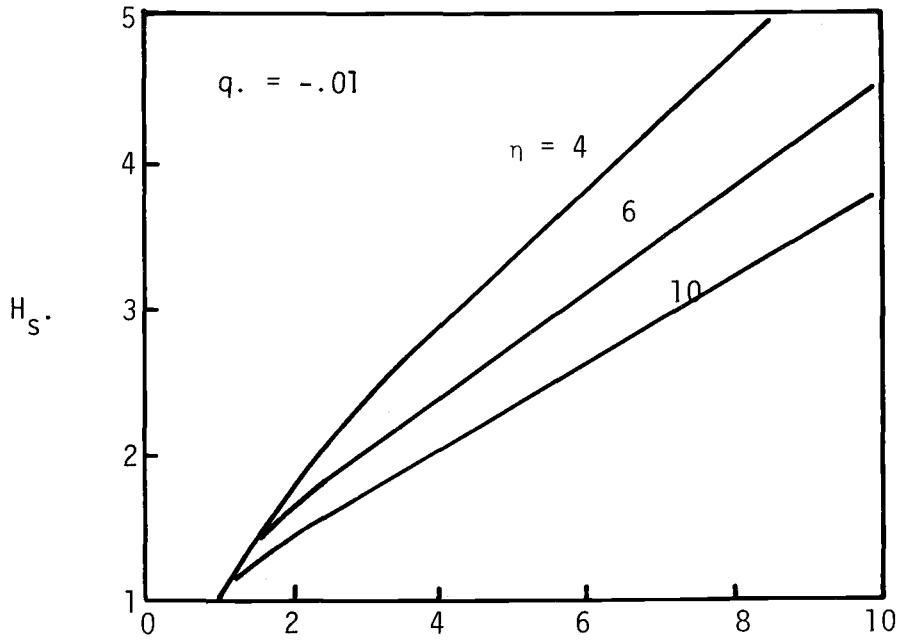

Figure II-12. Scaled effective saturated height as a function of scaled water table depth, steady downward flow

the effects of $q.$ upon $H_s.$ have not been evaluated in detail.

The value of H_s, itself, is not directly related to the specific yield of the soil. The difference in H_s between two successive water table positions, as given in Equation (II-37), corresponds with the ordinary conception of specific yield. That is, the specific yield for a given water table depth is proportional to the inverse slope of the curves of Figures II-11 and II-12.

SECTION III.

EFFECT OF CAPILLARY FLOW ON DRAIN PERFORMANCE

INTRODUCTION

Mathematical evaluations of drainage problems have been utilized for drain design for over a century. Colding, a Danish engineer, is credited as being the first to develop such an analysis, which he applied to the case of drainage in equilibrium with constant, uniform percolation. In the years since, many investigators have contributed to drainage theory to bring it to the present state of considerable mathematical sophistication. Except for very idealized cases, the mathematical complexity of the differential equations has required very naive consideration of the influence of soil water retained by capillary forces above the water table. As proved by the successful use of such equations, neglecting the capillary influence does not seriously impair the utility of these equations for a great many instances to which they are applied.

As mathematical sophistication of drainage equations progressed, investigators began attempts to account for flow above the water table. Most such attempts to date have, by one means or another, approximated the capillary region by an equivalent saturated region having the same capacity to transmit water.

The research committee feels, however, that an understanding of capillary effects and acknowledgement of their existence can reduce the incidence of inadequate drain installation and reduce drainage costs resulting from overdesign. This section of the paper describes the work of the research committee toward describing effects of the capillary region upon drain performance.

III.1 FLOW IN SLOPING AQUIFERS by R. H. Brooks and R. R. Tebbs

It appears that the criteria for determining whether capillary effects are significant must be expressed in relative terms so that specific problems may be compared with models having similar characteristics and whose performance can be predicted.

The similarity criteria of Brooks and Corey may be used to establish criteria for evaluating the importance of the flow region above the water table.

This section deals with an application of similarity criteria to the solution of a very simple one-dimensional flow problem. The purpose is to establish, in quantitative terms, conditions for which the capillary region should be considered.

III.1.1 THEORY

The model under consideration here consists of a uniformly sloping aquifer bounded on the lower surface by an impermeable layer and on the upper surface by the soil-atmosphere interface where no evapotranspiration is permitted as shown in Figure III-1. The aquifer may be homogeneous-isotropic or homogeneous-anisotropic (homogeneous layers parallel to the boundaries). The aquifer is assumed to be infinite in extent and dips at an angle, β, with respect to the horizontal. A steady source of water is maintained at an infinite distance upstream such that the flow within the aquifer is parallel to its boundaries. It is further assumed that relationships among permeability, capillary pressure, and saturation are known for the aquifer or for each layer within the aquifer.

The existence of a water table and its location in the aquifer as well as the hydraulic properties of the aquifer will determine the relative importance of the flow in the capillary region. This can be illustrated best by using the notation and symbols shown in Figure III-1.

The variation of capillary pressure, p_c, along any direction, s, can be expressed through Darcy's Law, i.e.

$$\frac{dp_c}{ds} = \frac{q_s \mu}{K} - \gamma \sin\beta \quad . \tag{III-1}$$

Using the Brooks-Corey scaling criteria (see Section II), Equation (III-1) reduces to

$$\frac{dp.}{dS.} = \frac{q.s}{K.} - \gamma \sin\beta \tag{III-2}$$

where $p. = p_c/p_b$, $S. = s\gamma/p_b$, $q. = q/K_1$, K_1 is the saturated hydraulic conductivity, and $K.$ is the scaled conductivity, K/K_1. The derivative in Equation (III-2) is valid for any element of width dw.

Since all characteristic lengths are scaled by p_b/γ, the thickness of the aquifer in Figure III-1 becomes $D. = D\,\gamma/p_b$ and the position of the water table above the lower boundary becomes $h. = h\,\gamma/p_b$.

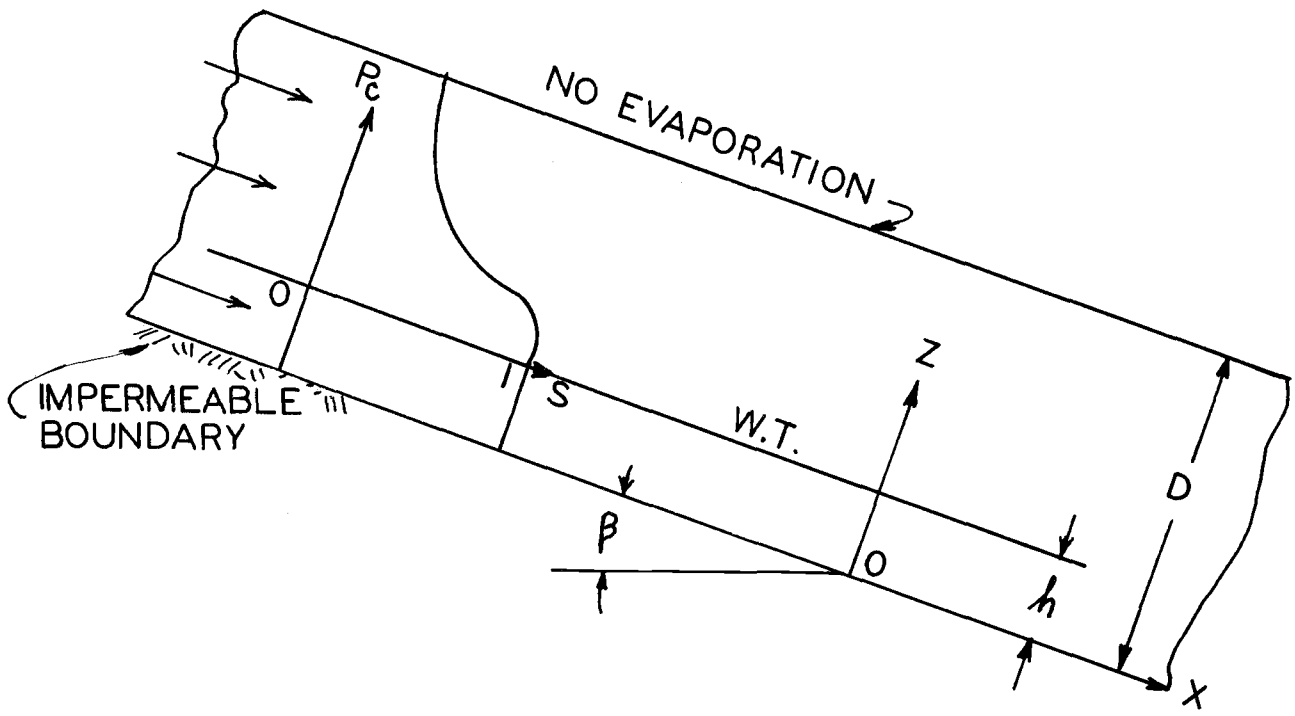

Figure III-1. Definition sketch for flow in a sloping aquifer showing the coordinate system and the water content distribution curve for a particular water table position.

If the direction s in Equation (III-2) is taken along x in Figure III-1, then

$$\frac{q._x}{K._x} = \sin\beta \ , \qquad \text{(III-3)}$$

since $dp./dx.$ along a streamline parallel to the boundary is zero. The total relative flux through the aquifer is obtained by integrating Equation (III-3) over the thickness of the aquifer, i.e.,

$$Q. = \int_o^{D.} q._x dz. = \sin\beta \int_o^{D.} K._z dz. \qquad \text{(III-4)}$$

where $K._x = K._z$. It should be noted that for a particular value of $z.$, $q.$ and $K.$ are both constants in that direction x , but in the $z.$-direction $q._z = 0$ and $K._z$ is a function of z .

An approximation for the variation of hydraulic conductivity in the $z.$-direction may be obtained by writing Darcy's Law in the $z.$-direction and using the Brooks-Corey equation of permeability as a function of capillary pressure as shown in the following development.

Equation (III-2) written along the $z.$-direction reduces to

$$\frac{dp.}{dz.} = \sin(90°-\beta)$$

or after separating the variables,

$$dp. = \cos\beta dz. \ .$$

The variation of $p.$ in the $z.$-direction is obtained by the equation

$$\int_o^{p.} dp. = \cos\beta \int_{h.}^{z.} dz. \ .$$

The locus of points where $p. = 0$ (water table) is given by $z. = h.$ Integrating the above produces

$$p. = \cos\beta(z.-h.) \quad . \tag{III-5}$$

From the Brooks-Corey equations

$$K. = (p.)^{-\eta} \quad \text{for} \quad p. \geq 1.0$$

and (III-6)

$$K. = 1.0 \qquad \text{for} \quad 0 \leq p. \leq 1.0 \quad .$$

When Equation (III-5) is substituted into Equation (III-6) and redefining the limits according to Figure III-1 the result is

$$K. = [\cos\beta(z.-h.)]^{-\eta} \quad \text{for} \quad z. \geq (h.+\sec\beta) \tag{III-7}$$

and

$$K. = 1.0 \qquad \text{for} \quad (h.+\sec\beta) \geq z. \geq 0 \quad . \tag{III-8}$$

The total scaled flux in the aquifer may be expressed in terms of the aquifer properties and boundary conditions by substituting Equations (III-7) and (III-8) into (III-4). The result is

$$Q. = \sin\beta \int_{0}^{(h.+\sec\beta)} dz. + \sin\beta \int_{(h.+\sec\beta)}^{D.} [\cos\beta(z.-h.)]^{-\eta} dz. \quad . \tag{III-9}$$

Integrating (III-9) and rearranging yields

$$Q. = \sin\beta \left[h.+\sec\beta+ \left(\frac{(D.-h.)^{1-\eta} - (\sec\beta)^{1-\eta}}{(1-\eta)(\cos\beta)^{\eta}} \right) \right] \tag{III-10}$$

where $Q.$ is the total scaled quantity of liquid flowing in the aquifer per unit

width. In terms os the scaling quantities already used,

$$Q_{\cdot} = Q\gamma/K_1$$

where Q is the actual volume flow per unit time in the aquifer per unit width.

It is convenient to reduce Equation (III-10) to a form that relates to the aquifer thickness. This is accomplished by dividing Equation (III-10) by $D_{\cdot} \sin\beta$. The result is

$$\frac{Q_{\cdot}}{D_{\cdot} \sin\beta} = \frac{h_{\cdot}}{D_{\cdot}} + \frac{\sec\beta}{D_{\cdot}} + \left[\frac{(1-\frac{h_{\cdot}}{D_{\cdot}})^{1-\eta} - (\sec\beta)^{1-\eta}}{(1-\eta)(\cos\beta/D)^{\eta}} \right] . \qquad \text{(III-11)}$$

The maximum possible flow in the aquifer for a given thickness and dip is $Q_{\cdot m} = D_{\cdot} \sin\beta$. Obviously then, $Q_{\cdot}/D_{\cdot} \sin\beta$ is the ratio of the scaled flow in the aquifer to the maximum scaled flow and the sum of the 3 terms on the right side of Equation (III-11) must be equal to or less than unity. If they are equal to unity, the maximum aquifer thickness for a given water table position aquifer dip is

$$D_{\cdot m} = h_{\cdot} + \sec\beta \qquad \text{(III-12)}$$

and

$$Q_{\cdot m} = D_{\cdot m} \sin\beta \quad .$$

The three terms on the right side of Equation (III-10) are the ratio of the flow in the three regions of the aquifer to the maximum flow, $Q_{\cdot m}$. These three regions are designated: $Q_{\cdot s}$, the saturated region, $Q_{\cdot f}$, the capillary fringe region and $Q_{\cdot c}$, the capillary region, i.e.,

$$\frac{Q_{\cdot s}}{Q_{\cdot m}} = \frac{h_{\cdot}}{D_{\cdot}} \quad ,$$

$$\frac{Q_{\cdot f}}{Q_{\cdot m}} = \frac{\sec\beta}{D_{\cdot}} \quad , \tag{III-13}$$

and

$$\frac{Q_{\cdot c}}{Q_{\cdot m}} = \frac{\left(1 - \frac{h_{\cdot}}{D_{\cdot}}\right)^{1-\eta} - \left(\frac{\sec\beta}{D_{\cdot}}\right)^{1-\eta}}{(1-\eta)(\cos\beta/D)^{\eta}} \quad .$$

III.1.2 THEORETICAL RESULTS

It will be useful to compare the quantity of flow in each of the three regions of the aquifer to the total flow in the aquifer for a given pore size distribution, η , aquifer thickness, $D_{\cdot}$, and angle of dip, β . The relative flow in each region was obtained by summing Equation (III-13) and dividing each by the sum.

Inasmuch as $h_{\cdot}/D_{\cdot}$ is the relative position of the water table with respect to the aquifer thickness as well as being proportioned to the flow in the saturated region, it was selected as a boundary condition along with the aquifer thickness and angle of dip. The pore size distribution, η , is the only aquifer property.

The relative flow in each region of the aquifer is plotted as a function of aquifer thickness for various water table positions, angles of dip and pore size distributions. These results are shown in Figures III-2 through III-4.

In Figure III-2, the effect of the relative position of the water table upon the flow in the three regions is shown for $\eta=2$, and $\beta=10°$. When $\eta=2$, the pore size distribution for the aquifer is the widest distribution possible. For this aquifer property, the flow in the capillary region is very significant when the water table is in the lower half of the aquifer. If the water table is coincident with the lower boundary, the flow in the capillary region becomes as large as the flow in the capillary fringe region when the aquifer becomes large.

Figure III-3 is for the same aquifer geometry but for a pore size distribution that is much more narrow, i.e., $\eta=8$. If the water table does not occupy less than

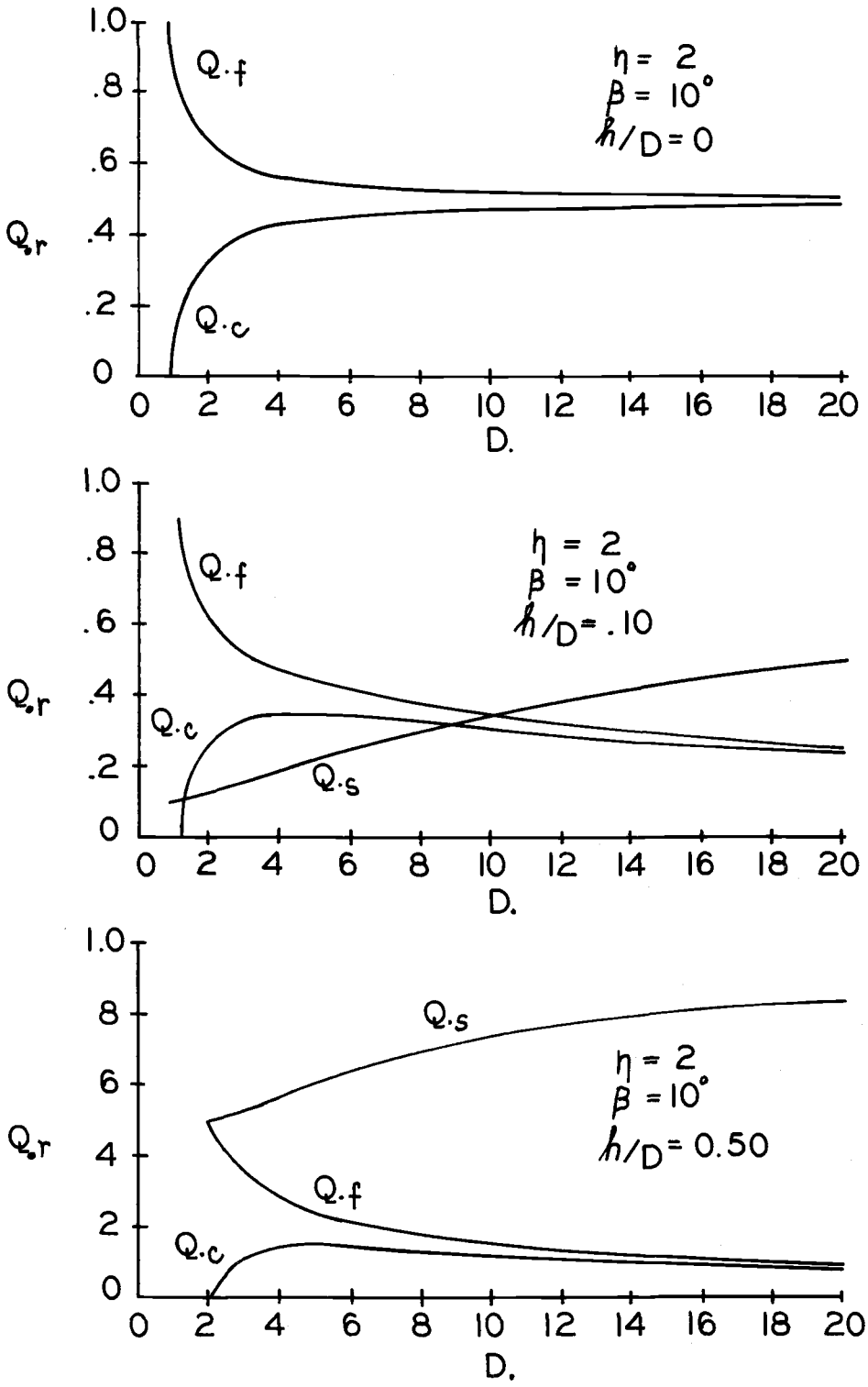

Figure III-2. Relative scaled discharge for three regions in an aquifer for $\eta=2$ dipping at 10° as a function of aquifer thickness and for various water table positions.

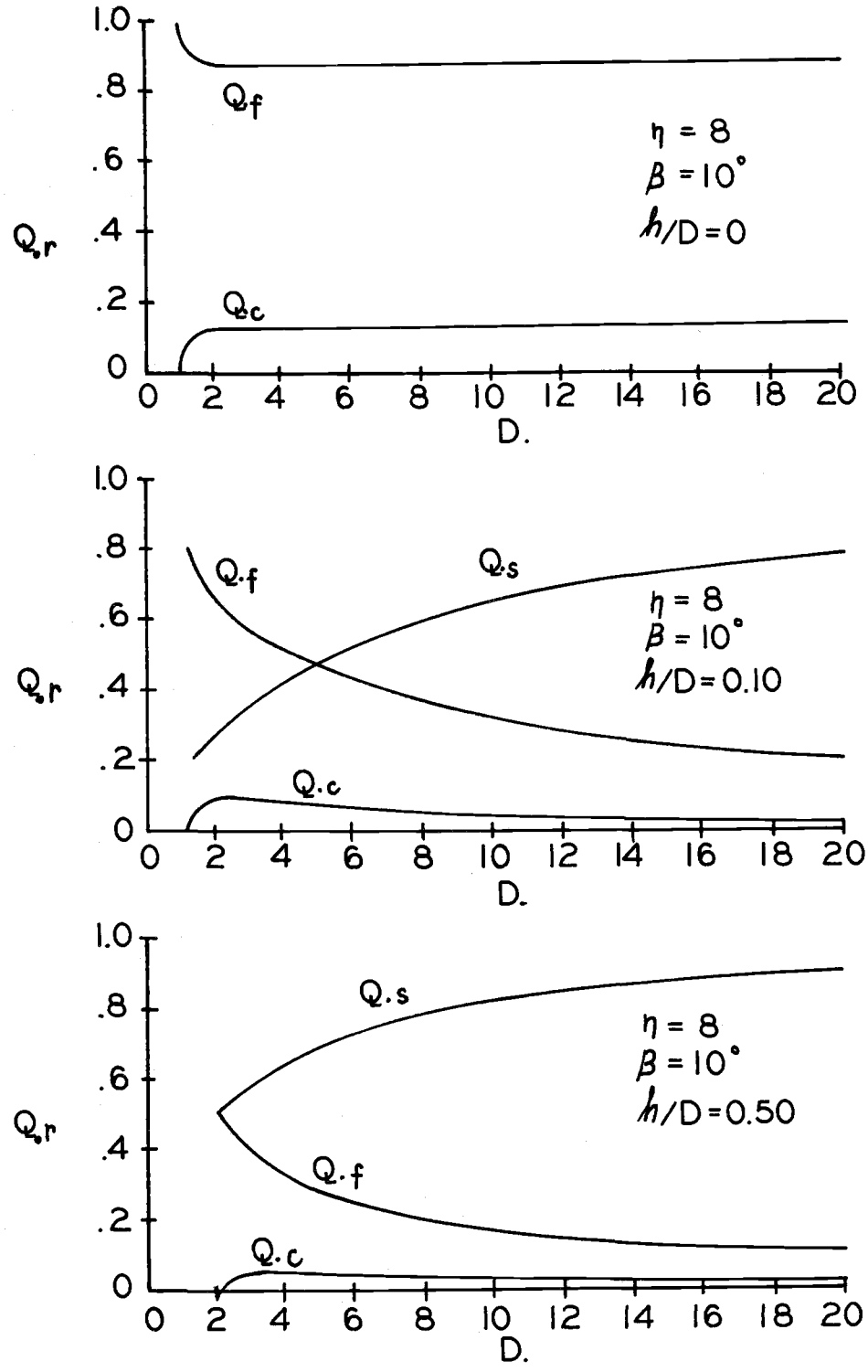

Figure III-3. Relative scaled discharge for three regions in an aquifer for η=8 dipping at 10° as a function of aquifer thickness and for various water table positions.

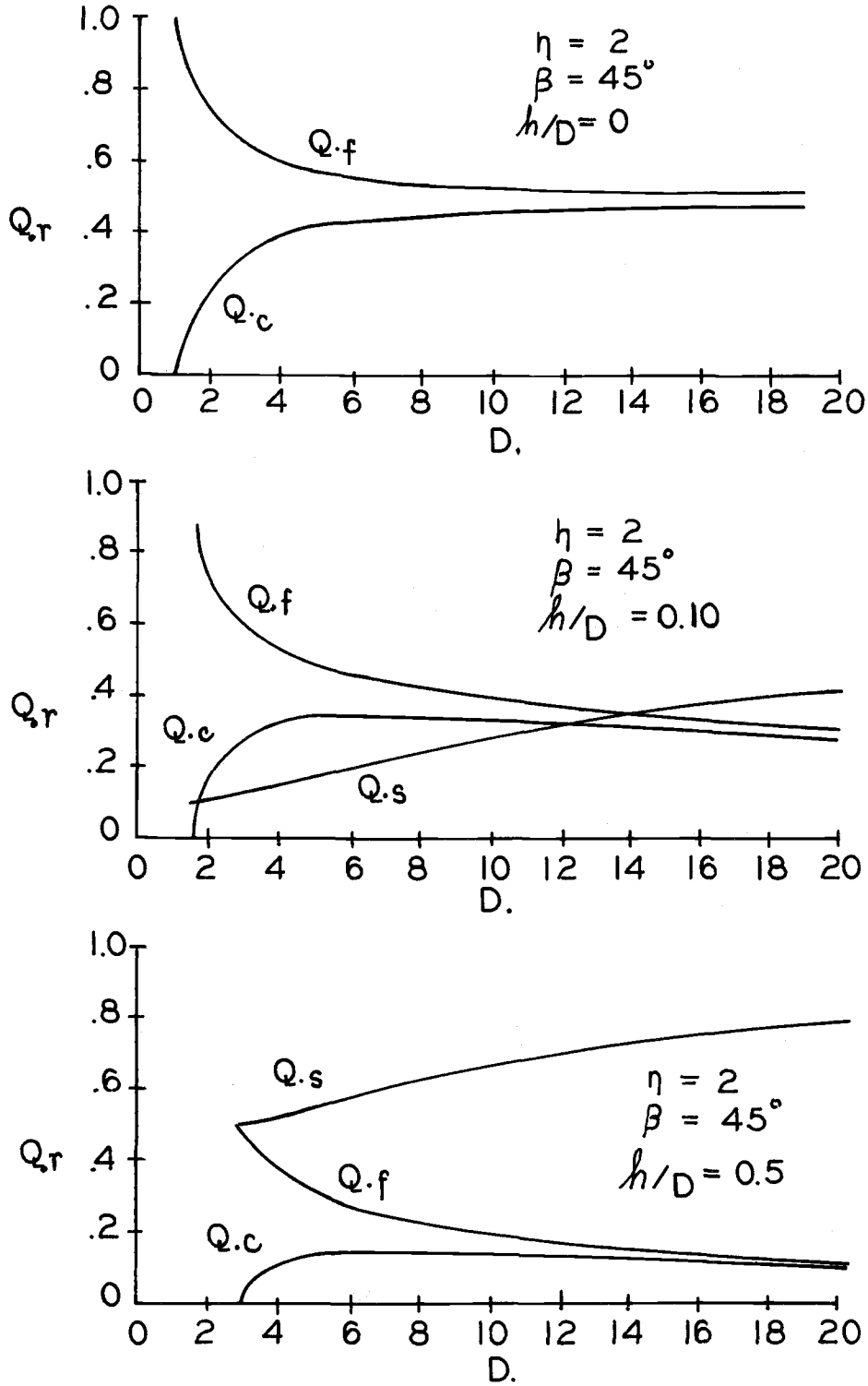

Figure III-4. Relative scaled discharge for three regions in an aquifer for $\eta=2$ dipping at 45° as a function of aquifer thickness and for various water table positions.

one-tenth of the thickness of the aquifer, the flow in the capillary region is less than 10 percent. The curve for the saturated region and the capillary fringe region is nearly symmetrical for all water table positions.

In Figure III-4, the angle of dip has been increased to 45° for aquifers having the same water table positions and pore size distribution as for Figure III-2. The angle of aquifer dip does not substantially change the distribution of flow within the three regions. The greatest reduction of flow in the three regions of the aquifer when the angle of dip is increased occurs for relatively thin aquifers.

In Figure III-5, the water table position in the aquifer may be obtained for a particular aquifer thickness that will produce the maximum flow in the aquifer. The maximum flow will occur in an aquifer when Q_c is zero. For example, if an aquifer has a scaled thickness of 5 and its dip is 10°, the water table must occupy 0.8 of the aquifer to eliminate the flow in the capillary region.

III.1.3 CONCLUSIONS

Most subsurface agricultural drainage occurs in relatively thin aquifers having little or no slope and the total flow toward the drains passes thru the three regions mentioned above.

The relative flux in the capillary region is less for aquifers with uniform pore size distributions than for aquifers with a wide range of pore sizes.

For relatively thin aquifers, the flow in the "fringe" region may be a significant part of the total flow, particularly when the water table occupies less than half of the total relative thickness of the aquifer. The effect is changed only slightly by a more narrow range of pore sizes in the aquifer.

In general, for relatively thin aquifers, when the water table occupies a position less than half of the relative thickness of the aquifer, the flow above the water table will make a significant contribution to the total flow.

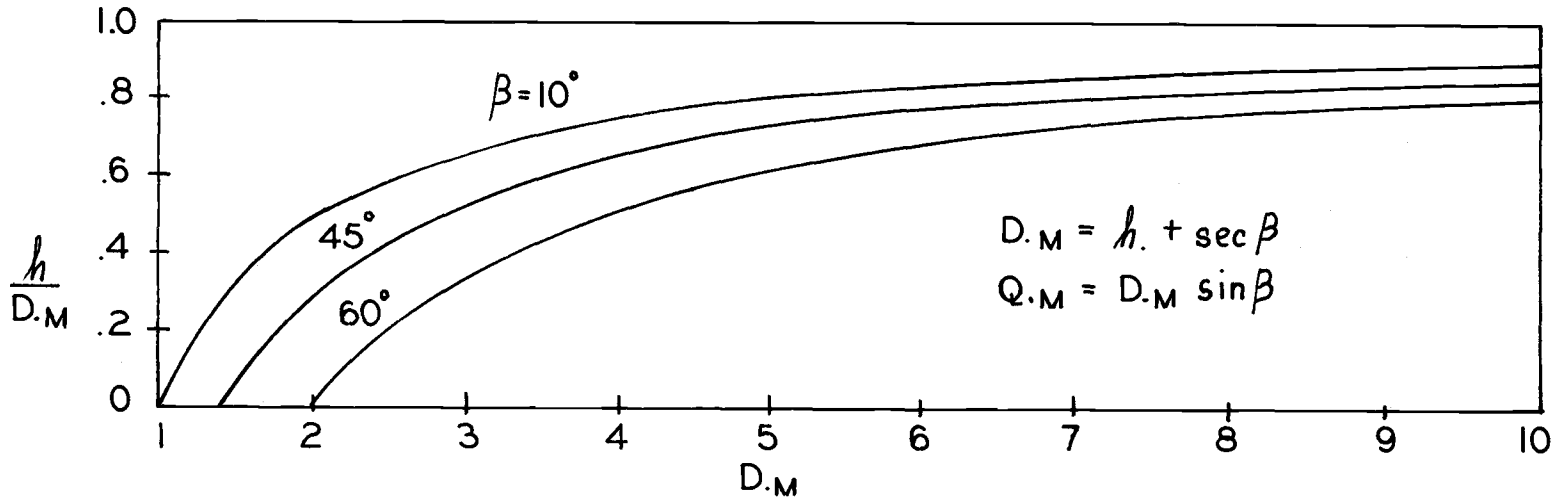

Figure III-5. Relative water table positions as a function of maximum aquifer thickness that will produce a maximum discharge for various angles of aquifer dip.

For example, if the bubbling pressure head is 1.0 feet, then an aquifer six feet thick will have a relative thickness of 6.0 and if the water table is 0.6 feet above the impermeable layer or occupies one-tenth of the aquifer thickness, then the flow above the water table will be from 48 to 77 percent of the total flow depending upon the pore size distribution. The flow in the capillary region above the "fringe" on the other hand will be from 6 to 35 percent of the total flow.

When one considers the importance of flow above the water table, it must be considered in relative terms. Hopefully, this simple flow geometry will provide engineers with an additional qualitative tool for making a decision as to the importance of considering flow above the water table.

III.2 WATER TABLE RESPONSE TO PARALLEL DRAINS by H. R. Duke

A preceding section illustrated how the effects of capillary conductivity and capillary storage can be evaluated from measurable soil properties. This analysis provides a method by which the shape and position of the water table can be evaluated even when the capillary region significantly influences the distribution of flux.

This section of the paper describes the results of a mathematical model, based upon the Dupuit-Forchheimer assumptions, used to analyze the combined effects of saturated and partially saturated flow on the performance of drains in shallow aquifers.

Admittedly, current technology could provide a more rigorous mathematical approach than has been attempted here, since this approach accepts the Dupuit-Forchheimer approximation. In later sections of this paper, the predicted performance is shown to agree quite well with experimental data. This observation is accepted as evidence of the adequacy of the approach used.

This study is limited to shallow, horizontal aquifers underlain at uniform depth by an impermeable boundary. The drainage systems considered are restricted to fully penetrating, parallel, open ditches of sufficient length that fluxes have components in only two dimensions. The soils encountered are assumed to be homogeneous, isotropic, and stable with time.

Under these conditions, the position of the water table is evaluated as affected by the depth of tailwater in the ditch, rate of uniform infiltration, bubbling pressure head, and distribution of pore sizes in the soil.

III.2.1 INADEQUACY OF CLASSICAL DRAINAGE THEORIES

A series of laboratory experiments was performed using a large sand-filled flume to illustrate the effect of the capillary region, and to verify the results of the numerical model. The experimental data are compared with two analytical solutions; one typical of the classical solutions to equilibrium drainage and the other to transient drainage problems. The ellipse equation and Glover's equation for the case of the drain on the impermeable boundary, respectively, are compared with experimental data to illustrate that neglecting the effects of the capillary region can lead to

significant errors. Figure III-6 shows a comparison of the solution to the ellipse equation with the steady state water table measured in the large flume. The measured

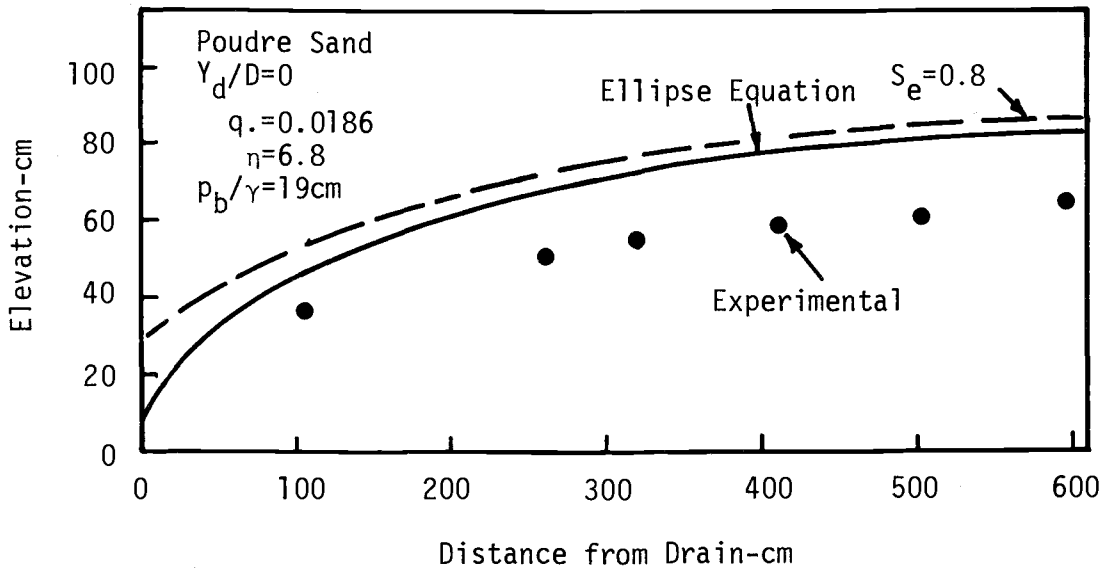

Figure III-6. Comparison of solution to the ellipse equation with experimentally determined equilibrium water table position

water table is lower at the centerline than predicted by the ellipse equation. This observation indicates that the ellipse equation results in an underestimation of the spacing which will maintain the desired water table position.

Figure III-7 compares the solution of Glover's equation with the experimental data of Hedstrom et al (1971). Glover's equation predicts a significantly slower decline of the water table than observed experimentally. Thus, like the equilibrium equation, the classical equation for transient drainage underestimates the spacing for a given water table response.

The degree of deviation of experimental data from theory shown in Figures III-6 and III-7 may not be observed in field installations designed by an experienced drainage engineer. The design values of specific yield and water table depth are usually based upon previous experience with similar drainage systems in similar soils. As a result, the value of specific yield normally used in design calculations is an artificial value, which forces the fit between experimental data and theory. Duke (1972) discussed the hazard of using such artificial values of specific yield when the depth to water table differs significantly from that at which the specific yield was evaluated.

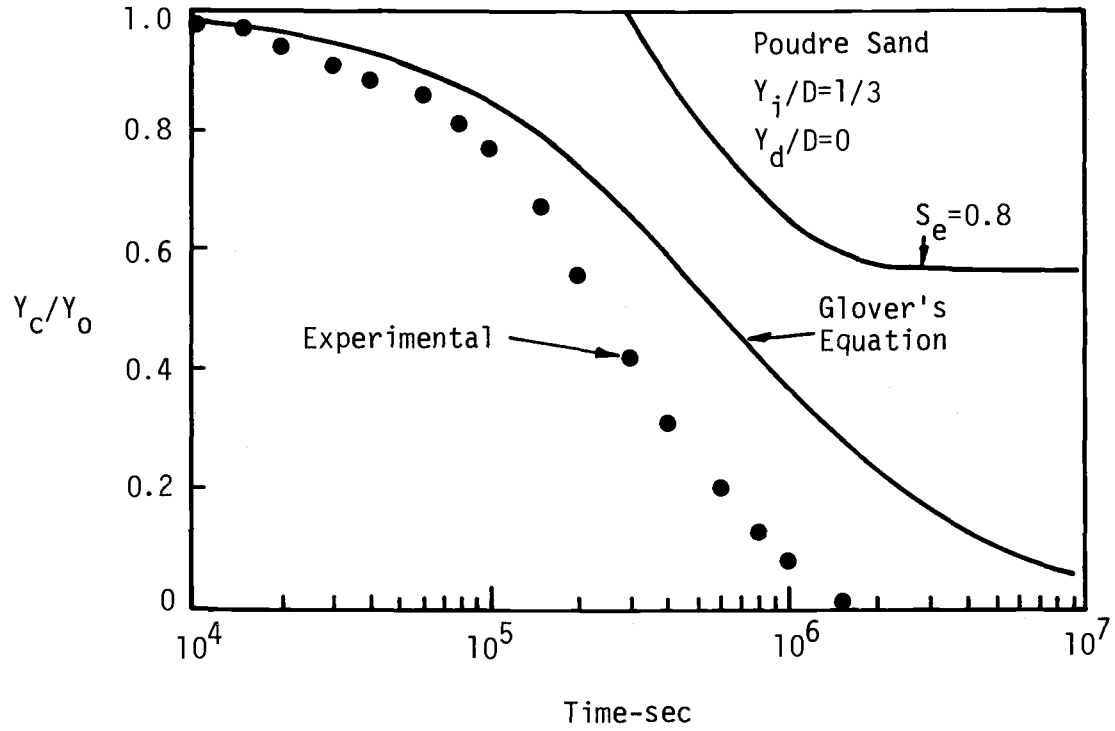

Figure III-7. Comparison of solution to Glover's equation with experimentally observed decline of the water table

Such "rule of thumb" practices undoubtedly give satisfactory results in areas where considerable past experience is available, but fail to give due consideration to those parameters that can result in significant differences in the flow situation.

III.2.2 SHAPE AND POSITION OF THE WATER TABLE

The numerical model was used to simulate 156 combinations of boundary and initial conditions, soil properties, and infiltration rates. The numerical results discussed represent typical examples of the cases evaluated.

III.2.2.1 Steady state. The effect of the capillary region upon the equilibrium position of the water table depends on the effective permeable height of the capillary region. Figure III-8 indicates the effect of increasing H_k by increasing the bubbling pressure head.

The upper curve of this figure represents the solution to the ellipse equation, i.e., capillary flow is neglected. As the effective permeable height, H_k, is

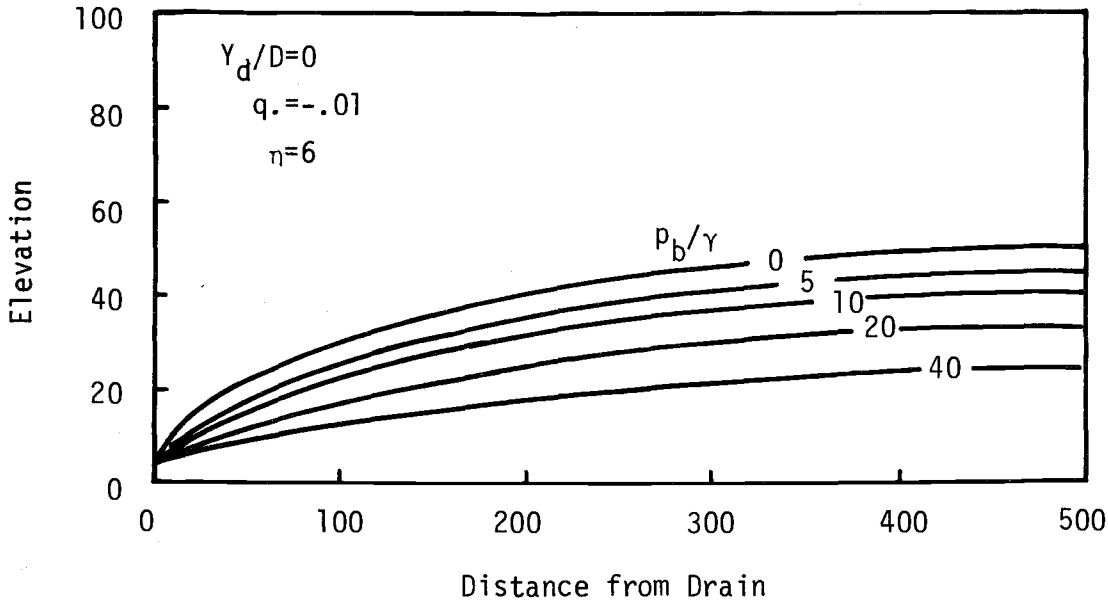

Figure III-8. Relative effect of bubbling pressure head upon equilibrium water table position

increased, the area, through which horizontal flow can occur, is increased. Since the uniform flux is constant, the result of increasing H_k is that smaller gradients are required and the water table becomes flatter. Since H_k is directly proportional to p_b/γ, the effect of increasing p_b/γ is significantly reflected in the water table position.

The water table position is not nearly as sensitive to η as it is to p_b/γ, since H_k is affected relatively little by η. The primary result of increased infiltration is to increase the water table elevation. This increase in water table elevation reduces the fraction of the flow moving through the capillary region by increasing the depth of saturated soil relative to H_k. As long as the water table is shallow, H_k itself is little influenced by this increased flux, since increasing $q.$ tends to increase H_k, while the higher water table results in a smaller distance from water table to soil surface and tends to decrease H_k. As a result, the magnitude of the error in water table elevation resulting from neglecting capillary flow is relatively independent of flux. The relative error, however, decreases as the infiltration rate is increased.

III.2.2.2 Transient flow. When the water table position changes with time, the contribution of the capillary region depends on both the conductivity and the saturation characteristics of the soil in the capillary zone. Hedstrom et al (1971) demonstrated that the capillary region significantly affects transient performance of drains. Their techniques, however, did not allow evaluation of the relative effects of the effective permeable height, H_k, and the effective saturated height, H_s, upon transient drainage. The numerical model developed for this study is capable of such analyses, and can simulate no capillary effects (H_k and H_s assumed zero), the influence of capillary conductivity only ($H_s = 0$) or the combined effects of capillary conductivity and capillary storage. Figure III-9 shows one such analysis, considering each of the three alternatives for treating the capillary region.

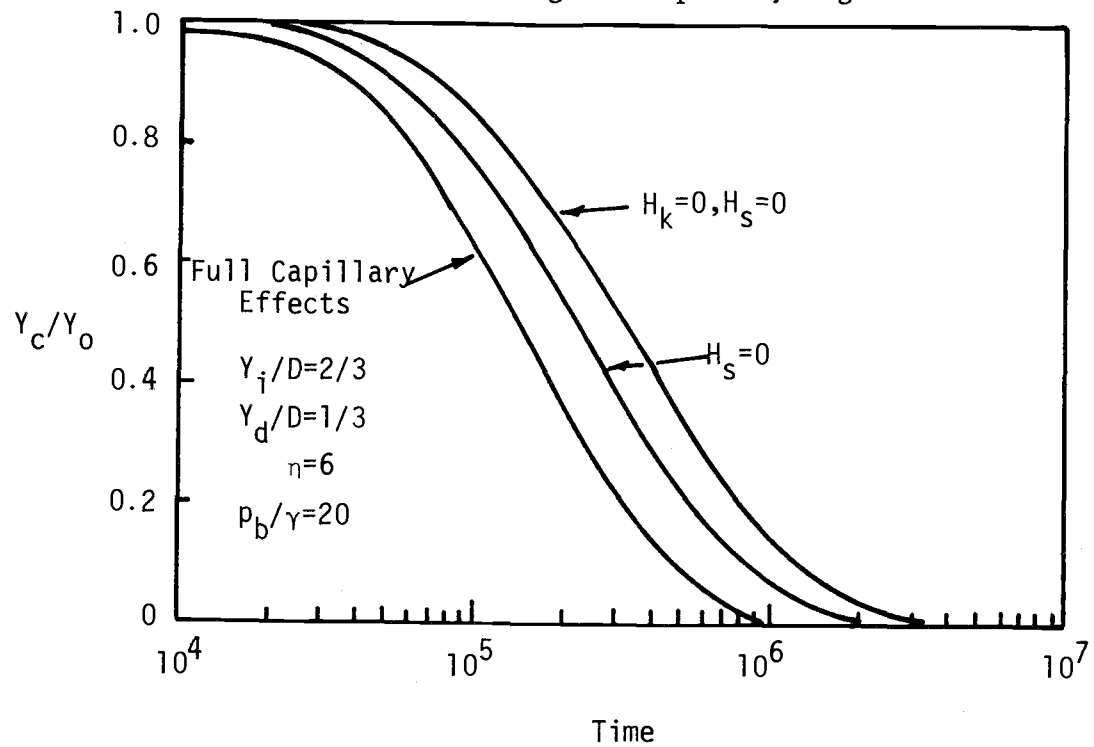

Figure III-9. Comparison of the relative importance of capillary conductivity and capillary storage to decline of the water table at the centerline

For the boundary conditions of the analysis shown, the effects of H_k and H_s are of the same order of magnitude. As in the steady state problem, the capillary region tends to increase the depth through which flow can occur. This increased flow depth tends to increase the rate of flow, and, consequently, increases the rate of water table decline. Since H_s increases less rapidly than does water table depth, the apparent specific yield increases with increasing water-table depth. The low apparent specific yield at early time also increases the rate of water table decline,

since a smaller volume of water must be removed from the soil to obtain a given water table decline.

Capillary flow is directly proportional to the magnitude of H_k . Therefore, since H_k approaches a constant at relatively shallow water table depth, the conductivity contribution of the capillary region is little affected by water table depth, as long as this depth is significantly greater than p_b/γ . However, H_s is quite sensitive to water table depth over a wide range. The influence of H_s upon release of capillary water is not dependent upon the magnitude of H_s , but rather upon dH_s/dH (i.e., rate of change of H_s with respect to water table depth). Since dH_s/dH is largest for small water table depth, the effect of capillary storage is more pronounced when the water table is shallow.

The effects of increasing p_b/γ upon the rate of water table decline are illustrated in Figure III-10. As in the case of steady drainage, the capillary zone has a

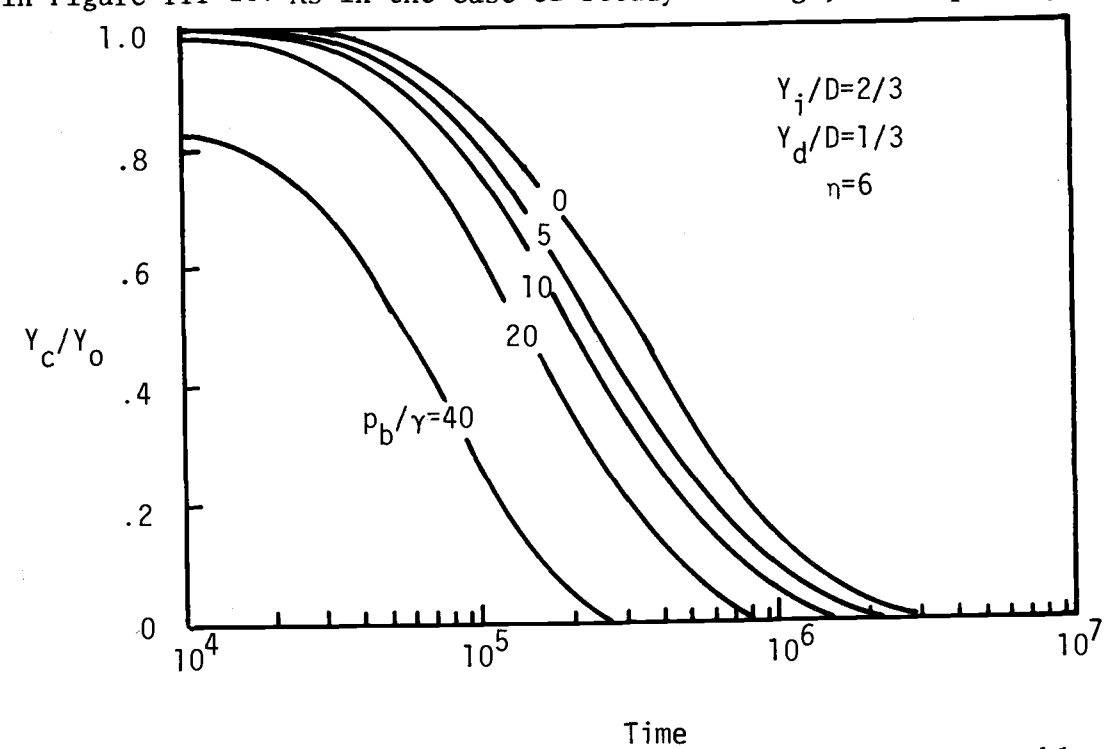

Figure III-10. Effect of bubbling pressure head upon transient water table response

capacity to transmit flow toward the drain. As a result, increasing p_b/γ increases the effective permeable height, H_k , and drainage proceeds more rapidly. Since H_s is also directly proportional to p_b/γ , the effect of capillary storage becomes more pronounced as p_b/γ is increased. For the initial condition illustrated in Figure III-9,

the soil was initially saturated to the surface for $p_b/\gamma = 40$. As a result, the water table decline at the centerline was almost instantaneous to the point where the surface soil began to desaturate, thus accounting for the low water table at early time.

The rate of water-table decline is not as sensitive to η as to p_b/γ . The sensitivity to changes in η decreases as η becomes large. So long as p_b/γ is finite, the water table must drop more rapidly than indicated by analyses neglecting capillary flow, regardless of the value of η . Note that as $\eta \to \infty$, H and H_s approach p_b/γ , rather than zero.

Because of differences in shape of drawdown curves, it is rather impractical to compare the entire curve for various initial, boundary, and capillary conditions. Further comparisons of water table response are based on the time required to achieve an arbitrarily selected fraction of the total available drawdown. The relative drawdown, Y_c/Y_o , selected for such comparisons is 0.8.

Figure III-11 illustrates the time to reach this 80% of the initial water table height relative to the corresponding time if capillary effects are neglected. Again, this figure illustrates the reduced effectiveness of the capillary region at high bubbling pressures. The extremely fast response at high bubbling pressure for the case $Y_i/D = 2/3$, $Y_d/D = 1/3$ is because the soil profile remains saturated to the surface during early time over a significant portion of the distance between drains. Figure III-11 also illustrates the effect of the initial water table level upon drain response. At early time, the capillary region provides a larger flow area compared to the depth below the water table as the initial water table depth is decreased. This larger area for flow results in more rapid drawdown for the lower initial water table. As bubbling pressure head is increased, this difference in effective flow depth is offset by increased convergence losses in the capillary region.

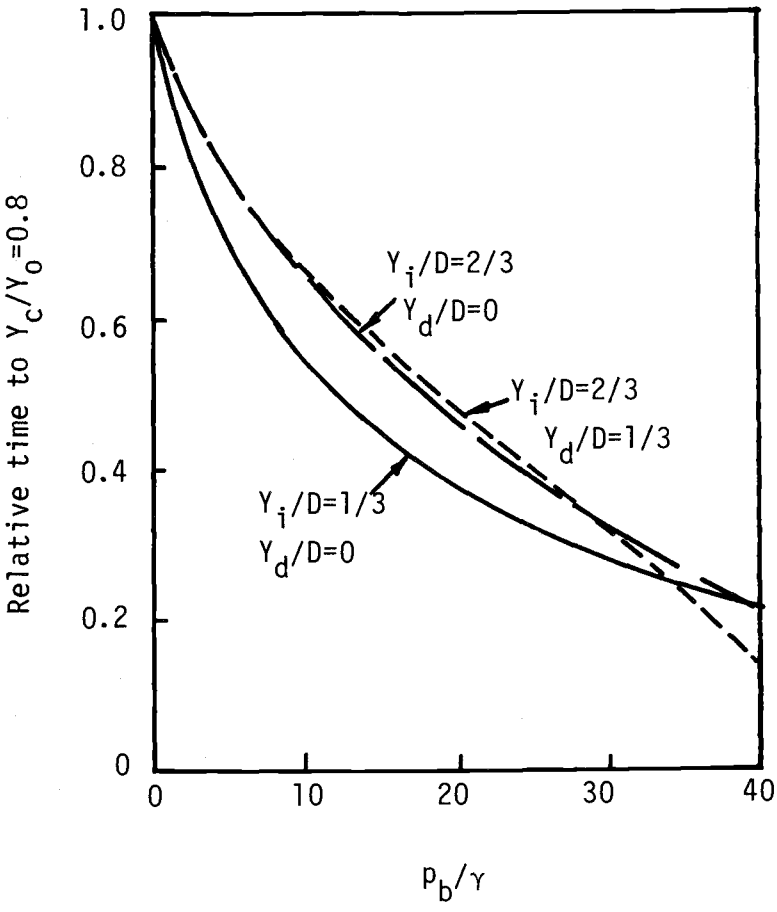

Figure III-11. Effect of bubbling pressure head upon relative time required to lower water table to 80 percent of the initial drainable depth.

III.3 SOIL PROFILE AERATION by H. R. Duke

Although aeration of the crop root zone is one of the primary objectives of agricultural drainage, present methods of design consider this factor only insofar as the depth of water table is specified. In reality, the position of the water table is of little direct importance. More important is the effect of the water table upon movement of water and air within the partially saturated root zone. The results of investigations by Stegman et al (1966) implied that adequate soil aeration may be achieved by maintaining the effective saturation below some maximum value within the root zone.

Thus, besides determining the position of the water table (considering both saturated and partially saturated flow), adequate drain design should include evaluation of soil water content above the water table and its effect on soil aeration.

III.3.1 REGION OF AERATION

A preceding section has indicated the manner in which the water table position is affected by the capillary flow region. This section is devoted to a discussion of the effects of the region of insufficient aeration above the water table upon drain design. The effect of the capillary region upon design spacing of drains is evaluated by assuming that the upper limit of this zone of insufficient aeration satisfies the same aeration requirements as the water table calculated by neglecting capillary flow. Thus, an equivalent spacing is defined that will give a water table elevation (neglecting capillary flow) equal to the elevation of the zone of insufficient aeration. For purposes of this discussion, it is assumed that the soil is adequately aerated whenever the effective saturation is less than 0.8.

For a given soil and flux of water, the ability of the soil to support a significant rate of gaseous diffusion is severely restricted for some distance above the water table. In fact, the gaseous phase is not continuous below the elevation at which the capillary pressure equals the bubbling pressure. Above this elevation, z', the fraction of air increases with elevation. At some distance above the water table, z_A, the air phase may reach such a magnitude that gaseous transfer with the atmosphere is sufficient to maintain plant growth.

The critical effective saturation, S_A, may be expressed in terms of its corresponding critical capillary pressure, p_A by the Brooks-Corey expression, as

$$S_A = (p_b/p_A)^{\lambda} \quad . \tag{III-14}$$

Then

$$p_A/\gamma = (p_b/\gamma)\ S_A^{-1/\lambda} \tag{III-15}$$

and the problem is to determine the elevation, z_A, above the water table at which p_A occurs.

III.3.1.1 Static equilibrium. When the soil water profile is in static equilibrium with the water table $z = p_c/\gamma$, and Equation (III-15) can be written employing the previous scaling criteria, i.e., $z_A. = \gamma z_A/p_b$, as

$$z_A. = S_A^{-1/\lambda} \quad . \tag{III-16}$$

Note that this equation is valid only for $H. > 1$, since no air phase exists when $p_c \leq p_b$.

III.3.1.2 Steady downward flow. When steady percolation toward the water table occurs, capillary pressures are reduced, and z_A occurs at a greater elevation (if at all) than in the case of static equilibrium. Since the surface capillary pressure decreases with increasing flow rate, z_A must be less than the surface capillary pressure head if S_A exists within the soil profile. Thus, a maximum percolation rate exists, beyond which a suitable root environment is nonexistent. At this limit

$$-\varepsilon q. \leq (p_b/p_A)^{\eta} \quad . \tag{III-17}$$

Substituting Equation (III-17) into (III-16) and solving for the maximum percolation rate gives

$$-q. \leq \frac{S_A^{\eta/\lambda}}{\varepsilon} \quad . \tag{III-18}$$

Assuming that this limitation of $q.$ is satisfied, and noting that z_A can exist

only in the region $z' < z_A \leq z''$, then the relation between elevation and pressure is described by

$$d_z = \frac{p_b}{\gamma} \frac{dp.}{(1 + q.p.^{\eta})} \quad . \tag{III-19}$$

Integrating Equation (III-19) between the limits $z. = 1$ at $z = z'$ and $z. = S_A^{-1/\lambda}$ at $z = z_A$, and expressing the result in terms of scaled variables gives

$$z_{A.} = \frac{1}{1+q.} + \int_1^{S_A^{-1/\lambda}} \frac{dp.}{1 + q.p.^{\eta}} \tag{III-20}$$

where $q.$ has a negative value.

Figure III-11 illustrates the effect of η upon $z_{A.}$ when the vertical flux is zero. Elevation $z_{A.}$ is very sensitive to changes in η for small η , but changes less than 20 percent as η increases from 6 to infinity. The effect of η upon $z_{A.}$ depends strongly on the selected value of S_A . At large S_A , η has little effect upon $z_{A.}$, but for smaller S_A , the variation of $z_{A.}$ with η becomes very large.

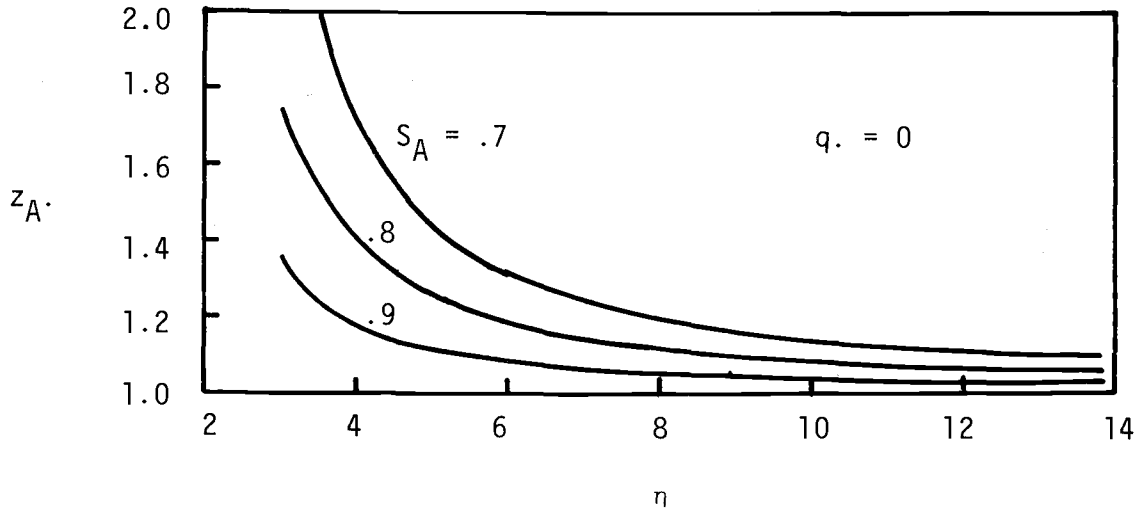

Figure III-12. Effect of η upon scaled height of insufficient aeration, static equilibrium

Figure III-13 shows the relation between $z_{A.}$ and downward flux $(-q.)$ for $S_A = 0.8$. From this figure, it is seen that $z_{A.}$ differs from the static equilibrium value in excess of 10 percent only for $-q.$ greater than about 0.07. Therefore, the static equilibrium value should be an adequate approximation to z_A , over a wide range of $q.$. Again, however, this relationship between $q.$ and $z_{A.}$ is dependent

upon the selected value of S_A . For lower values of S_A , the range of $q.$, over which the equilibrium value is adequate, is considerably smaller.

When a downward flux persists, there is a minimum saturation that can exist. Conversely, for any value of S_A and η there is a maximum downward flow rate beyond which the selected S_A cannot exist. This maximum flow rate, given by Equation (III-18) is shown graphically as a function of η in Figure III-14. The maximum flux is most sensitive to η at low values of η . Unless a very low S_A is required (or the saturated hydraulic conductivity is quite low) this restriction on $q.$ is not likely to eliminate the zone of aeration under typical drainage conditions.

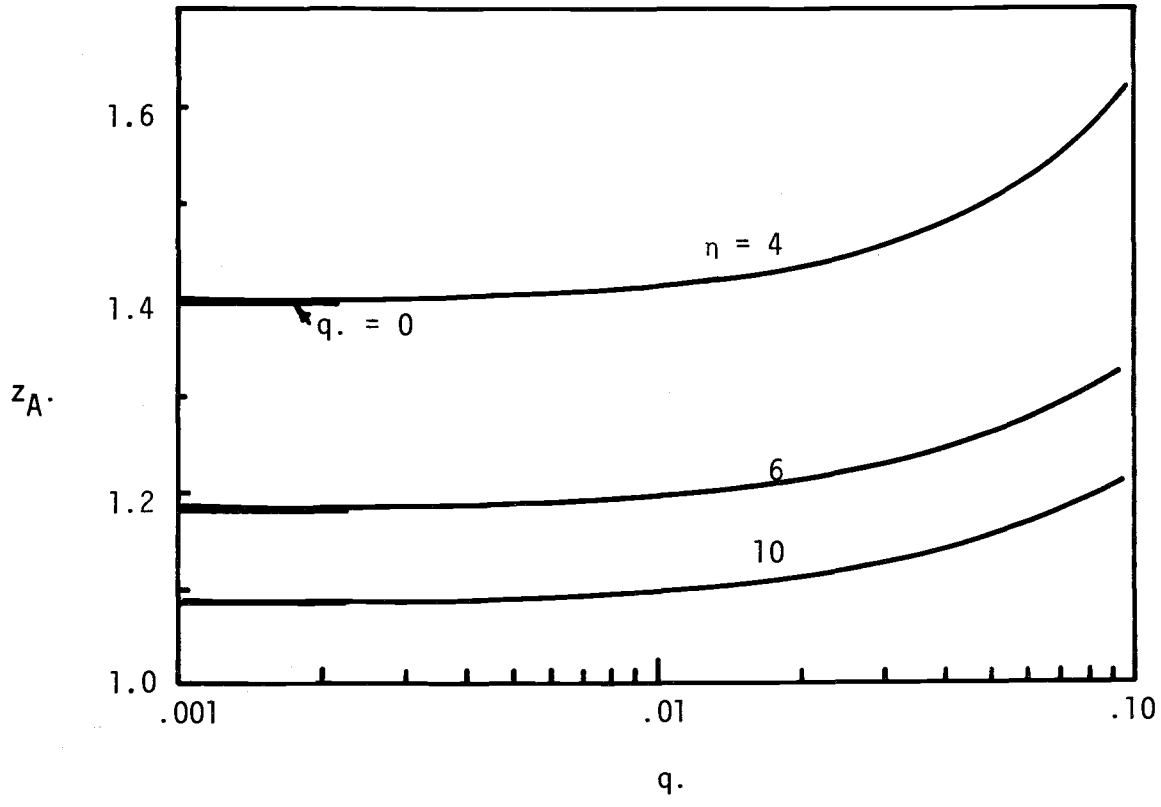

Figure III-13. Effect of downward flux on height of zone of insufficient aeration

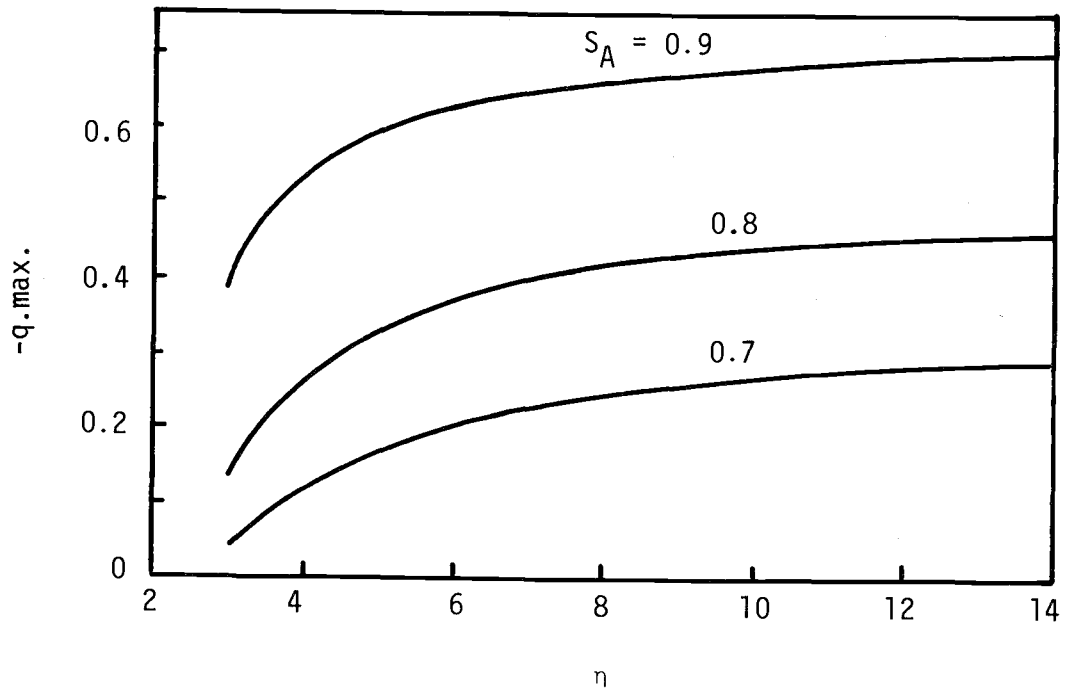

Figure III-14. Effect of η upon the maximum downward flux at which a given S_A can exist

III.3.2 AERATION ABOVE THE WATER TABLE

In the preceding discussions, it has been shown that the effect of η upon H_K, H_S, and z_A are relatively small for large values of η. However, the same conclusion cannot be drawn regarding the effect of bubbling pressure head, p_b/γ. Since p_b/γ is the scaling parameter for the dimensionless form of each of these terms, the effective permeable and saturated heights and the height of the zone of inadequate aeration are directly proportional to p_b/γ. Therefore, except for very low η values, such as may be characteristic of clay soils, the value of bubbling pressure head is expected to be a more important parameter than is η.

Having evaluated the height of the zone of insufficient aeration, we can determine the adequately aerated root zone by adding z_A to the water table elevation discussed in a previous section.

III.3.2.1 Steady state. Figure III-15 illustrates the equilibrium position of the surface where $S_A = 0.8$ for the water table profiles discussed in the previous

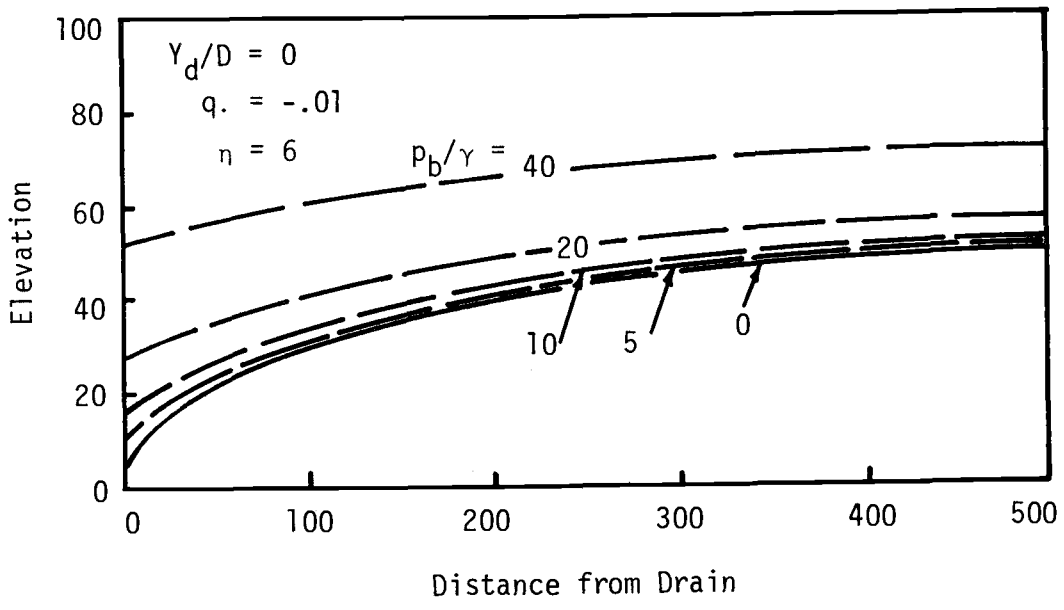

Figure III-15. Effect of bubbling pressure head upon aeration profile, steady state drainage

section. In every case, the height of the zone of insufficient aeration, z_A, (calculated from Equation (III-20)) is greater than the depression of the water table resulting from consideration of capillary flow. As a result, increasing the bubbling pressure head results in a decreased depth of adequately aerated soil, even though the water table elevation is decreased.

The sensitivity to changes in η decreases with increasing η, just like water-table response. The position of the aerated zone is much less sensitive to η than to p_b/γ, as indicated by Equation (III-20) (i.e., z_A is directly proportional to p_b/γ).

Figure III-16 illustrates the effects of p_b/γ upon the height of the zone of insufficient aeration, Y_A, at the centerline between drains. Since the water table decrease is always less than p_b/γ, Y_A continues to increase with increasing bubbling pressure head. The effect of p_b/γ upon Y_A decreases somewhat as the water level in the ditch is decreased. This results from the increased effect of p_b/γ upon water table elevation for small Y_d, and the fact that Y_A is independent of water table depth.

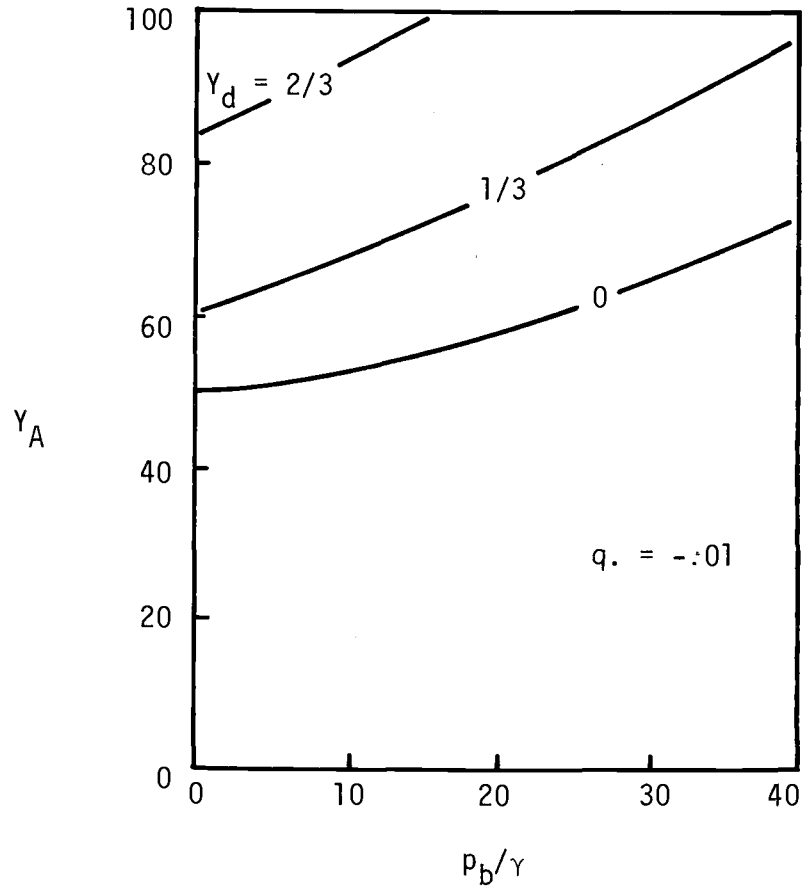

Figure III-16. Effect of p_b/γ upon height of zone of insufficient aeration at centerline

As evidenced by the curve for $Y_d/D = 2/3$, it is entirely possible that the soil will have no zone of adequate aeration at the centerline, if the bubbling pressure is sufficiently large and the water table is near the surface.

The effects of the capillary region upon drain design are presented in terms of a relative spacing. This relative spacing is the effective spacing (the spacing calculated by neglecting capillary flow, which will result in a water table at the same elevation as Y_A calculated by considering capillary flow) divided by the actual drain spacing. Thus, this relative spacing is an indication of the spacing error resulting from neglecting the effects of the capillary region.

Figure III-17 illustrates the effect of bubbling pressure head and of tailwater level upon the relative spacing. Because of relatively small effects of capillary flow

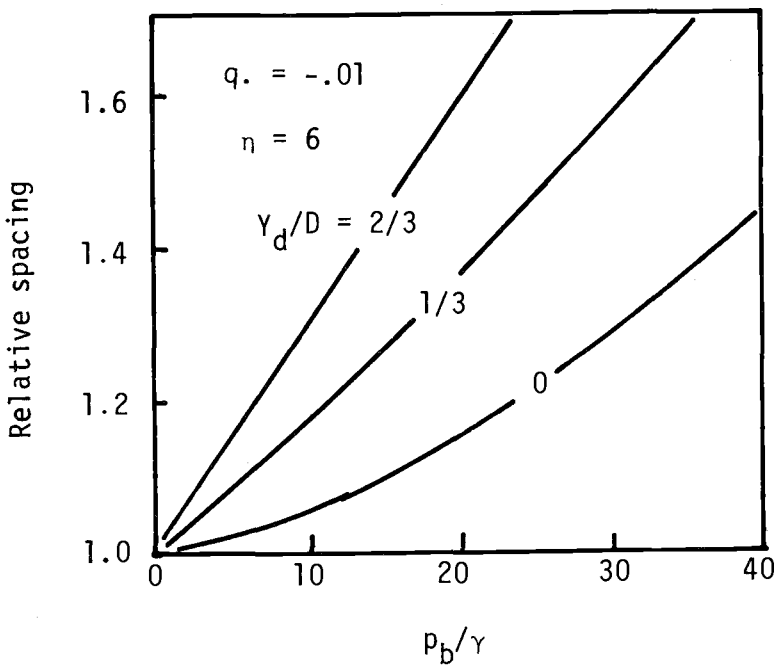

Figure III-17. Effect of bubbling pressure head and tailwater level upon relative drain spacing

upon water table position, the relative spacing increases as depth of tailwater increases (i.e., as gradient decreases). The influence of convergence upon the effectiveness of the capillary zone is again apparent for $Y_d/D = 0$, since the rate of change of relative spacing with respect to p_b/γ increases with increasing bubbling pressure head.

The relative spacing is increased by either reducing the percolation rate or by raising the tailwater level. Either of these changes results in smaller water table gradients. As discussed earlier, the effect of the capillary region upon the position of the water table is small when small water table gradients exist. Since z_A is independent of water table gradient and depth to water table, water table gradients are small that result in the greatest effects upon Y_A. Such small water table gradients exist whenever the infiltration rate is low or the tailwater depth (thus the equivalent flow depth) is large.

III.3.2.2 Transient drainage. During transient drainage, the zone of insufficient aeration above the water table is assumed to have a constant thickness with time. That is z_A is assumed to be the equilibrium value given by Equation (III-16). The

basis for comparison of drain performance is arbitrarily selected as the time required to reduce the zone of inadequate aeration at the centerline between drains, Y_A, to 0.8 of the original drainable water table depth. Figure III-18 illustrates the effect of bubbling pressure head upon the rate of decline of the surface of aeration. Although the rate of decline of the water table is increased by large values of p_b/γ,

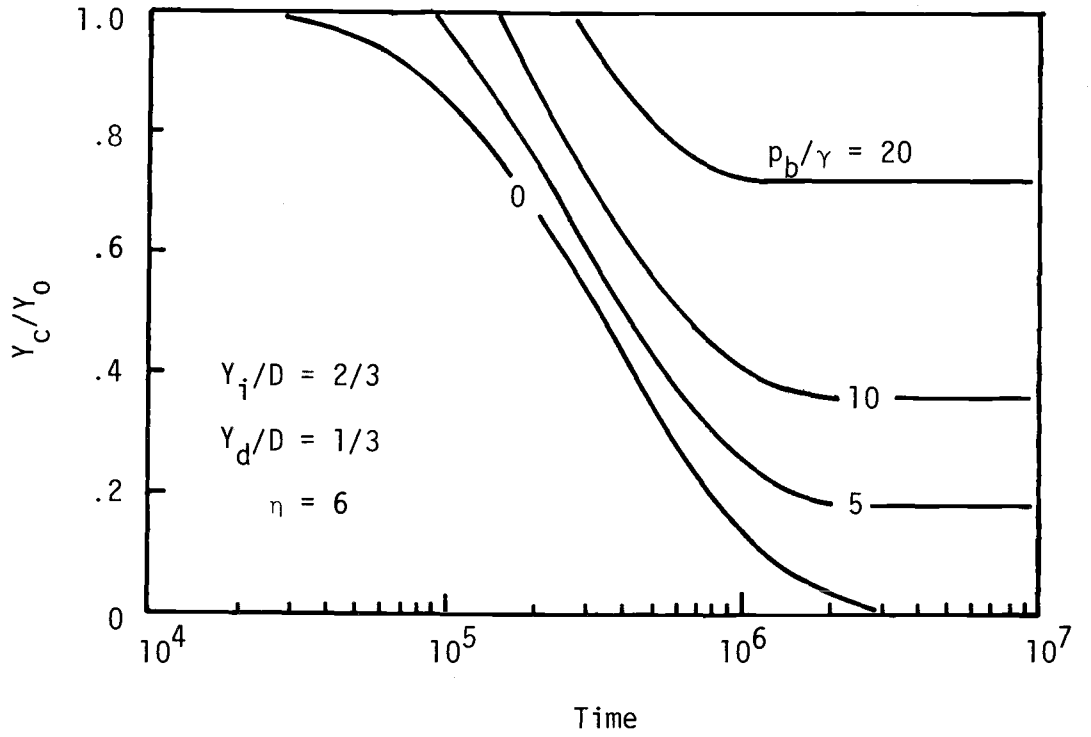

Figure III-18. Effect of bubbling pressure head upon rate of decline of the zone of insufficient aeration

the effect of the capillary zone upon position of the water table is not as large as the value of z_A. As a result, increasing the bubbling pressure head delays the rate of decline of the zone of insufficient aeration. If z_A is greater than the initial drainable depth, the aerated zone will never decline below the initial water elevation, as apparent for the case $p_b/\gamma = 40$ in Figure III-18. As drainage progresses toward the final water table elevation, Y_d, the zone of inadequate aeration, Y_A, approaches the constant elevation, $Y_d + z_A$.

Since the final water-table elevation, Y_d, is independent of effects of the capillary region, the ultimate effects of η upon Y_A are somewhat larger than for the case of equilibrium. During early stages of aeration within the region considered, water table gradients are larger for large η. The resulting higher water table tends to compensate for small values of z_A. As a result the effects of η are initially small and tend to increase with time.

From the discussion of equilibrium drainage, one would expect the relative spacing to increase as the drainable depth (i.e., $Y_i - Y_d$) decreases. Figure III-19 illustrates the effect of the initial and final water table depths upon relative

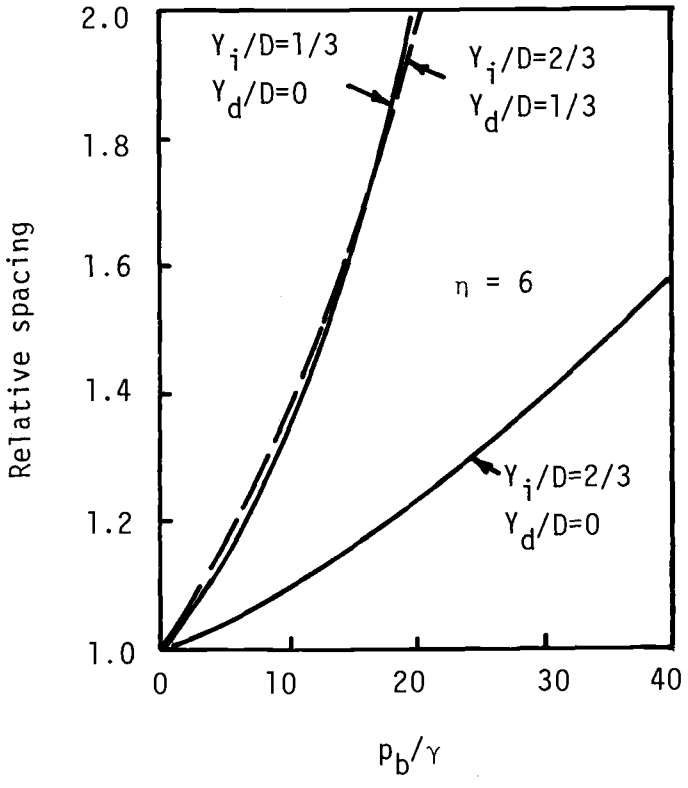

Figure III-19. Effect of bubbling pressure head on relative spacing for various initial and final boundary conditions

spacing. The effects of increased convergence losses, due to smaller saturated thickness are reflected in the slightly larger relative spacing shown for the case where the tailwater depth is zero.

The magnitude of the errors resulting from spacing calculations, based upon the assumption of no capillary flow, depends upon the degree of aeration required. If the effective saturation required for adequate aeration is less than the value (0.8) selected in this discussion, the relative spacing will be even greater than that indicated. From the standpoint of drain design, this means that drains must be spaced more closely, and possibly deeper, to maintain an optimum environment for plant roots.

The previous discussion has shown that neglecting the effects of the capillary region on drain performance can result in serious design deficiencies. The use of

classical drainage theories to evaluate drain spacing always results in an overestimate of the maximum spacing. The degree of overestimation depends on the soil characteristics, the infiltration rate, initial and boundary conditions, and the degree of aeration required within the root zone.

The analyses performed for this study are insufficient in scope to justify any general design criteria. They do, however, indicate the manner in which various parameters affect the error resulting from neglecting the capillary region.

The bubbling pressure head, p_b/γ is the most significant soil property affecting the adequacy of classical drainage theories. As p_b/γ increases, the classical theories provide a less accurate description of actual drain performance. The pore-size distribution, η , is significantly less important in evaluating drain performance than is p_b/γ , especially for large values of η . This suggests that, if p_b/γ can be determined accurately, then η (which is considerably more difficult to evaluate) could possibly be estimated with sufficient accuracy from a qualitative inspection of the particle-size distribution.

In general, the classical theories provide the least adequate evaluation of drainage when water table gradients are small. Such conditions may result from low infiltration rates, q , high hydraulic conductivity, K , (although large K is usually associated with small p_b/γ), a large saturated thickness of soil, or a large capillary region with respect to the total soil depth.

REFERENCES CITED

1. Brooks, R. H., and A. T. Corey. 1964. Hydraulic properties of porous media. Hydrology Paper No. 3, Colorado State University, Fort Collins, Colorado.

2. Brooks, R. H., B. Ng, G. L. Corey, A. T. Corey. 1971. Drainage of soil profiles. Journal of the Irrigaton and Drainage Division, American Society of Civil Engineers, IR3:455-467, September 1971.

3. Brutsaert, W. 1968. The permeability of a porous medium determined from certain probability laws for pore-size distribution. Water Resources Research 4(2): 425. April.

4. Bouwer, H. 1964. Unsaturated flow in ground-water hydraulics. Journal of the Hydraulics Division, American Society of Civil Engineers, HY5:121-144.

5. Bouwer, H. 1966. Rapid field measurement of air entry value and hydraulic conductivity of soil as significant parameters in flow system analysis. Water Resources Research 2:729-739.

6. Burdine, N. T. 1953. Relative permeability calculations from pore-size distribution data. Petro. Trans., Amer. Inst. Mining Metal. Eng. 198:71-78.

7. Carman, P. C. 1937. Fluid flow through granular beds. Trans. Inst. Chem. Eng., London 15:150.

8. Childs, E. C. 1960. The nonsteady state of the water table in drained land. Journal of Geophysical Research 65:780-782.

9. Corey, A. T. 1954. Interrelation between gas and oil relative permeabilities. Pennsylvania State University, Mineral Industries Experiment Station Bulletin 64:29-35.

10. Corey, G. L., A. T. Corey, and R. H. Brooks. 1965. Similitude for non-steady drainage of partially saturated soils. Hydrology Paper No. 9, Colorado State University, Fort Collins, Colorado. August.

11. Donnan, W. W. 1947. Model tests of a tile-spacing formula. Soil Science Society of American Proceedings 11:131-136.

12. Douglas, J., Jr. and B. F. Jones, Jr. 1963. On predictor-corrector methods for non-linear parabolic differential equations. Journal of the Society for Industrial and Applied Math. 11:195-204.

13. Duke, H. R. 1972. Capillary properties of soils-influence upon specific yield. Transactions, American Society of Agricultural Engineers 15(4):688-691.

14. Fatt, I., and H. Dykstra. 1951. Relative permeability studies. J. Petro. Tech. 3(9):249-255. September.

15. Hayden, C. W., and W. H. Heinemann. 1968. A hand-operated undisturbed core sampler. Soil Science 106(2):153-156. August.

16. Hedstrom, W. E., A. T. Corey, and H. R. Duke. 1971. Models for sub-surface drainage. Hydrology Paper No. 48, Colorado State University, Fort Collins, Colorado. 56 pp.

17. Irmay, S. 1954. On the hydraulic conductivity of unsaturated soils. Transactions of the American Geophysical Union 35(3):463-467. June.

18. Kozeny, J. 1927. Ueber kapillare leitung des wassers in boden. Sitzungsber. Wien. Akad. Wissensch 136(2a):271-306.

19. Laliberte, G. E. and R. H. Brooks. 1967. Hydraulic properties of disturbed soil materials affected by porosity. Proceedings, Soil Science Society of America 31(4):451-454, July-August.

20. Laliberte, G. E., R. H. Brooks and A. T. Corey. 1968. Permeability calculated from desaturation data. Journal of the Irrigation and Drainage Division, American Society of Civil Engineers IR1:57-71, March.

21. Marshall, T. J. 1958. A relation between permeability and size distribution in pores. Journal of Soil Science 9:1-8.

22. Millington, R. J., and J. P. Quirk. 1961. Permeability of porous solids. Trans. Faraday Soc. 57:1200-1206.

23. Purcell, W. R. 1949. Capillary pressures, their measurement using mercury and calculations of permeability therefrom. J. Petro. Tech. 1(2):39-46.

24. Reeve, R. C., and R. H. Brooks. 1953. Equipment for subsampling and packing fragmented soil samples for air and water permeability tests. Soil Science Society of America Proceedings 17:333.

25. Rose, W. 1949. Theoretical generalization leading to evaluation of relative permeability. J. Petro. Tech. 1(5):111-125. May.

26. Sinclair, L. R. 1970. Hydraulic characteristics of undisturbed, unsaturated agricultural soils. Master's thesis. Department of Agricultural Engineering, University of Idaho, Moscow. August.

27. Sinclair, L. R. 1973. Permeability of unsaturated field soils predicted from desaturation data. Ph.D. dissertation, Department of Agricultural Engineering, University of Idaho, Moscow.

28. Stegman, E. C., A. E. Erickson and E. H. Kidder. 1966. Characterization of soil aeration during sprinkler irrigation. Summer Meeting, American Society of Agricultural Engineers, Paper No. 66-214, 18 pp.

29. Todd, D. K. 1959. Ground water hydrology. John Wiley and Sons, New York, 336 pp.

30. White, N. F., H. R. Duke, D. K. Sunada, and A. T. Corey. 1970. Physics of desaturation in porous materials. Journal of the Irrigation and Drainage Division, American Society of Civil Engineers, 96(IR2):165-191. June.

APPENDIX A

DEFINITION OF SYMBOLS USED

c	shape factor [n.d]
D	thickness of soil profile [L]
$D(\theta)$	soil water diffusivity function $[L^2T^{-1}]$
F	number of pores desaturating within a finite pressure increment [n.d.]
h	hydraulic head [L]
H	distance from water table to soil surface [L]
$H.$	dimensionless distance from water table to soil surface, $H\gamma/p_b$ [n.d.]
H_k	equivalent permeable depth of capillary zone [L]
$H_k.$	dimensionless permeable depth of capillary, $H_k\ \gamma/p_b$ [n.d.]
Hs	equivalent saturated depth of capillary zone [L]
$H_s.$	dimensionless saturated depth of capillary, $H_s\ \gamma/p_b$ [n.d.]
k	intrinsic permeability $[L^2]$
$k_{1.0}$	saturated permeability $[L^2]$
$k.$	dimensionless permeability, $k/k_{1.0}$ [n.d.]
K	hydraulic conductivity $[LT^{-1}]$
K_o	standard flux unit (later shown to be $K_{1.0}$) $[LT^{-1}]$
$K_{1.0}$	saturated hydraulic conductivity $[LT^{-1}]$
$K.$	dimensionless hydraulic conductivity (numerically equal to k. for same fluid properties), $K/K_{1.0}$ [n.d.]
L	geometric dimension [L]
L_o	standard length unit (later shown to be p_b/γ) [L]
ND	number of finite increments considered [n.d.]
p_A	capillary pressure above which aeration is adequate $[ML^{-1}T^{-2}]$

p_b bubbling pressure, pressure at which a continuous air phase first exists $[ML^{-1}T^{-2}]$

p_c capillary pressure, pressure in the nonwetting phase (air) minus pressure in the wetting phase (water) $[ML^{-1}T^{-2}]$

p_o standard pressure unit (later shown to be p_b) $[ML^{-1}T^{-2}]$

$p_.$ dimensionless capillary pressure, p_c/p_b [n.d.]

PA average capillary pressure head in a finite pressure increment [L]

q volumetric flux per unit area of porous medium $[LT^{-1}]$

$q_.$ dimensionless volumetric flux per unit area, $q/K_{1.0}$ [n.d.]

Q total horizontal flux per unit thickness of soil $[L^2T^{-1}]$

$Q_.$ dimensionless horizontal flux per unit thickness of soil, $Q/K_{1.0}$ [n.d.]

$Q._c$ dimensionless flux through partially saturated region [n.d.]

$Q._f$ dimensionless flux through capillary fringe [n.d.]

$Q._s$ dimensionless flux below the water table [n.d.]

r radius of a pore [L]

R hydraulic radius of a pore [L]

RA average pore radius corresponding to a finite pressure increment [L]

s arbitrary coordinate direction [L]

S saturation, the fraction of interconnected pore volume occupied by the wetting fluid (n.d.]

S_A maximum saturation at which aeration is adequate for root growth [n.d.]

S_e effective saturation, fraction of drainable pore volume occupied by the wetting phase [n.d.]

S_r residual saturation, fraction of pore volume occupied by wetting phase when $K \to 0$ [n.d.]

S_m maximum saturation attainable, may be < 1.0 if air is entrapped [n.d.]

SA average saturation corresponding to a finite pressure increment [n.d.]

t time [T]

t_o standard time unit [T]

T	tortuosity factor [n.d.]
V	volume of liquid [L^3]
V_d	volume of drainable liquid per unit area [L]
V_r	volume of water released per unit area by decline in water table [L]
V_s	bulk volume of soil [L^3]
X	horizontal space coordinate [L]
Y	water table elevation referred to impermeable boundary [L]
Y_A	minimum height at which aeration is adequate, referred to impermeable boundary [L]
Y_c	water table elevation midway between drains, referred to level in ditch [L]
Y_d	water level in ditch, referred to impermeable lower boundary [L]
Y_i	initial saturated thickness [L]
Y_k	apparent permeable depth [L]
Y_o	initial drainable depth referred to level in ditch [L]
Y_s	apparent saturated depth [L]
z	vertical space coordinate [L]
z_A	minimum height at which aeration is adequate, referred to water table [L]
$z.$	dimensionless elevation above arbitrary datum, $z\gamma/p_b$ [n.d.]
z'	elevation above water table at which $p_c = p_b$ [L]
z''	elevation above water table at which $K = \varepsilon/q/$ [L]
α	contact angle of liquid-air interface with solid [n.d.]
β	slope of impermeable lower boundary of aquifer [n.d.]
γ	specific weight of wetting phase fluid [$M.^{-2}T^{-2}$]
∇	gradient operator [L^{-1}]
∇	dimensionless gradient operator, $(p_b/\gamma)\nabla$ [n.d.]
ε	constant, greater than but arbitrarily close to unity [n.d.]

η negative slope of log-log plot of p_c/γ vs. K. [n.d.]

θ volumetric water content [n.d.]

λ pore size distribution index, negative slope of log-log plot of p_c/γ vs. S_e [n.d.]

μ viscosity of wetting phase $[ML^{-1}T^{-1}]$

σ surface tension coefficient $[MT^{-2}]$

ϕ total interconnected porosity of medium [n.d.]

ϕ_e effective or drainable porosity of medium $\phi(1-S_r)$ [n.d.]

APPENDIX B

PUBLICATIONS OF WRRC W-51 RELATED TO EFFECTS OF CAPILLARY FLOW

Anat, A., H. R. Duke and A. T. Corey. 1965. Steady upward flow from water tables. Colorado State University Hydrology Paper No. 7, 34 pp.

Brooks, R. H. and A. T. Corey. 1964. Hydraulic properties of porous media. Colorado State University Hydrology Paper No. 3, March.

Brooks, R. H. and A. T. Corey. 1964. Hydraulic properties of porous media and their relation to drainage design. Transactions ASAE 7(1).

Brooks, R. H. and A. T. Corey. 1966. Properties of porous media affecting fluid flow. J. Irrigation and Drainage Division, ASCE, June.

Brooks, R. H., B. Ng, G. L. Corey and A. T. Corey. 1971. Drainage of soil profiles. J. Irrigation and Drainage Division, ASCE, 97(IR3).

Corey, G. L. and A. T. Corey. 1967. Similitude for drainage of soils. J. Irrigation and Drainage Division, ASCE, 93(IR3):3-23.

Corey, G. L., A. T. Corey and R. H. Brooks. 1965. Similitude for non-steady drainage of partially saturated soils. Colorado State University Hydrology Paper No. 9.

Duke, H. R. 1972. Capillary properties of soils - influence upon specific yield. Transactions, ASAE, 15(4), 688-691.

Duke, H. R. 1973. Drainage design based upon aeration. Colorado State University Hydrology Paper No. 61, 59 pp.

Hedstrom, W. E., A. T. Corey and H. R. Duke. 1970. Models for subsurface drainage. Colorado State University Hydrology Paper No. 48. 56 pp.

Laliberte, G. E. and R. H. Brooks. 1967. Hydraulic properties of disturbed soil materials affected by bulk density. Proceedings, Soil Science Society of America, 31:451-454.

Laliberte, G. E. and A. T. Corey. 1967. Hydraulic properties of disturbed and undisturbed earth materials. Permeability and Capillarity of Soils, ASTM STP 417, Am. Society of Testing Matls., 56-71.

Laliberte, G. E., A. T. Corey and R. H. Brooks. 1968. Permeability calculated from desaturation data. J. Irrigation and Drainage Division, ASCE, 94(IR1): 57-71.

Laliberte, G. E., A. T. Corey and R. H. Brooks. 1966. Properties of unsaturated porous media. Colorado State University Hydrology Paper No. 17, November.

White, N. F., H. R. Duke, D. K. Sunada and A. T. Corey. 1970. Physics of desaturation in porous materials. J. Irrigation and Drainage Division, ASCE (IR2):165-191.

White, N. F., D. K. Sunada, H. R. Duke and A. T. Corey. 1972. Boundary effects in desaturation of porous media. Soil Science 113(1):7-12.

APPENDIX C

COMPUTER PROGRAM OF STAUFFER AND COREY FOR CALCULATING SOIL CAPILLARY PARAMETERS

Although the digital computer has been used to obtain solutions to many of the problems discussed in this paper, only the computer program in this section is included to provide a convenient, objective method for determining the Brooks-Corey capillary properties from pressure-desaturation data.

This program, written in FORTRAN IV, selects the value of residual saturation resulting in the most nearly linear relation between log S_e and log P_c. Least squares linear regression is then applied to the experimental data (log S_e vs. log P_c/γ) to calculate the pore size distribution index, λ . From these parameters, the relative permeability-capillary pressure function is generated.

```
      PROGRAM SORPT (INPUT,OUTPUT)
      DIMENSION S(20),PC(20)

C        PROGRAM ACCEPTS MAXIMUM 20 PAIRS OF SATURATION-CAPILLARY PRESSURE DATA.
      REAL L,L1
      PRINT 1
    1 FORMAT (1H1,/)
      READ 2,NR

C        ENTER NO. SETS OF DATA INCLUDED IN THE CURRENT ANALYSIS
    2 FORMAT (I2)
    3 READ 4,IDN,N

C        ENTER SAMPLE ID NO., NO. OF DATA PAIRS IN THAT SAMPLE.  MAX N=20.
    4 FORMAT(2I5)
      DO 5 I=1,N
    5 READ 6, S(I),PC(I)
    6 FORMAT(2F10.4)

C        ENTER SATURATION AND CORRESPONDING CAP. PRESSURE, ONE PAIR OF VALUES
C       PER CARD, IN ORDER OF DECREASING CAP PRESSURE.  ENTER ONLY DATA PAIRS FOR
C       WHICH  S IS LT 1.0.
C        INITIALIZE VARIABLES-
      J=0 $ K=0 $ JR=0
      DL=0.1 $ R1=0. $ R2=0. $ R3=0. $ SS=0. $ SS2=0.
      DO 7 I=1,N

C        SUMS AND SUM OF SQUARES OF S
      SS=SS+S(I)
    7 SS2= SS2+S(I)**2

C        OBTAIN FIRST ESTIMATE OF SR AND LAMBDA
      PC1=PC(1)
      PC2=PC(2)
      PCL1=ALOG(PC1)
      PCLN=ALOG(PC(N))
      S1=S(1)
      S2=S(2)
      FPC1=(1./PC1)**2
      FPC2=(1./PC2)**2
      SR=(FPC2*S1-FPC1*S2)/(FPC2-FPC1)
      IF(SR.LT.0.) SR=0.
      SEL1=ALOG((S1-SR)/(1.-SR))
      SELN=ALOG((S(N)-SR)/(1.-SR))
      L=-(SELN-SEL1)/(PCLN-PCL1)
    8 SFPC=0.
      SPS=0. $ SFPC2=0.
```

```
C          CALCULATE CORRELATION COEFFICIENT FOR SELECTED SR AND LAMBDA
        DO 9 I=1,N
        FPCI=(1./PC(I))**L
        SFPC=SFPC+FPCI
        SFPC2=SFPC2+FPCI**2
      9 SPS=SPS+FPCI*S(I)
        R=(SFPC2-SFPC**2/N)*((SPS-SFPC*SS/N)**2)/(SS2-SS**2/N)

C          INCREMENT LAMBDA TO FIND VALUE AT WHICH CORRELATION COEFFICIENT IS MAX.
        IF(JR.EQ.1) R1=R
        IF(JR.EQ.3) R3=R
        IF(K.EQ.2) GO TO 17
        IF(R3.NE.0.) GO TO 12
        IF(R2.NE.0.) GO TO 10
        R2=R
        L1=L
        L=L1-DL
        GO TO 8
     10 IF(R1.NE.0.) GO TO 11
        R1=R
        L=L1+DL
        GO TO 8
     11 R3=R
     12 IF((R2-R1)*(R2-R3)) 13,13,16
     13 IF(R1.GT.R3) 14,15
     14 R3=R2
        R2=R1
        JR=1
        L1=L1-DL
        L=L1-DL
        GO TO 8
     15 R1=R2
        R2=R3
        JR=3
        L1=L1+DL
        L=L1+DL
        GO TO 8
     16 C=(R1+R3-2.*R2)/(2.*DL**2)
        B=(R3-R2-C*DL**2)/DL
        L=L1
        L=L-B/(2.*C)
        DL=DL/10.
        R1=0. $ R2=0. $ R3=0.
        JR=0
        K=K+1
        GO TO 8

C          CALCULATE SR, ETA, BUBBLING PRESSURE
     17 B=(SPS-SS*SFPC/N)/(SS2-SS**2)
        SR=(SS-SFPC*B)/N
        PB=1./(B+SFPC/N-B*SS/N)**(1./L)
        E=3.*L+2.
```

```
C          PRINT RESULTS
      PRINT 18,IDN
   18 FORMAT(1H ,*SOIL IDENTIFICATION NUMBER*, I5,///)
      PRINT 19
   19 FORMAT(1H ,5X,*SATURATION*,8X,*CAP. PRESSURE*,6X,*REL.PERMEABILITY*,4X,*E
     1FF. SATURATION*,//)
      DO 20 I=1,N
      RK=((S(I)-SR)/(1.-SR))**(E/L)
      FPC=(PB/PC(I))**L
   20 PRINT 21, S(I),PC(I),RK,FPC
   21 FORMAT(7X,3(F6.5,13X),/)
      PRINT 22; E,L,SR,PB,R
   22 FORMAT(///,*ETA =*,F10.3,/,*LAMBDA =*,F10.3,/,*RESIDUAL SATURATION =*,F10.
     13,/,*BUBBLING PRESSURE =*,F10.3,* CM*,/,*CORRELATION COEFFICIENT =*E16.6,
     2/////)
      NR=NR-1
      IF(NR.GT.0) GO TO 3
      END
```